Application and Assessment of Open-system vs. Closed-system Kerogen Isolation Methods for Characterization of Gas Shale Kerogens

---

A Thesis

Presented to

the Faculty of the Department of Earth and Atmospheric Sciences

University of Houston

In Partial Fulfillment

of the Requirements for the Degree

Masters of Science

By

Denet Pernia

August 2012

Application and Assessment of Open-system vs. Closed-system Kerogen Isolation Methods for Characterization of Gas Shale Kerogens

_____

Denet Pernia

APPROVED:

_____

Dr. K.K. Bissada, Chairman

_____

Dr. Regina Capuano

_____

Dr. Robert Stewart

_____

Dr. Joseph Curiale

Chevron Energy Technology Company

_____

Dean Mark A. Smith, College of Natural Sciences and Mathematics

ACKNOWLEDGEMENTS

I would like to thank my advisor Dr. Adry Bissada for all of his help and guidance as well as Dr. Joseph Curiale, without whom this project would have not been possible. Thank you to my committee members, Dr. Regina Capuano and Dr. Robert Stewart, for all of your support. I am very grateful to Chevron Energy Technology Company for providing me with the samples and for funding this study. I would like to thank Rice Energy for providing me with the Marcellus sample for this study. I am also very grateful to the University of Houston Center for Petroleum Geochemistry for providing the facilities as well as financial support. Also thank you to Mike Darnell, Ewa Szymczyk, Thomas Szymczyk, Maria Andrades, Maria Gutierez, and Gregory Sills. I would like to acknowledge Dr. Lawrence Alemany at Rice University for his indispensible help with the NMR analysis. Thank you to the whole Chevron geochemistry group for their comments and suggestions at the AAPG in Long Beach. I am most grateful for the support of my family and especially my husband, Zheng Huang.

Application and Assessment of Open-system vs. Closed-system Kerogen Isolation Methods for Characterization of Gas Shale Kerogens

---

An Abstract of a Thesis

Presented to

the Faculty of the Department of Earth and Atmospheric Sciences

University of Houston

In Partial Fulfillment

of the Requirements for the Degree

Masters of Science

By

Denet Pernia

August 2012

ABSTRACT

Increasing interest in unconventional natural gas resources has spurred much research into the origin as well as the mode of entrapment and expulsion of natural gas. A pre-requisite of all such research is the isolation and separation of the kerogen, the insoluble organic matter from which hydrocarbons are formed, in its purest and most intact form from the rock matrix. Previous work showed that the isolation methods, closed-method versus open-method, used can impact kerogen recovery, purity, and elemental composition of the kerogen. This study takes it further and also addresses the effects of the isolation processes on the elemental, isotropic, spectroscopic, and structural (physical) properties of the kerogen recovered.

Four major gas shales, including the Barnett, the Marcellus, the Haynesville, and a Polish gas shale, were chosen to test the impact of the closed-conservative versus open-conventional isolation methods on the properties of kerogen. The Monterey shale, though not strictly a gas shale, was included to address the effects on sulfur-rich, Type II-S kerogens. Standard screening procedures including Total Organic Carbon analysis, RockEval Pyrolysis, and X-ray Diffraction (XRD)-mineralogy were carried out on the native rocks, as well as sulfur forms. The carbon and sulfur isotopic compositions, organic elemental composition, solid-state ^{13}C Nuclear Magnetic Resonance (NMR) spectroscopic properties, and Pyrolysis-GC pyrolytic behavior of the isolated kerogens were investigated.

Higher ash content of kerogens isolated via the open-method and corresponding XRD results show more impurities than the closed-method kerogens. The closed-method

resulted in higher kerogen recovery efficiencies. Pyrolysis-GC n-alkene/n-alkane ratios and relative quantities of alkanes, alkenes, and aromatics show much variability across samples isolated by the three methods, as though the same sample's kerogen-cracking behavior has been altered. The ^{13}C NMR yielded no significant change in the kerogen structure. The closed-method kerogens generally had higher carbon weight % than the open-method. Stable carbon isotopes showed no significant differences in the kerogen $\delta^{13}C$, whereas the stable sulfur isotopes showed significant change in the kerogen $\delta^{36}S$. Still to be investigated are the impacts of the isolation methods on the kerogen's gas-retention and storage capacity as well as its density.

TABLE OF CONTENTS

Chapter 1: Introduction ***1***

1.1 Introduction **2**

1.2 Research Objective **2**

1.3 Scope **3**

Chapter 2: Background ***6***

2.1 Kerogen Defined **7**

2.2 Physical and Chemical Means for Kerogen Isolation: **9**

2.3 Commonly Used Chemical Kerogen Isolation Methods **11**

2.3.1 Closed-conservative Method (CCM) 11

2.3.2 Open-conventional Method (OCM) 14

Chapter 3: Sample Set ***17***

Chapter 4: Methods ***25***

4.1 Total Organic Carbon (TOC) **26**

4.2 RockEval Pyrolysis **26**

4.3 Bitumen Extraction **29**

4.4 Whole-Rock Sulfur Forms **30**

4.5 X-Ray Diffraction (XRD) **31**

4.6 Ash Content **32**

4.7 Kerogen Recovery Efficiency **32**

4.8 Visual Kerogen Assessment by Microscopy **34**

4.9 Stable Isotope Analysis **35**

4.9.1 Stable Carbon Isotope Analysis ($\delta^{13}C$) 35

4.9.2 Stable Sulfur Isotope Analysis ($\delta^{34}S$) 36

4.10 Elemental Analysis **37**

4.11 Pyrolysis-GC **38**

4.12 Solid-state ^{13}C Nuclear Magnetic Resonance (NMR) **39**

Chapter 5: Results ***43***

5.1 Total Organic Carbon (TOC) Results **44**

5.2 RockEval Pyrolysis Results **44**

5.3 Bitumen Extraction Results **46**

5.4 Sulfur Forms Results **47**

5.5 X-Ray Diffraction Results **50**

5.6 Ash Content Results ____ **56**

5.7 Kerogen Recovery Efficiency Results ____ **57**

5.8 Visual Kerogen Assessment Results ____ **57**

5.8.1 Vitrinite Reflectance (R_o) ____ 57

5.8.2 Thermal Alteration Index (TAI) ____ 66

5.9 Stable Isotope Analysis Results ____ **68**

5.9.1 Stable Carbon Isotope Analysis ($\delta^{13}C$) Results ____ 68

5.9.2 Stable Sulfur Isotope Analysis ($\delta^{34}S$) Results ____ 69

5.10 Elemental Analysis Results ____ **70**

5.11 Pyrolysis-GC Results ____ **72**

5.12 Solid-state ^{13}C Nuclear Magnetic Resonance (NMR) Results ____ **83**

Chapter 6: Discussion ____ ***90***

6.1 Whole-Rock Properties ____ **91**

6.2 Kerogen Recovery and Purity ____ **94**

6.3 Kerogen Elemental Properties ____ **95**

6.4 Kerogen Structural (Physical) Properties ____ **97**

6.5 Kerogen Isotopic Properties ____ **97**

6.6 Kerogen Molecular Properties ____ **99**

6.7 Kerogen Spectroscopic Properties ____ **102**

Chapter 7: Summary and Conclusions ____ ***104***

Chapter 8: Recommendations ____ ***109***

References ____ ***112***

Appendix ____ ***115***

LIST OF FIGURES

Figure 2.1.1: Composition of organic matter in sedimentary rocks modified from Tissot and Welte (1978). 7

Figure 2.1.2: Coal macerals and kerogen-type: evolution paths upon geological burial. Three main types are identified, from Type I starting at low maturity with high H/C and low O/C to Type III starting at low maturity with low H/C and high O/C. FromVandenbroucke and Largeau (2007). 8

Figure 2.3.1: Automated, closed-system kerogen isolation instrument from Ibrahimov and Bissada (2010). 12

Figure 2.3.2: A flow diagram summarizing the open-conventional method #1(OCM #1) for kerogen isolation used in this study. 15

Figure 2.3.3: A flow diagram summarizing the open-conventional method #2 (OCM #2) for kerogen isolation used in this study. 16

Figure 3.1: Location of the Barnett (mature and immature), the Haynesville, the Marcellus, the Monterey shales, and undisclosed Poland shale. Source: United-States-Map.com, Enchantedlearning.com/Europe/Poland. 18

Figure 3.2: Map of Barnett shale play. Source: NETL (2009). 21

Figure 3.3: Map of Marcellus shale play. Source: NETL (2009). 22

Figure 3.4: Map of Haynesville shale play. Source: NETL (2009). 23

Figure 3.5: Monterey shale play. Source: Australian Oil Company. Source: Australian Oil Company (2010). 24

Figure 4.2: Principle of the RockEval II and the TOC module from Bordenave et al. (1993). 28

Figure 4.12: The NMR spectrometer consists of a superconducting magnet, a probe, a radio transmitter, a radio receiver, an analog-to-digital converter (ADC), and a computer. The magnet consists of a solenoid of superconducting Nb/Ti alloy wire immersed in liquid helium. A current flows around the solenoid creating a strong magnetic field. The probe is a coil of wire positioned around the sample and it transmits and receives radio frequency signals. The computer has the transmitter send a pulse of radio frequency to the probe, after which the signal from the probe is amplified, converted to audio frequency signal and sampled producing a list of numbers. The computer determines the time and intensity of the pulses from the transmitter and then receives and processes the digital information from the ADC. After performing a Fourier transform the resulting spectrum is displayed on the computer screen. From Jacobsen (2007). 41

Figure 5.4.1: Bar graph showing the sulfur weight percentages (wt%) of the different sulfur forms from the whole-rock. From left to right: Total Sulfur, Sulfate Sulfur, Pyritic Sulfur, and Organic Sulfur. 48

Figure 5.4.2: Pie charts showing the sulfur forms in terms of percentages of the total sulfur. 49

Figure 5.5.1: X-Ray diffractograms for the immature Barnett whole-rock in black, OCM #1 in purple, OCM #2 in orange, and CCM in green. 51

Figure 5.5.2: X-Ray diffractograms for the Monterey whole-rock in black, OCM #1 in purple, OCM #2 in orange, and CCM in green. 52

Figure 5.5.3: X-Ray diffractograms for the Marcellus whole-rock in black, OCM #1 in purple, OCM #2 in orange, and CCM in green. 53

Figure 5.5.4: X-Ray diffractograms for the Polish Shale whole-rock in black, OCM #1 in purple, OCM #2 in orange, and CCM in green. 54

Figure 5.5.5: X-Ray diffractograms for the Haynesville whole-rock in black, OCM #2 in orange, and CCM in green. 55

Figure 5.6.1: Bar graph comparing ash content results. The OCM kerogens have higher ash contents than the CCM. 56

Figure 5.7.1: Bar graph comparing the results of kerogen recovery efficiency of initial kerogen of the three labs. The two OCM approaches show lower recovery compared to the CCM. 57

Figure 5.8.1: Zones of hydrocarbon generation, expulsion, and preservation. Modified from Bissada (1979). 59

Figure 5.8.2: Histograms for the immature Barnett based on the vitrinite reflectance values of the kerogens. 60

Figure 5.8.3: Histograms for the immature Barnett and matured Barnett based on the vitrinite reflectance values of the kerogens. 61

Figure 5.8.4: Histograms for the Monterey based on the vitrinite reflectance values of the kerogens. 62

Figure 5.8.5: Histograms for the Marcellus based on the vitrinite reflectance values of the kerogens. 63

Figure 5.8.6: Histograms for the Polish Shale based on the vitrinite reflectance values of the kerogens. 64

Figure 5.8.7: Histogram for the Haynesville based on the vitrinite reflectance values of the kerogen. 65

Figure 5.9.1: Carbon isotopic composition of the various kerogens isolated by the three approaches (error bars based on twice the standard deviation). 69

Figure 5.9.2: Sulfur isotopic composition of the various kerogens isolated by the three approaches (values are within ± 0.3‰). 70

Figure 5.10.1: Elemental analysis results of the kerogen. Note variance in the values across the labs. 71

Figure 5.10.2: Elemental analysis results normalized to 100 %. Above the Barnett immature (outcrop) sample and the Barnett matured samples' compositions were compared. The Monterey non-bitumen extracted and bitumen-extracted kerogen's compositions were compared. 72

Figure 5.11.1: N-alkene/n-alkane ratios for the immature Barnett kerogens. Note the variability in the ratios across methods. Greatest variability in the ratios was seen in the C1 to C5 range. 74

Figure 5.11.2: N-alkene/n-alkane ratios for the Monterey kerogens. Note the variability in the ratios across methods. The open-method #2 (OCM #2) kerogen significantly varies in the ratios from the other two methods. 75

Figure 5.11.3: N-alkene/n-alkane ratios for the Marcellus kerogens. Note the variability in the ratios across methods. The most significant variability was seen in the C1-C5 range. 75

Figure 5.11.4: N-alkene/n-alkane ratios for the Polish Shale kerogens. Note the variability in the ratios across methods. The most significant variability was seen in the C1-C5, C11-C14, and C15+ ranges. 76

Figure 5.11.5: N-alkene/n-alkane ratios for the Haynesville kerogens. Note the variability in the ratios across methods. There was significant variability in all the ranges. 76

Figure 5.11.6: Pyrograms for the three Barnett (immature) kerogens with a summary table for each result. 78

Figure 5.11.7: Pyrograms for the three Monterey kerogens with a summary table for each result. 79

Figure 5.11.8: Pyrograms for the three Marcellus kerogens with a summary table for each result. 80

Figure 5.11.9:Pyrograms for the three Polish Shale kerogens with a summary table for each result. 81

Figure 5.11.10: Pyrograms for the three Haynesville kerogens with a summary table for each result. 82

Figure 5.12.1: Solid-state 13C NMR results for the immature Barnett kerogen. On the left are the cross-polarization results and on the right are the dipolar dephasing results. 84

Figure 5.12. 2: Solid-state 13C NMR results for the Barnett kerogen comparing the thermally immature and the mature Barnett samples. On the left are the cross-polarization results and on the right are the dipolar dephasing results. 85

Figure 5.12.3: Solid-state 13C NMR results for the Monterey kerogen. On the left are the cross-polarization results and on the right are the dipolar dephasing results. 86

Figure 5.12.4: Solid-state 13C NMR results for the Marcellus kerogen. On the left are the cross-polarization results and on the right are the dipolar dephasing results. 87

Figure 5.12 5:Solid-state 13C NMR results for the Polish Shale kerogen. On the left are the cross-polarization results and on the right are the dipolar dephasing results. 88

Figure 5.12.6:Solid-state 13C NMR results for the Haynesville kerogen. On the left are the cross-polarization results and on the right are the dipolar dephasing results. 89

Figure 6.1.1: Modified van Krevelen Plot of RockEval Pyrolysis results. Plot from Ibrahimov an d Bissada (2010). 91

Figure 6.1.2: Plot of TOC vs. THGP to determine oil- vs. gas-proneness of samples. Plot from Ibrahimov an d Bissada (2010). 93

Figure 6.3.1: Chemical characterization of kerogen by van Krevelen method. Plot from Ibrahimov an d Bissada (2010). 97

Figure 6.5.1: Results of the sulfur isotopes (±0.3‰) of the kerogens showing the sulfur form results for the whole-rock with the percentages of sulfate, pyritic, and organic sulfur. Note the relationship between high amounts of pyritic sulfur and greater variance in the sulfur isotopes. 99

Figure 6.6.1: The above plots compare the alkanes, alkenes, and aromatics for the samples based on the Py-GC of the kerogens. Overall the values follow the same pattern but with varying intensities based on the isolation

method used. Presence of impurities (inorganic mineralogy) in the OCM kerogen may help explain the different cracking behaviors of the kerogen. 101

LIST OF TABLES

Table 2.3.1: List of protocols for University of Houston closed-conservative method (CCM) for kerogen isolation. 13

Table 3.1: Summary table for major gas shales in the United States. Highlighted in blue are the gas shales that are a part of this study. From Bissada (2012) Poza Rica, Mexico conference. 19

Table 5.1.1: TOC results for the whole-rock samples given in wt%. 44

Table 5.2.1: RockEval Pyrolysis results for the whole-rock (top) and the bitumen-free rocks (bottom). 46

Table 5.3.1: Quantified bitumen for whole-rock samples. 47

Table 5.8.1: Summary table of the vitrinite reflectance work. Mean R_o is based on the representative kerogen seen in blue in the histograms shown in Figures 5.8.2-5.8.4. Note the very little variance in thermal maturity results across methods used. 59

Table 5.8.2: Summary table of TAI results for the samples. 67

Table 5.11.1: Table showing the aromaticity of the kerogen from the Py-GC results. Aromaticity was determined from the percent of aromatics out of all the measured compounds. 73

Table 6.1.1: Organic richness of the native shale samples (Richness scale modified from Baskin, 1997). 93

Table 6.1.2: Permeability and porosity calculations for the Marcellus shale in this study. Increasing depth from A to F. 94

Table 7.1: Summary table of the elemental, isotopic, molecular, and spectroscopic results. Note the variance in the results. Aromaticity is given from the Py-GC and the NMR which differ greatly. 108

Chapter 1: Introduction

1.1 Introduction

Kerogen is the predominant form of organic matter in sedimentary rocks and the precursor to hydrocarbon generation. Its characterization is crucial for understanding the origin of oil and gas, basin thermal history, and source rock depositional environments. Understanding the kerogen properties and characteristics is also critical to better understanding the way gas shales store and release natural gas. This cannot be accomplished without the isolation of the kerogen from the rock matrix. Kerogen isolation can be done through either an open-conventional method (OCM) or a closed-conservative method (CCM). In the study by Ibrahimov and Bissada (2010) of open- versus closed-kerogen isolation methods, it was found that open-methods for kerogen isolation yielded kerogens that were not good representatives for chemical analysis while the closed-method for kerogen isolation did. The conventional open-system approach yields fractionated, impure, and otherwise unrepresentative kerogen not useful for chemical investigations (Ibrahimov and Bissada, 2010). Research-quality kerogen for chemical and physiochemical studies requires special conservative separation procedures that preclude fractionation and ensure quantitative recovery, effective mineral removal, chemical preservation, and maintenance of the organic matter (Ibrahimov and Bissada, 2010).

1.2 Research Objective

The first aim of this study is to conduct a comparative analysis of the effects that the two different kerogen isolation methods, closed-conservative vs. open-conventional, may have on kerogen's elemental, isotopic, spectroscopic, and structural (physical) properties. Any observed differences, including isotopic fractionation, will be examined

to determine how they may affect subsequent interpretation of the kerogen's origin, thermal maturity, and internal structure. The second aim of this study is to conduct a comparative analysis between the gas shales and the oil shale in the study in terms of their whole-rock and kerogen properties.

1.3 Scope

The samples include three gas shales located in the United States (the Marcellus, the Barnett, and the Haynesville), as well as one gas shale from Poland. The Monterey oil shale was also included in the sample set in order to assess any effects the different kerogen isolation methods may have on a Type II-S kerogen. All of the sample preparation and most of the geochemical analyses were carried out at the University of Houston (UH) Center for Petroleum Geochemistry. A brief description of the analytical methods is provided below:

Analysis of Whole-rock:

1. The whole-rock samples were crushed and ground to pass through a 60 mesh (250 microns) sieve, homogenized using a Micro-Rifler, and then separated into three aliquots for analysis.
2. Total organic carbon (TOC) and total sulfur (TS) weight percentages were determined using a LECO Carbon/Sulfur Combustion Analyzer (CS230CH).
3. RockEval Pyrolysis was done for each sample using a RockEval II-Plus instrument.
4. X-ray Diffraction (XRD) was carried out at the UH with a Panalytical X'Pert Pro XRD machine, in order to determine whole-rock mineralogy and pyrite content.

5. Whole-rock organic microscopy was conducted using a Leitz Orthoplan microscope, for visual determination of organic matter type.
6. Sulfur forms, specifically organic sulfur, sulfate sulfur, and pyritic sulfur weight percentages, were determined using sequential leaching. Sulfur forms analysis was carried out at UH.
7. Bitumen extraction was done with a Soxhlet extractor. Once the samples were bitumen-free they were treated to recover the kerogen.
8. Ultra-pure kerogen isolation was done via the closed-conservative method at the UH. Non-ultra-pure kerogen isolation was done via the open-conventional method at two different commercial laboratories.

Analysis of Isolated Kerogen:

1. Pyrolysis-Gas Chromatography (Py-GC) was carried out at Weatherford Laboratories (see Appendix).
2. Solid-state ^{13}C NMR spectroscopic analysis was conducted at Rice University to assess aromaticity distribution.
3. Organic elemental analysis for carbon, hydrogen, oxygen, nitrogen, and sulfur (CHONS) was contracted to Intertek QTI (see Appendix). Analyses were carried out on a Perkin-Elmer 2400 Elemental Analyzer fitted with an oxygen accessory kit.
4. X-ray Diffraction was carried out to determine mineralogy and pyrite content to assess the purity of the recovered kerogen. The work was carried out at the UH with a Panalytical X'Pert Pro XRD machine.
5. Maceral rock microscopy, including visual kerogen assessment (VKA) for maceral distribution and vitrinite reflectivity equivalent (VReq) for thermal maturity, was

done. Thermal Alteration Index (TAI) was determined using a Leitz Orthoplan microscope on dispersed kerogen slides. Thermal maturity levels were determined directly using a Zeiss Photoscope equipped with reflectance photometry capability for vitrinite equivalent reflectance measurements (R_o eq) on organic particles in the recovered kerogens.

6. Stable carbon ($\delta^{13}C$) and sulfur ($\delta^{34}S$) isotope compositions were determined to assess isotope fractionation. Carbon isotopic compositions were done at UH on a Finnigan Mat Delta S stable-isotope mass spectrometer. Sulfur isotope analyses were contracted out to Isotech (see Appendix).
7. Ash content, measured at UH, was used to determine the effectiveness of each isolation method in the removal of inorganic material.

Chapter 2: Background

2.1 Kerogen Defined

At the most basic level there are two main types of sedimentary organic matter on Earth, kerogen and bitumen. Kerogen is the more abundant of the two sedimentary organic matters and is defined as insoluble in common organic solvents (Forsman and Hunt, 1958; Durand, 1980). Bitumen is defined sedimentary organic matter that is soluble in common organic solvents. Figure 2.1.1 is a graphical representation of the types of sedimentary organic matter given by Tissot and Welte (1978).

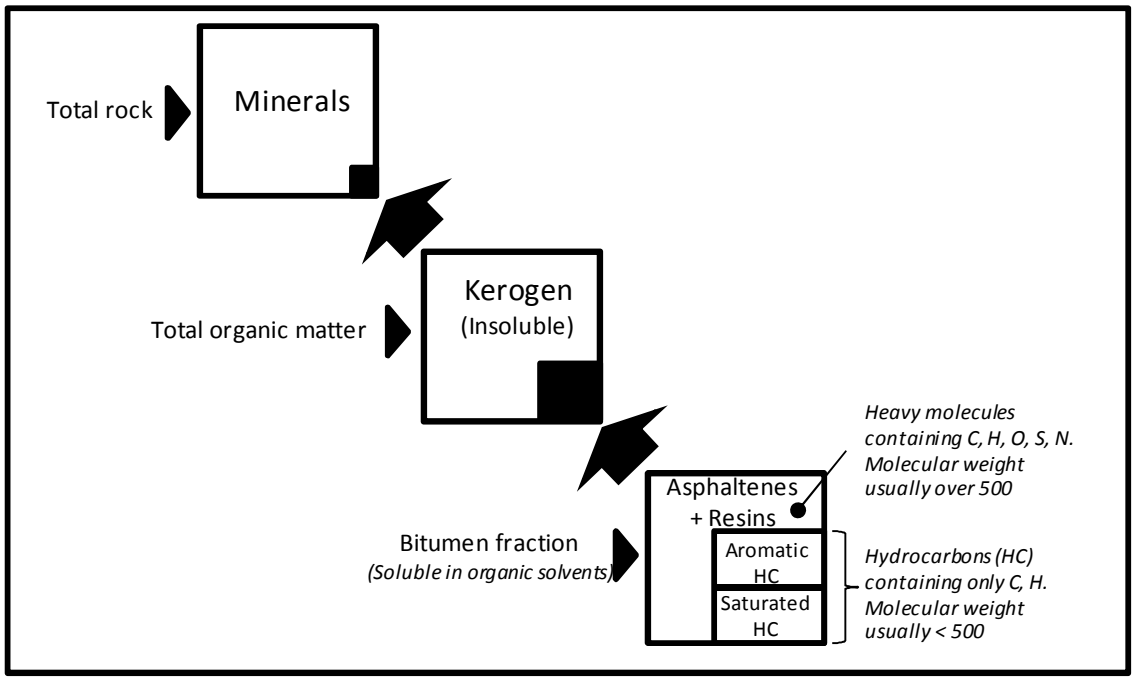

Figure 2.1.1: Composition of organic matter in sedimentary rocks modified from Tissot and Welte (1978).

According to Vandenbroucke and Largeau (2007), Durand and Espitalie (1973) proposed the classification of source rock kerogen into three types along with evolution paths for each one based on thermal maturation. Tissot et al. (1974) recognized that the evolution paths for the three types of kerogen resembled carbonization paths of coal macerals so that the three main types of kerogen could be plotted on a modified van Krevelen diagram (Figure 2.1.2). This made it possible for the adoption of the study of

coal macerals by coal and palynology sciences to the study of organic matter composition and determination of source-rock potential and maturity. Type I kerogen (Sapropellic), which resembles Alginites, is highly aliphatic, oil-prone, has a high H/C ratio, has a relatively low O/C ratio, and is sourced from algal-lacustrine and algal-marine sources. Type II kerogen (Exinitic or Mixed), which resembles Exinites, is oil-prone and gas-prone, has relatively high H/C ratios, has low O/C ratios, and can come from a mixture of sources from Type I and Type III. Type III kerogen (Humic), which resembles Vitrinites, is gas-prone, is highly aromatic, has high O/C ratios, has relatively low H/C ratios, and is sourced mainly from higher plants and terrestrial material that accumulate in non-marine environments.

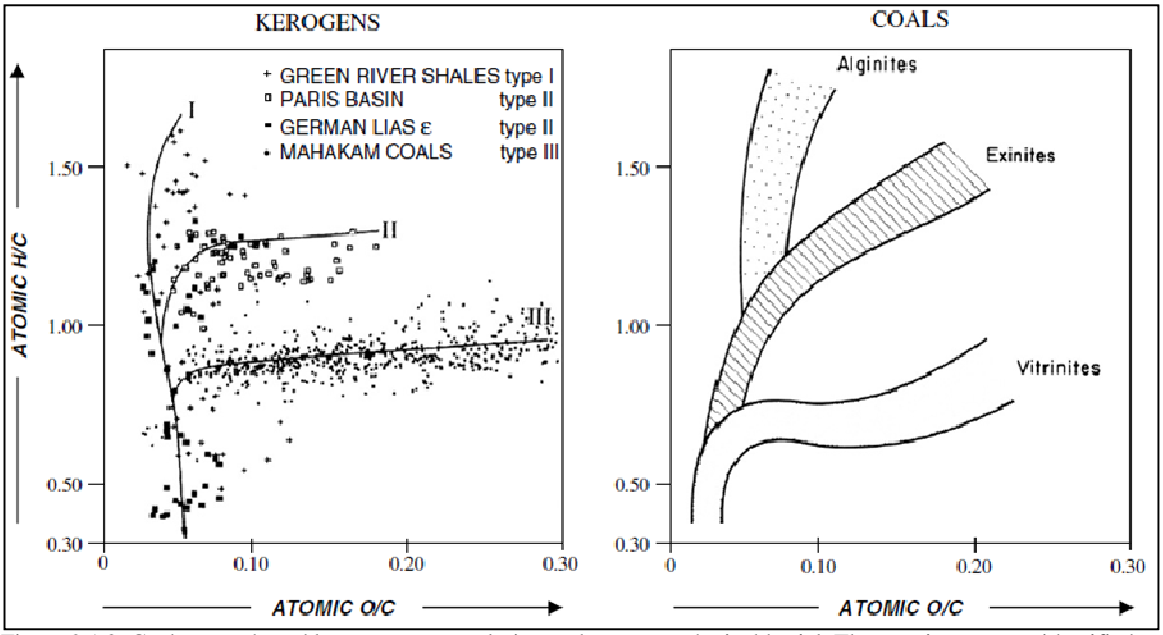

Figure 2.1.2: Coal macerals and kerogen-type: evolution paths upon geological burial. Three main types are identified, from Type I starting at low maturity with high H/C and low O/C to Type III starting at low maturity with low H/C and high O/C. From Vandenbroucke and Largeau (2007).

2.2 Physical and Chemical Means for Kerogen Isolation:

To study kerogen it must first be isolated from the rock matrix with which it is intimately associated. There are two basic ways to isolate kerogen, physically or chemically. Physical means of isolation are mainly used by palynologists and coal scientists. Kerogen is commonly isolated via chemical means, using strong acids, for the recovery of organic matter present in a rock.

2.2.1 Physical means for isolation:

The different physical separation methods, similar to those used for ore mineral processing, include flotation, centrifugation techniques, ultrasonic techniques, electrostatic and electromagnetic processes, and using the different wetting properties of organic and inorganic matter (Saxby, 1970 (a); Durand and Nicaise, 1980).The physical methods of isolation were preferred by some because they did not heavily alter the kerogen chemically. However, physical isolation methods have low recoveries of the organic matter, they do not accomplish total isolation of the kerogen, and are not useful when only small amounts of organic matter are available (Saxby, 1970 (a)). Physical means of isolation will not be discussed any further since the focus of this study are the chemical methods of isolation.

2.2.2 Chemical means of isolation:

The issues encountered with the physical means of isolation can be overcome with the chemical means of isolation where smaller amounts of organic matter can be used (Saxby, 1970 (a)). The chemical reactions must be carried out at temperatures that

are high enough for carbonate dissolution (~70˚C), but low enough to prevent kerogen oxidation (Durand and Nicaise, 1980). Hydrochloric acid (HCl) is used to dissolve most carbonate species as well as sulphides, basic oxides, and basic hydroxides (Saxby, 1970 (a)). A mixture of Hydrofluoric acid (HF) and HCl can be used to dissolve away quartz, other silicates, and clay minerals (Saxby, 1970 (a); Saxby, 1970 (b); Vandenbroucke and Largeau, 2007).

Even after such robust acid treatments, pyrite will still remain in the organic matter. The residual pyrite can interfere with chemical characterization of the kerogen. Many different approaches have been used to remove pyrite. In the past, nitric acid (HNO_3) was used, but it oxidized the kerogen so it was not desirable (Forsman and Hunt, 1958; Saxby, 1970 (a)). Lithium aluminum hydride ($LiAlH_4$) was used but it altered the kerogen (Saxby, 1970 (a)). Sodium borohydride ($NaBH_4$) was used but it proved ineffective in removing the pyrite (Saxby, 1970 (a)). The pyrite removal problem was finally resolved by Acholla and Orr (1993) with the use of acidic chromous chloride ($CrCl_2$) under nitrogen (N_2), to prevent oxidation and remove pyrite without significant alteration of the kerogen. This method must be accompanied with fine grinding and multiple treatments to ensure effective removal of pyrite (Acholla and Orr, 1993). Another common method used today for the removal of pyrite is heavy liquid separation with zinc bromide. The problem with this method is it results in fractionation of the organic matter and incomplete removal of the pyrite (Ibrahimov and Bissada, 2010).

There are some complications with chemical means of kerogen isolation, including the formation of complex fluorides with the use of HF when clay minerals and feldspars are present (Forsman and Hunt, 1958). For example, ralstonite forms under

low-temperature (down to 40˚C) reactions carried out in fluorine-rich conditions (Hitchon et al., 1976). Thus, a critical first step is to remove all calcium and magnesium from the system. It was found that to prevent new fluorides from forming a mixture of HF and HCl and effective water washings would help (Durand and Nicaise, 1980). A subsequent rinse with HCl after the removal of silicates has been found to prevent the formation of new fluorides (Vandenbroucke and Largeau, 2007). Another complication is the presence of virtually insoluble minerals in the kerogen. Durand and Nicaise (1980) found zircon, rutile, anatase, brookite, tourmaline, and barite to be commonly left behind after treatment of the kerogen with the acids.

There are two ways to chemically isolate kerogen; one is via a closed-conservative method and the second is via an open-conventional method. These two methods were used in this study and are briefly described below.

2.3 Commonly Used Chemical Kerogen Isolation Methods

2.3.1 Closed-Conservative Method (CCM)

Kerogen isolation via the closed-conservative (CCM) was carried out as described by Ibrahimov and Bissada (2010), in a sealed system under an inert N_2 atmosphere that is computer automated. The whole-rock specimens were loaded into Teflon cells and into the CCM apparatus, where they were flushed numerous times with HCl (to dissolve carbonates, sulfates, and soluble sulfides), HF (to dissolve siliciclastics), de-ionized (DI) water (in between steps for rinsing), and ammonium hydroxide (NH_4OH) to neutralize the system and remove HCl soluble gels (Ibrahimov and Bissada, 2010). Finally, the kerogen in the sealed reaction cells were treated numerous times with acidic $CrCl_2$ in

order to dissolve any pyrite present (Acholla and Orr, 1993). Figure 2.3.1 shows the instrument used for kerogen isolation via the UH CCM and Table 2.3.1 shows a detailed list of protocols used to recover the kerogen.

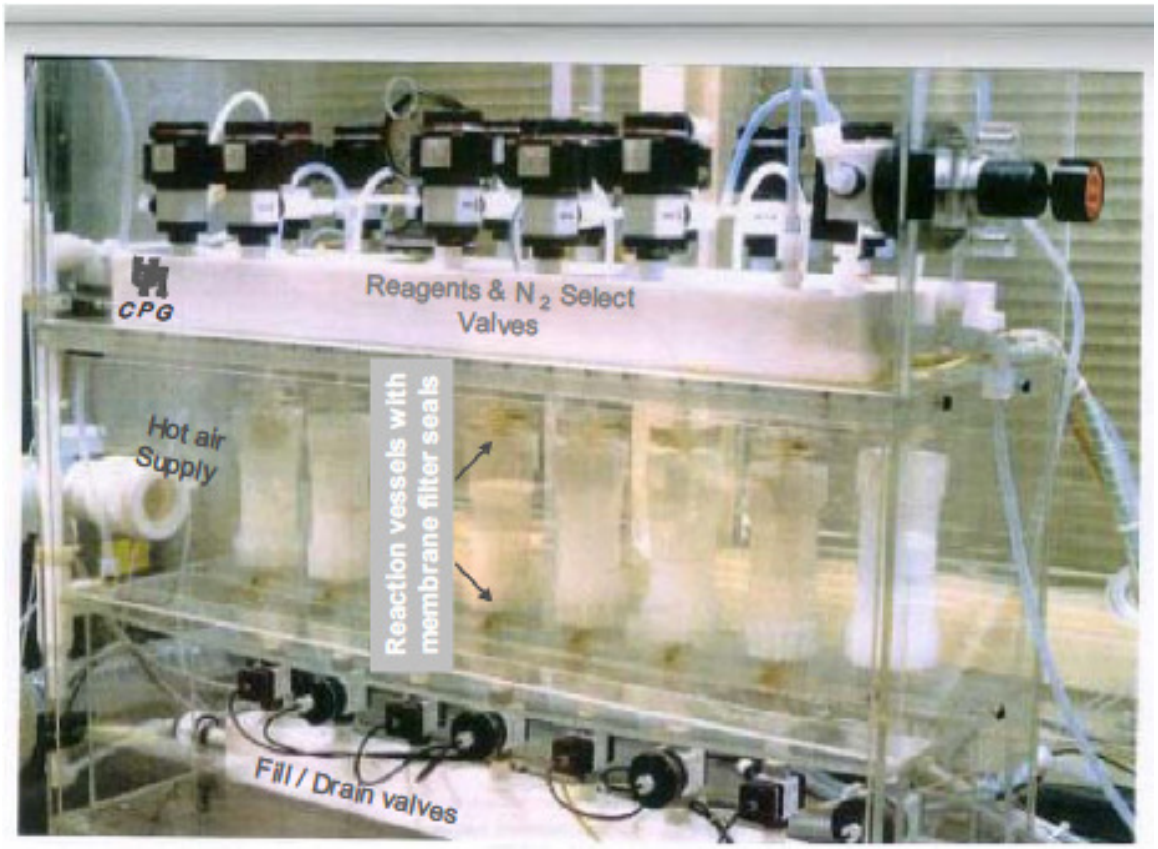

Figure 2.3.1: Automated, closed-system kerogen isolation instrument from Ibrahimov and Bissada (2010).

1	FILL HCl	27	FILL HF:HCl	53	FILL H_2O	79	FILL H_2O
2	DRAIN	28	DRAIN	54	DRAIN	80	DRAIN
3	FILL HCl	29	FILL HF:HCl	55	FILL H_2O	81	FILL HCl
4	TIME/DRAIN	30	TIME/DRAIN	56	DRAIN	82	DRAIN
5	FILL HCl	31	FILL HCl	57	FILL NH_4OH	83	FILL H_2O
6	TIME/DRAIN	32	DRAIN	58	DRAIN	84	DRAIN
7	FILL H_2O	33	FILL H_2O	59	FILL H_2O	85	FILL H_2O
8	DRAIN	34	DRAIN	60	DRAIN	86	DRAIN
9	FILL H_2O	35	FILL H_2O	61	FILL H_2O	87	FILL $CrCl_2$
10	DRAIN	36	DRAIN	62	DRAIN	88	DRAIN
11	FILL HCl	37	FILL NH_4OH	63	FILL HF:HCl	89	FILL HCl
12	DRAIN	38	DRAIN	64	TIME/DRAIN	90	DRAIN
13	FILL HCl	39	FILL H_2O	65	FILL HCl	91	FILL $CrCl_2$
14	TIME/DRAIN	40	DRAIN	66	DRAIN	92	DRAIN
15	FILL HCl	41	FILL H_2O	67	FILL HF:HCl	93	FILL HCl
16	TIME/DRAIN	42	DRAIN	68	TIME/DRAIN	94	DRAIN
17	FILL H_2O	43	FILL HF:HCl	69	FILL HCl	95	FILL $CrCl_2$
18	DRAIN	44	DRAIN	70	DRAIN	96	DRAIN
19	FILL H_2O	45	FILL HF:HCl	71	FILL HCl	97	FILL HCl
20	DRAIN	46	TIME/DRAIN	72	DRAIN	98	DRAIN
21	FILL NH_4OH	47	FILL HCl	73	FILL H_2O	99	FILL H_2O
22	DRAIN	48	DRAIN	74	DRAIN	100	DRAIN
23	FILL H_2O	49	FILL H_2O	75	FILL H_2O	101	FILL H_2O
24	DRAIN	50	DRAIN	76	DRAIN	102	DRAIN
25	FILL H_2O	51	FILL HCl	77	FILL HCl	103	FILL H_2O
26	DRAIN	52	DRAIN	78	DRAIN	104	DRAIN

Table 2.3.1: List of protocols for University of Houston closed-conservative method (CCM) for kerogen isolation.

2.3.2 Open-conventional Method (OCM)

Kerogen isolation via the open-conventional method (OCM) in this study involved two commercial labs. In this method, all the wet chemistry was done in open beakers under fume hoods. Samples were decanted during the acid treatments and kerogen was recovered from the material that was floating in the containers after heavy liquid separation for pyrite removal. The samples were treated with HCl, HF, and DI water several times to ensure that all the carbonates and silicates were removed. A brief summary of the methods provided by the two commercial labs is given below.

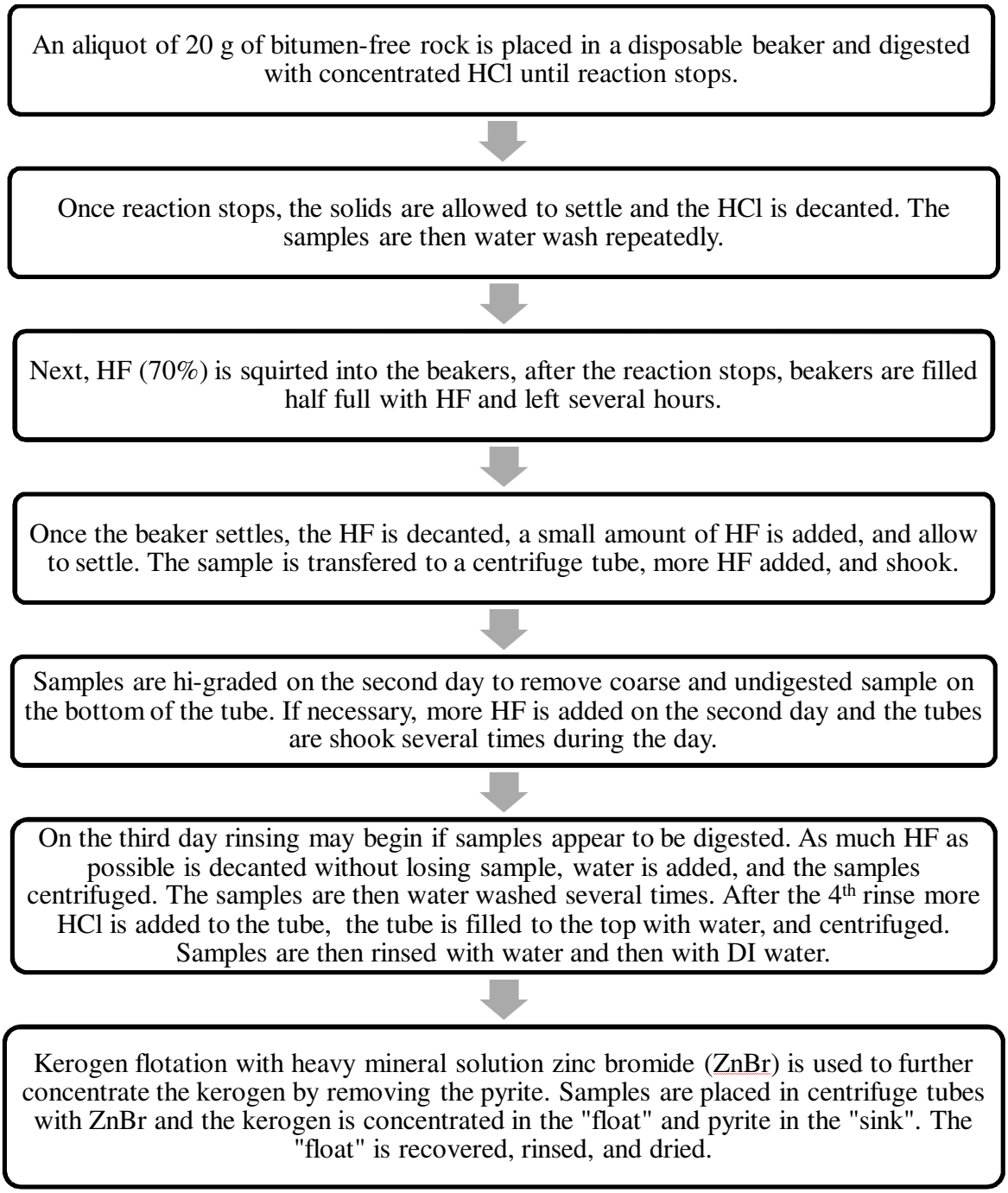

Figure 2.3.2: A flow diagram summarizing the open-conventional method #1 (OCM #1) for kerogen isolation used in this study.

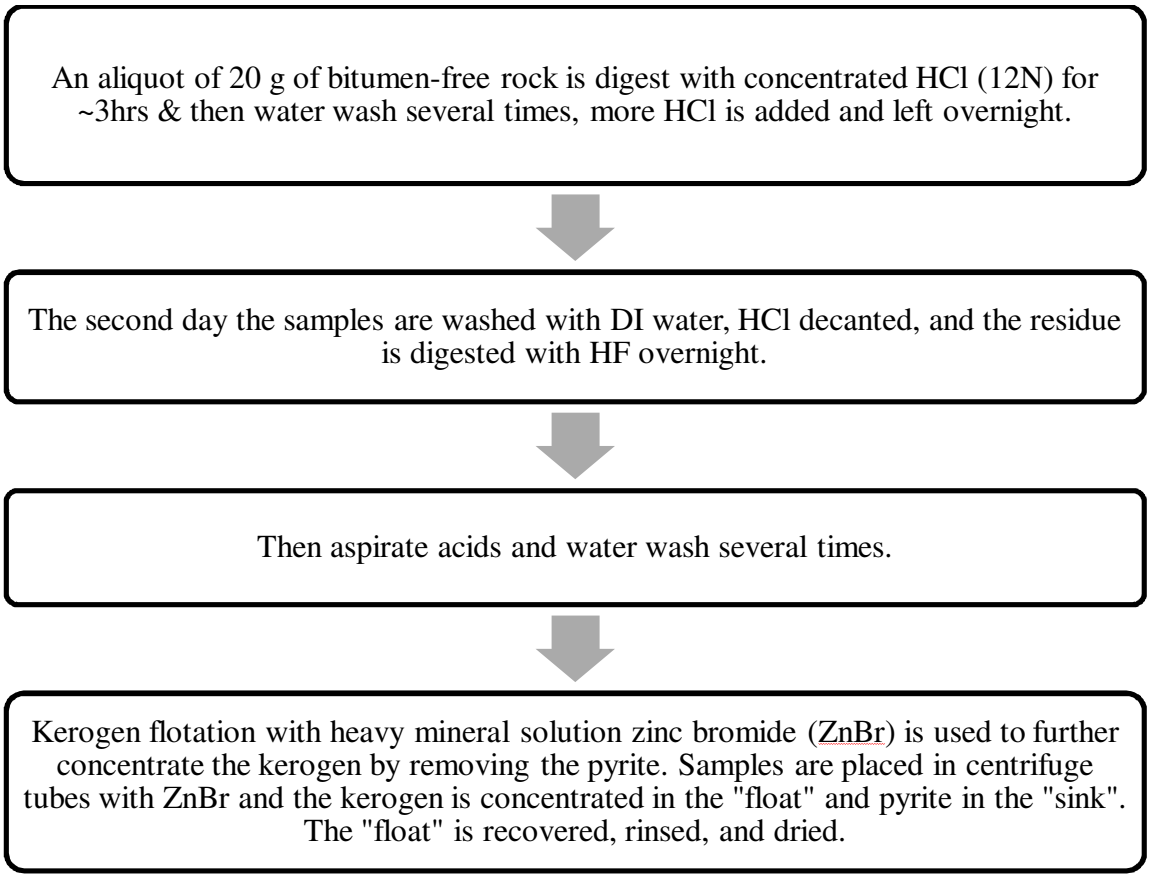

Figure 2.3.3: A flow diagram summarizing the open-conventional method #2 (OCM #2) for kerogen isolation used in this study.

Chapter 3: Sample Set

The suite of samples used in this study include specimens of four gas shales, three from the United States (the Marcellus, the Barnett, and the Haynesville) and one from Poland (Figure 3.1). The Monterey shale, while not strictly a gas shale, is included in the suite to test the effects of the isolation methods on sulfur-rich, Type II-S kerogens. The specimens include both conventional core and cuttings mostly from wells drilled with water-based drilling fluids. The Barnett shale specimens include an outcrop sample ($Barnett_{imm}$) from a quarry in San Saba County and a matured ($Barnett_{mat}$) core sample from the Fort Worth Basin. The outcrop Barnett sample was selected especially to represent the immature counterpart of the highly mature Barnett core sample. A brief description of the specimens is given below.

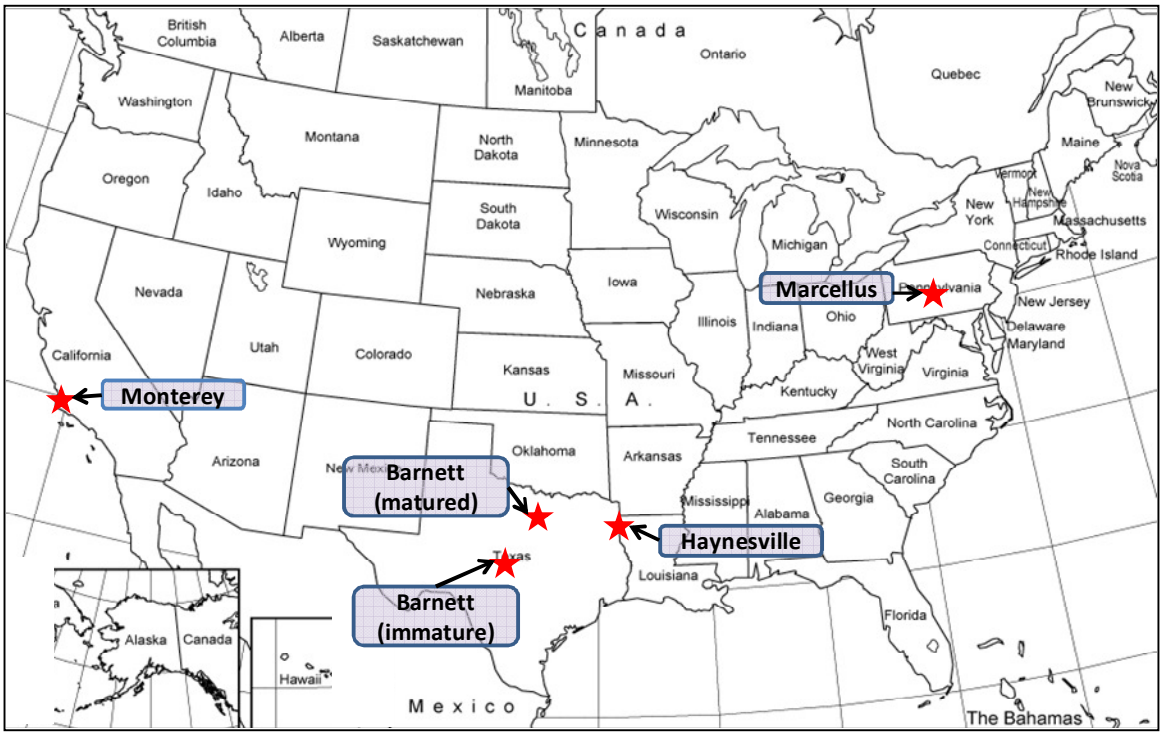

Figure 3.1: Location of the Barnett (mature and immature), the Haynesville, the Marcellus, the Monterey shales, and undisclosed Poland shale. Source: United-States-Map.com, Enchantedlearning.com/Europe/Poland.

Gas Shales in the USA							
Gas-Shale Basin	**Marcellus (Six States NE-Penn, NY, WV)**	**Barnett (Fort Worth Basin)**	**Fayetteville (Arkoma Basin)**	**Haynesville/Bossier (N. LA Salt Basin)**	**Woodford (S. Central Oklahoma)**	**Antrim (Michigan basin)**	**New Albany (Illinois Basin)**
Age	M. Devonian	Mississippian	Mississippian	U. Jurassic	Devonian	U. Devonian	Devon. - Miss.
Basin Area (sq mi)	95,000	5,000	9,000	9,000	11,000	12,000	43,500
Net Thickness (ft)	50 - 200	100 - 600	20 - 200	200 - 300	120 - 220	70 - 120	50 - 100
Original Gas-In-Place (tcf)	1,500	327	52	717	23	76	160
Gas Content (scf/ton)	60 - 100	300 - 350	60 - 220	100 - 330	200 - 300	40 - 100	40 - 80
Total Organic Carbon (wt%)	3 - 12	4.5	4 - 9.8	0.5 - 4	1 - 14	1 - 20	1 - 25
Total Porosity (%)	10	4 - 5	2 - 8	8 - 9	3 - 9	9	10 - 14
Depth (ft)	4,000 - 8,500	6,500 - 8,500	1,000 - 7,000	10,500 - 13,500	6,000 - 11,000	600 - 2,200	500 - 2,000
Est. Technically Recoverable Resources (tcf)	262	44	41.6	251	11.4	20	19.2

Table 3.1: Summary table for major gas shales in the United States. Highlighted in blue are the gas shales that are a part of this study. Modified from NETL (2009).

3.1 Barnett Shale

The Barnett Shale is located in the Fort Worth Basin near Fort Worth, Texas. This Mississippian siliceous shale has generated both low-sulfur oil and natural gas. The hydrocarbons from the Barnett Shale were generated from a marine Type II kerogen that is mainly composed of amorphous organic matter and has yielded incredible amounts of natural gas (Hill et al., 2007). The Barnett was deposited in a marginal deep water basin in the southern margin of the Laurussian platform (Ruppel and Kane, 2009). The Barnett has a total porosity between 4 to 5 % (see Table 3.1). Total porosity is the total pore volume per unit volume of rock.

The main Barnett shale sample used in this study is a thermally immature sample from an outcrop in a quarry in San Saba County with a TOC content of 10.7%, hydrogen index (HI) of 371 mg HC/g TOC and a total hydrocarbon generation potential (THGP) of 40.5 mg HC/g rock. A thermally matured sample of the Barnett was included for comparing the elemental and spectroscopic properties of the immature versus mature kerogen. The thermally matured Barnett has a TOC of 3.4%, a HI of 5 mg HC/g TOC, T_{max} 540˚C and a THGP of 0.3 mg HC/g rock.

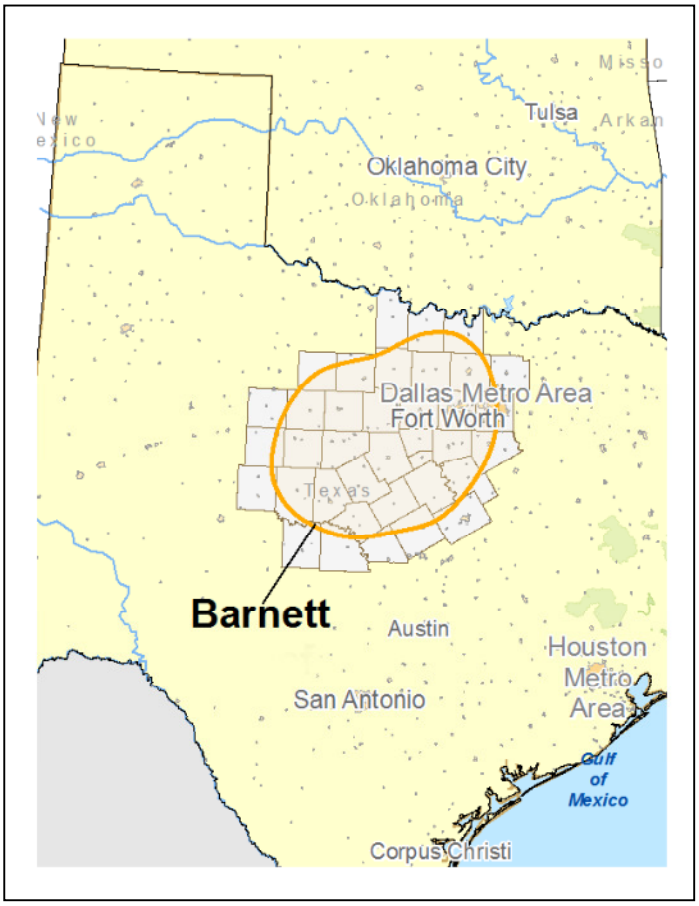

Figure 3.2: Map of Barnett shale play. Source: NETL (2009).

3.2 Marcellus Shale

The Marcellus shale in this study, donated by Rice Energy, is from Washington County, Pennsylvania with a TOC of 10.10%. The Marcellus is a black shale of Devonian age and a marine Type II kerogen with a HI of 33 mg HC/ g TOC and a THGP of 26.82 mg HC/g rock. The Marcellus was deposited in the Appalachian foreland basin at a time when subsidence was greater than sedimentation (Ettensohn, 1992). This tectonic setting led to deep-water environment with water stratification and anoxia allowing the deposition and accumulation of organic-rich sediments (Ettensohn, 1992). The Marcellus shale has a total porosity of about 10% (see Table 3.1).

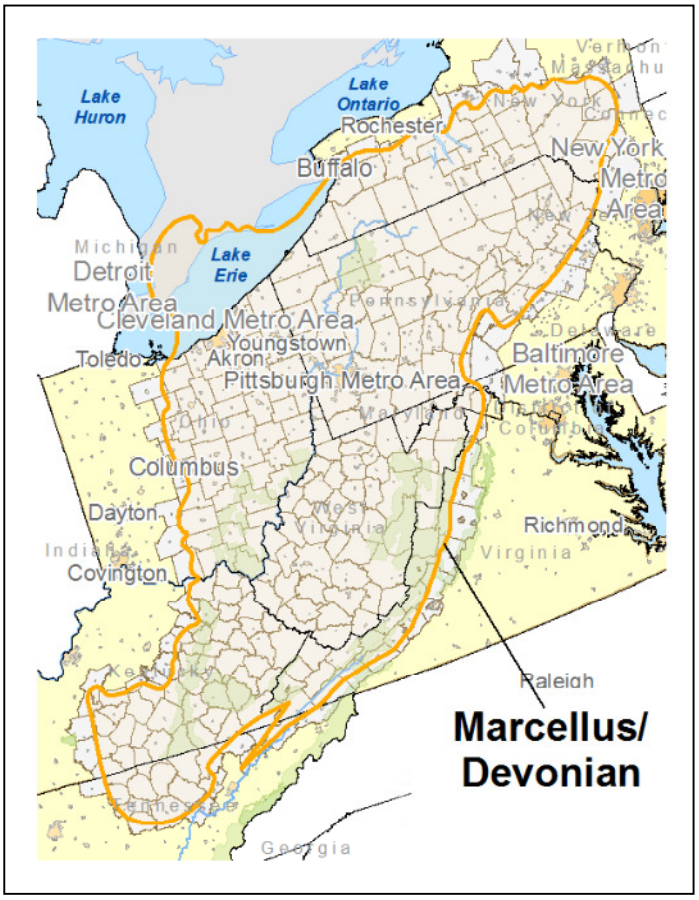

Figure 3.3: Map of Marcellus shale play. Source: NETL (2009).

3.3 Haynesville Shale

The Haynesville shale in this study is located in the northeast part of Texas and is an Upper Jurassic black shale with a TOC of 2.00%. It is a marine Type II kerogen with a HI of 18 mg HC/ g TOC and a THGP of 0.82 mg HC/ g rock. The Haynesville is a transgressive shale which was deposited below storm-wave base in mostly anaerobic conditions (Hammes and Frebourge, 2011). The Haynesville shale has a total porosity of about 8 to 9 % (see Table 3.1).

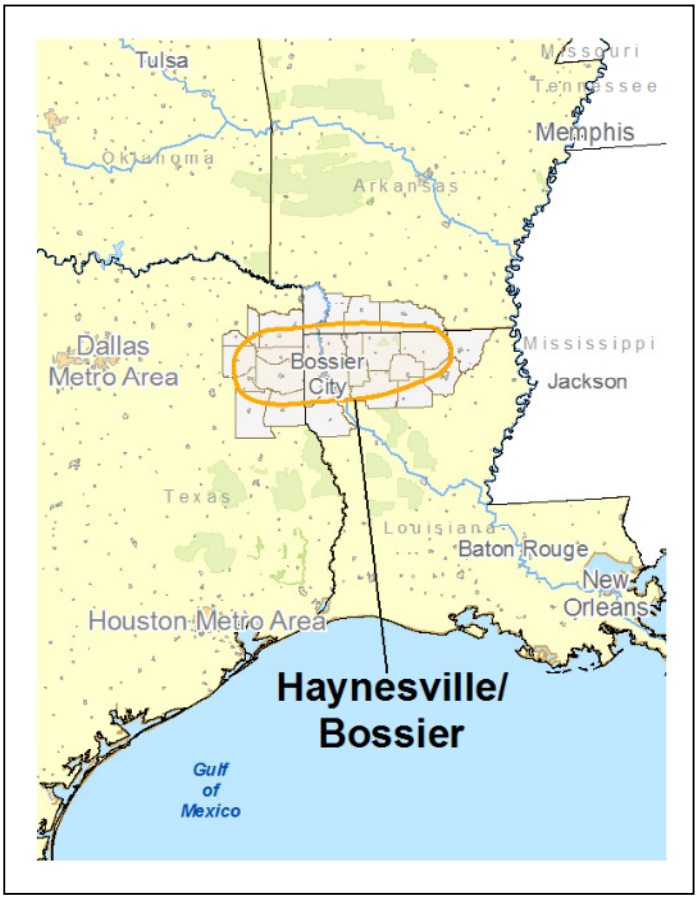

Figure 3.4: Map of Haynesville shale play. Source: NETL (2009).

3.4 Polish Shale

The Polish shale in this study is a gas shale with a TOC of 4.53%. It is a marine Type II kerogen shale with a HI of 5 mg HC/g TOC and a THGP of 0.30 mg HC/g rock. The location of the Polish shale was not disclosed.

3.5 Monterey Shale

The Monterey shale in this study is from the southern coast of California (Santa Maria Basin). It is a Miocene siliceous shale of Type II marine kerogen, high in sulfur. Orr (1986) addressed the presence of the Type II-S kerogen especially in the Santa Maria

Basin. The Monterey in this study has a TOC content of 6.08%, a HI of 656 mg HC/g TOC, and a THGP of 42.04 mg HC/g rock. This shale is predominantly an oil-prone source rock, but it also produces natural gas. The Monterey shale was deposited in a dysaerobic to anoxic marine basin, which was sediment-starved (Curiale and Odermatt, 1988). According to Baskin and Peters (1992), the Monterey deposition was also occurred under highly reducing marine conditions. The Monterey shale has a total porosity of about 11 % (EIA, 2011).

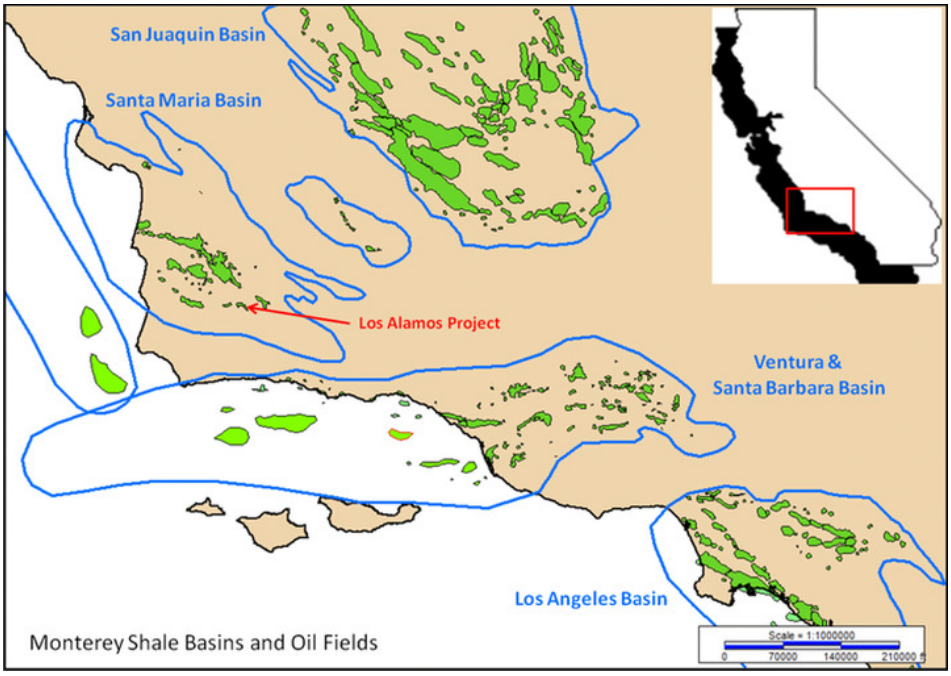

Figure 3.5: Monterey shale play. Source: Australian Oil Company. Source: Australian Oil Company (2010).

Chapter 4: Methods

Initial sample preparation began with a whole-rock which was then crushed with a hammer and jaw crusher. After the rock was crushed, the samples were placed in a grinder and ground to 60 mesh (250 microns). To ensure the data was representative, the samples were homogenized with a Rotary Micro Riffler. The Rotary Micro Riffler works by introducing the sample into a vibrating cup which dispenses the ground sample into test tubes which are rotating on a wheel. Each sample was run through the Rotary Micro Riffler 5 times to ensure homogenization. The analytical methods used in this study are described below.

4.1 Total Organic Carbon (TOC)

Total organic carbon (TOC) is used to describe the richness of the source rock and is commonly used as a screening tool to access the potential of a formation to generate hydrocarbons. To only measure the organic carbon, the inorganic carbon such as calcite and dolomite must first be removed. This is done by first acidizing the samples in HCl overnight as they sit in porous ceramic crucibles. The samples are thoroughly washed and then left to dry overnight in an oven. Once ready the samples are run through a LECO Carbon/Sulfur analyzer. The samples are combusted with ultra-high purity (UHP) oxygen forming CO_2 and SO_2 which are then measured for carbon and sulfur using an infrared detector. The carbon and sulfur values were reported in weight percent (wt%).

4.2 RockEval Pyrolysis

RockEval Pyrolysis is another screening procedure used to determine generation potential of the formation. While TOC is combustion in the presence of oxygen, pyrolysis is heating in the absence of oxygen. RockEval generates three peaks, S1, S2, and S3 and

calculates a T_{max}. T_{max} is calculated at the peak of the S2 curve and is an approximate measure of source rock maturity. S1 represents the free hydrocarbons in the pore space, S2 represents the hydrocarbons generated as a result of pyrolysis and reflects the remaining oil potential of the rock, and S3 represents the organic oxygen within the organic matter.

There are other parameters which can be calculated based on the TOC and RockEval data which are also used to characterize the formation. The total hydrocarbon generation potential (THGP) of the source rock is based on S1+S2. The kerogen transformation ratio (KTR), which is the extent of transformation of the kerogen, is based on S1/(S1+S2). The hydrogen index (HI) is based on S2/TOC. The HI is the equivalent of H/C atomic ratio and is an indicator of hydrogen enrichment. The Oxygen Index (OI) is based on S3/TOC. The OI is the equivalent of O/C atomic ratio and is a measure of oxygen enrichment.

RockEval II instrument (Figure 4.2.1) was used for the analysis and the RockPlus 1.6 software for data reduction. Samples were weighed, based on TOC wt% values, and placed in steel crucibles. Weight of the sample is based on TOC values to avoid saturation of the detector in the RockEval instrument and thus incorrect values. The steel crucibles were cleaned by heating in a furnace.

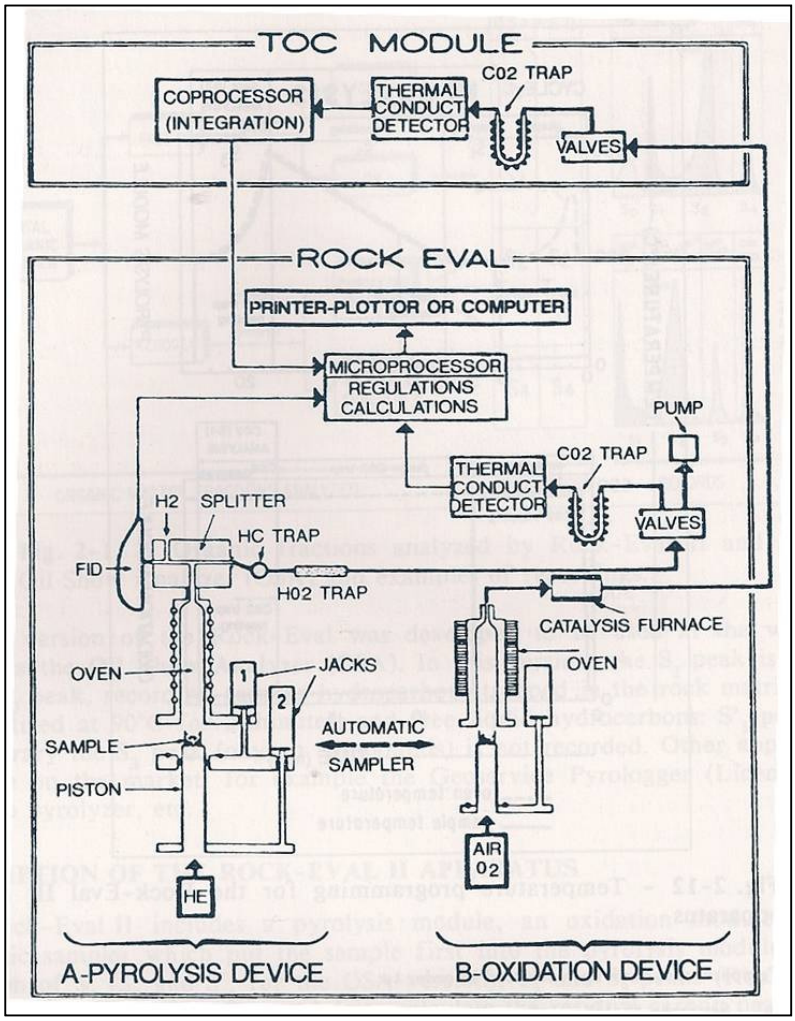

Figure 4.2: Principle of the RockEval II and the TOC module from Bordenave et al. (1993).

4.3 Bitumen Extraction

Bitumen is the second type of sedimentary organic matter, which unlike kerogen, is soluble in common organic solvents. Bitumen is removed before isolating the kerogen. Bitumen extraction was done using a soxhlet extractor for the whole-rock and a high pressure extractor for the UH CCM kerogen. The soxhlet method, which recycles the dichloromethane (DCM), was done on the whole-rocks for a period of 3-5 days. The bitumen that was captured in the flasks by the DCM was then filtered using a 45µm filter in order to remove any solids that may have fallen into the flasks. After filtering, the DCM was separated from the bitumen with a Rotovap (rotary evaporator) by using a water bath set at 40˚C to evaporate the DCM from the flask. The samples were further concentrated into 4 oz vials. The high pressure bitumen extraction method was carried out on the kerogen isolated via the UH CCM that had bitumen even after isolation. The sample was loaded into a filter assembly with a 45µm filter and nitrogen was used to flush the sample with DCM at high pressure. Results are reported in parts per million (ppm).

To quantify the bitumen recovered the following formula was used:

$$\boldsymbol{Quantified\ Bitumen\ (ppm)} = \left(\frac{\textbf{Bitumen weight (g)}}{\textbf{native rock weight (g)}}\right) \times \mathbf{100}\%$$

Equation 4.1

4.4 Whole-Rock Sulfur Forms

Sulfur forms were done on the whole-rock to determine weight percent of the different sulfur forms (sulfate sulfur, pyritic sulfur, and organic sulfur) in the samples. The sulfur forms were carried out by a selective leaching process using increasingly stronger acids in successive steps. First, total sulfur was determined on a LECO Carbon/Sulfur analyzer. A weighed sample is combusted in the presence of oxygen to form SO_2, which is swept into an infrared detector for measurement and determination of total sulfur. Next, sulfate sulfur is determined as the portion of sulfur that is soluble in hot 3N HCl. A weighed portion of the sample is placed in a porous crucible and leached with the non-oxidizing acid bath overnight, cleaned with DI water, and once dry, run on the LECO for sulfur determination. The weight percent value that results is subtracted from the total sulfur to get the sulfate sulfur wt%. Next, a weighed portion of the sample, which has already been treated with the 3N HCl is then leached in a hot 3N HNO_3 bath for one hour, cleaned with DI water, and once dry, run on the LECO for sulfur determination. The sulfur wt% value that results is the organic sulfur wt% of the rock. The organic (residual) sulfur is the portion of sulfur that is neither soluble in HCl or in HNO_3. The pyritic sulfur is determined as the portion of sulfur that is not soluble in HCl, but soluble in HNO_3. In practice, pyritic sulfur is determined by calculation of the difference between HCl insoluble sulfur and HNO_3 insoluble sulfur. The assumption is that pyritic sulfur requires oxidation and, therefore, is not HCl soluble. Equation 4.2 shows the work flow for estimating the sulfur forms weight percentages.

$$\textbf{Total S (wt\%)} - \textbf{HCl Residue S (wt\%)} = \textbf{Sulfate S (wt\%)}$$

$$\textbf{HCl/HNO}_3\textbf{ Residue S (wt\%)} = \textbf{Organic S (wt\%)}$$

$$\textbf{Total S (wt\%)} - (\textbf{HCl/HNO}_3\textbf{ Residue S (wt\%)} + \textbf{Sulfate S (wt\%)}) = \textbf{Pyritic S (wt\%)}$$

Equation 4.2

4.5 X-Ray Diffraction (XRD)

X-ray diffraction (XRD), a non-destructive analysis, was conducted on an X'PERT PRO PANalytical X-ray Diffractometer. The basic premise of XRD is to place a sample between a source of X-rays with known wavelengths and an X-ray detector (Breeden and Shipman, 2004). As the X-ray tube and detector rotate around the sample the diffracted rays are record. Each mineral has a unique crystal lattice where the atoms are arranged in repeating planes and so based on the spacing between the planes is the angle at which the X-ray is reflected (Breeden and Shipman, 2004). Using Bragg's Law ($\lambda = 2d (\sin\theta)$), the "d" spacing (atomic spacing) of the sample is used to find the diffraction angle 2θ. The recorded intensity versus the angle of the diffracted ray is plotted allowing for determination of the crystalline solids (mineralogy).

In this study, the samples were placed on a zero background holder and standard XRD procedures were used to obtain the diffraction spectrum. Phase identification was accomplished by comparing the peaks from the samples against the large dataset provided by the International Center for Diffraction Data (ICDD). To confirm the

presence of specific minerals, the 2θ and d-spacing of the peaks were also searched in the American Mineralogist Crystal Structure Database online.

X-ray diffraction was carried out on all whole-rocks to determine starting mineralogy, pyrite content, and to determine the best protocol to use for kerogen isolation. X-ray diffraction was also used as a product-purity assessment to determine how efficient the three kerogen isolation methods were in removal of inorganics.

4.6 Ash Content

Ash content was also used as a product-purity assessment indicator to compare the efficiency of the three isolation methods in the removal of inorganic material. The ash represents the inorganic mineral components that are still present in the kerogen after isolation. Ash content is determined by combusting a small aliquot of the kerogen in a furnace overnight at ~800˚C. The difference in the weight of the empty crucible before heating and the crucible after heating with the sample inside is calculated and ash content found.

4.7 Kerogen Recovery Efficiency

Quantitative mass balance calculations for kerogen recovery efficiency were done using Equations 4.3-4.6. The first step is to calculate an initial kerogen content of the sample based on the TOC wt% of the whole-rock and the normalized elemental carbon wt% of the kerogen. The TOC represents only a fraction of the organic matter in the rock since the organic matter is also composed of other elements like nitrogen, sulfur, hydrogen, and oxygen. The initial kerogen content wt% is found by calculating how much of the organic matter the carbon truly represents (Equation 4.3). The next step is to

translate the initial kerogen content wt% into initial kerogen in grams, which is done by using the initial rock weight in grams that one starts with before isolation of the kerogen (Equation 4.4). The next step is to calculate the "true" weight of the kerogen recovered after kerogen isolation since the weight of the kerogen residue includes the organic component as well as the inorganics still present (i.e. the ash content). This is done by subtracting the weight of the ash from the kerogen residue (Equation 4.5). Once you have the initial kerogen content in grams and the "true" weight of kerogen recovered then the recovery efficiency can be calculated as shown by Equation 4.6.

$$\textbf{Initial Kerogen Content (wt\%)} = \frac{\textbf{TOC (wt\%)}}{\textbf{Kerogen Elemental Carbon Fraction (wt\%)}}$$

Equation 4.3

$$\textbf{Initial Kerogen (g)} = \textbf{Rock Wt (g)} \times \textbf{InitialKerogen Content (wt\%)}$$

Equation 4.4

$$\begin{aligned}\textbf{True Recovered Kerogen Wt (g)} &= \textbf{Kerogen Recovered Residue wt (g)} \\ &- (\textbf{Ash wt \%} \times \textbf{Kerogen Recovered Residue wt (g)})\end{aligned}$$

Equation 4.5

$$\textbf{Kerogen Recovery Efficiency (\%)} = \frac{\textbf{True Recovered Kerogen Wt (g)}}{\textbf{Initial Kerogen (g)}} \times \textbf{100}$$

Equation 4.6

4.8 Visual Kerogen Assessment by Microscopy

Maceral rock microscopy is a useful tool in determining organic matter composition, origin, as well as for thermal maturity estimates of the rock. Macerals in coals are like the minerals in a rock. A maceral represents the most basic optical microscopic part of coal and can be recognized by its optical properties: morphology, reflectance, and fluorescence (Hutton et al., 1994). According to Vandenbroucke and Largeau (2007), the first study to draw a connection between kerogen and coal and their precursors was Down and Himus (1941) followed by Forsman and Hunt (1958). These two early studies found that kerogen compositional differences were due to changes in plant sources (Vandenbroucke and Largeau, 2007). Subsequent to the studies on kerogen and coal macerals, Durand and Espitalie (1973) proposed the classification of source rock kerogen into three types along with evolution paths for each one based on maturation (Vandenbroucke and Largeau, 2007). Tissot et al. (1974) recognized that the evolution paths for the three types of kerogen resembled those of carbonization paths of coal macerals. For Type I kerogen it resembled Alginite, for Type II kerogen it resembled Exinite, and for Type III kerogen it resembled Vitrinite. The kerogen types were plotted on a modified van Krevelen diagram (Tissot et al., 1974).

The organic microscopy allowed for the assessment of the impact the different isolation methods on the physical structure of the kerogen and whether they were destructive or not. Vitrinite reflectivity (R_o) was carried out on a Zeiss Photoscope equipped with a reflectance photometry capability. Vitrinite is sourced from higher plant material and is only found in post-Ordovician section of the stratigraphic record (Ibrahimov and Bissada, 2010). Thermal alteration index (TAI) was determined with a

Leitz Orthoplan Microscope equipped with transmitted and fluorescence lights. In this study the whole-rock thin section slides, the kerogen vitrinite plugs, and the disperse kerogen slides were prepared by National Petrographic Service, Inc. (see Appendix) and Weatherford Laboratories. The R_o is based on the reflectance of vitrinite particles in an oil immersion fluid. The TAI is based on the color of spores in transmitted light.

4.9 Stable Isotope Analysis

One aspect of this study is to assess if there is any isotope fractionation as a result of the kerogen isolation method used. Isotope fractionation is defined as the separation of isotopes among two substances or phases of the same material with dissimilar isotopes ratios (Hoefs, 1997). Stable carbon and sulfur isotopes were used to address isotope fractionation and are described below.

4.9.1 Stable Carbon Isotope Analysis ($\delta^{13}C$)

The two stable isotopes of carbon are ^{13}C and ^{12}C, which are commonly used to correlate hydrocarbons to their source rocks. The correlation is based on the isotopic composition determined by converting the carbon into CO_2 which is then analyzed by a mass spectrometer and delta (δ) values are reported in per mil (‰). The ratio of the isotopically heavier $^{13}CO_2$ versus that of the isotopically lighter $^{12}CO_2$ is compared to a standard that determines whether the sample is isotopically light or heavy (Equation 4.7).

$$\boldsymbol{\delta^{13}C\ ‰} = \left(\frac{(^{13}C/^{12}C)_{sample} - (^{13}C/^{12}C)_{reference}}{(^{13}C/^{12}C)_{reference}}\right) \times 1000$$

Equation 4.7

Carbon isotope analysis was done at UH. The first step was to weigh 1-2 mg of the organic matter which was placed in a Pyrex tube with some fired cupric oxide to aid in the combustion. The Pyrex tubes were purified beforehand by heating in an oven for several hours at 800˚C. The cupric oxide was purified by heating in an oven for ~1 hour at 900˚C. The tubes were evacuated, to remove any atmosphere, by using a vacuum line and then sealed with a torch while the tube sat in a liquid nitrogen bath. Once sealed, the tubes were placed in a preheated oven at ~550˚C for ~10 hours to convert the organic matter into CO_2. The following day the tubes were placed in a cracking device on the vacuum line. A moisture trap was prepared by having a tube, through which the CO_2 must travel, immersed in a slurry of dry ice and iso-propanol. At the other end of the vacuum line the capture tube is placed in liquid nitrogen. The CO_2 is isolated and trapped under vacuum. The stable carbon isotopic composition of the kerogen isolated via the three methods was carried out on a Finnigan Mat Delta S stable-isotope mass spectrometer. Isodat 5.2 software was used for data reduction.

4.9.2 Stable Sulfur Isotope Analysis ($\delta^{34}S$)

Sulfur isotope analysis was contracted out to Isotech who did the analysis using a "continuous flow" elemental analyzer-isotope ratio mass spectrometry (EA-IRMS) technique. The solid kerogen samples were introduced into a Vario Elementar combustion furnace where they were combusted in the presence of excess oxygen and the resulting gases were separated, including the sulfur dioxide (SO_2), by a packed column gas chromatograph. After the gases were split they were sent to a Thermo ConFlo II interface by a helium carrier gas. The purpose of the interface is to make sure there is a stable gas glow into the mass spectrometer since the quality of the data is dependent on

the gas flow from the sample versus that of the reference gas in the mass spectrometer. From the interface, the sample gas was sent to a Thermo Delta V Plus where its isotope ratio was measured versus a reference gas as shown in Equation 4.8 below and reported in parts per mil.

$$\delta^{34}S\ ‰ = \left(\frac{(^{34}S/^{32}S)_{sample} - (^{34}S/^{32}S)_{reference}}{(^{34}S/^{32}S)_{reference}}\right) \times 1000$$

Equation 4.8

4.10 Elemental Analysis

Elemental analysis was contracted to QTI Intertek and was done to determine kerogen type and the origin and evolution of the sedimentary organic matter. The results were plotted as the H/C and O/C atomic ratios on a van Krevelen plot. Elemental analysis was also useful in assessing the effects of the different isolation methods on the composition of the kerogen.

Elemental analysis was conducted on a PE 2400 CHN Analyzer for carbon, hydrogen, nitrogen total and ratios fitted with an oxygen accessory kit. For carbon, hydrogen, and nitrogen approximately 2 mg of the sample were weighed into a tin sample boat and placed in the analyzer. Samples are combusted in an UHP oxygen environment to convert the sample to simple gases like CO_2, H_2O, and N_2. The resulting gases are then separated and measured as a function of thermal conductivity. Before analyzing for carbon, hydrogen, and nitrogen, the standard must check to within 0.1% of its theoretical value. The instrument has a detection limit 0.1%. For sulfur analysis the standard must check to within 0.4% of its theoretical value (qtionline.com).

Oxygen was determined using pyrolysis. Pyrolysis converts the oxygen to carbon monoxide which is then separated from the other pyrolozates and measured as a function of thermal conductivity. High levels of fluorine or inorganics can cause interference in the results because these inorganics attack the catalyst used and may yield incorrect results (qtionline.com). For oxygen the standard used must check within 0.3% of its theoretical value.

The sulfur was determined using colormetric titration where the sample is placed into an aluminum sample boat and wrapped in an ashless filter paper. The sample is then combusted in an oxygen combustion flask containing hydrogen peroxide and set aside for 20 minutes which allows for sulfate to form. The sulfate, in the presence of DMSA (dimercaptosuccinic acid) III, is the titrated with barium perchlorate to a distinct blue end point. The analysis for sulfur has a detection limit of 0.1%. Interferences in the sulfur values can be caused by the presence of fluorides, phosphorous, and iodides. Before analyzing for sulfur the standard must check to within 0.4% of its theoretical value (qtionline.com).

Elemental analysis data is also critical for kerogen structure determination as was shown by LaPlante (1974). The elemental analysis data helps to constrain the number of possible structures for the kerogen.

4.11 Pyrolysis-GC

Pyrolysis-gas chromatography (Py-GC) is a thermal degradation technique that can be used to study kerogen structure and composition (Van De Meent et al., 1980;

Horsfield, 1989). For this study, Py-GC pyrolysates were used to study the effects the three isolation methods had on the molecular properties of the kerogens.

Weatherford Laboratories conducted the Py-GC analysis using a 6890 Agilent GC with a specially designed inlet system. Between 1-25 mg of sample were placed in a quartz GC liner which was then inserted into the inlet. The inlet temperature was programmed from 320˚C-620˚C at 65˚C per minute. Then the samples were held at 620˚C for 1 minute. A split portion of the volatile hydrocarbons was trapped onto the front of the analytical column using a liquid nitrogen trap. The GC temperature was then programmed from 0˚C, held for 8 minutes, then ramped up to 320˚C at 5˚C per minute intervals, then held at 320˚C for 20 minutes.

This technique yields data in the form of a gas chromatogram with amplitude on the y-axis and retention time on the x-axis. The displayed peaks represent components immerging out of the column in a sequence mainly based on their boiling points so the ones with the lowest boiling points come out first. The amount of each compound is determined based on the area under the peak for the compounds as well as the height of the peaks.

4.12 Solid-state ^{13}C Nuclear Magnetic Resonance (NMR)

Nuclear magnetic resonance (NMR) is a quantitative technique for detecting specific chemical elements by measuring the energy absorbed from the radio-frequency coil around the sample (Shoolery, 1972). This technique takes advantage of the magnetic properties of nuclei to provide information on the molecular structure of the sample (Lambert and Mazzola, 2004).

When the atomic number and atomic mass are odd values, the nucleus has magnetic properties, meaning it spins (Lambert and Mazzola, 2004). For ^{1}H and ^{13}C the nuclei have a spin of 1/2 meaning they only spin in one of two directions (Lambert and Mazzola, 2004). When a sample is placed under the influence of a strong magnet, the nuclei go through magnetic polarization where the nuclei align either in the +1/2 or -1/2 direction (Shoolery, 1972; Lambert and Mazzola, 2004). A radio frequency is applied which causes energy to be either absorbed or emitted between this second field and the nucleus called resonance as the nuclei change between +1/2 and -1/2 (Lambert and Mazzola, 2004; Jacobsen, 2007). The absorption is detected creating a plot of frequency vs. absorption called an NMR spectrum (Lambert and Mazzola, 2004).

The chemical shifts seen in the spectra result from variations of the resonance frequency with shielding (Lambert and Mazzola, 2004). Shielding results from the local effect on the magnetic field by the electrons around the nucleus (Lambert and Mazzola, 2004). This property of nuclei allows for structural analysis of solids.

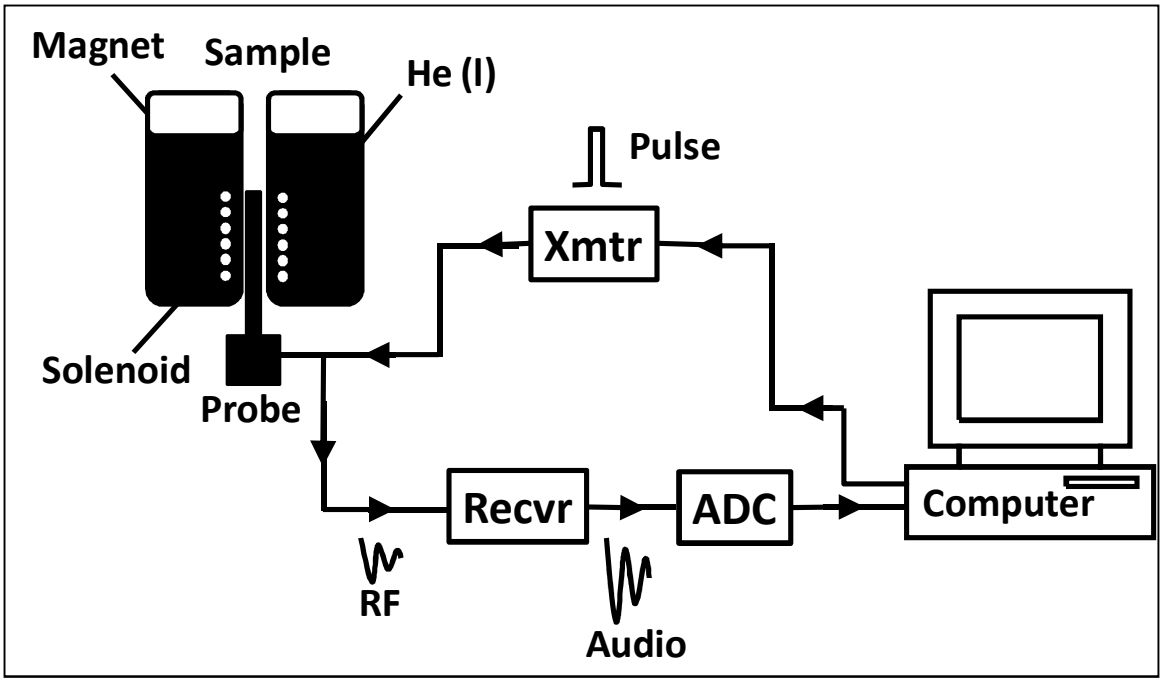

Figure 4.12: The NMR spectrometer consists of a superconducting magnet, a probe, a radio transmitter, a radio receiver, an analog-to-digital converter (ADC), and a computer. The magnet consists of a solenoid of superconducting Nb/Ti alloy wire immersed in liquid helium. A current flows around the solenoid creating a strong magnetic field. The probe is a coil of wire positioned around the sample and it transmits and receives radio frequency signals. The computer has the transmitter send a pulse of radio frequency to the probe, after which the signal from the probe is amplified, converted to audio frequency signal and sampled producing a list of numbers. The computer determines the time and intensity of the pulses from the transmitter and then receives and processes the digital information from the ADC. After performing a Fourier transform the resulting spectrum is displayed on the computer screen. Modified from Jacobsen (2007).

Solid-state ^{13}C NMR was conducted using a 200 MHz Bruker to study the spectroscopic properties of the kerogen and determine aromaticity. Aromaticity is the percentage of carbon atoms in the aromatic region versus the aliphatic region of the spectrum (Barwise et al., 1984). Aromatics are unsaturated with respect to hydrogen so they have resonating structures. Aliphatics are the opposite of aromatics and they can be saturates (single bonds, alkanes), unsaturated (double bonds, alkenes), or they can be joined by triple bonds (alkynes).

The results and interpretation for the spectroscopic analysis of the kerogen are dependent on the NMR parameters set and experiments run. In this study the ^{1}H-^{13}C

cross-polarization magic angle spinning (CPMAS) experiment was done to obtain two spectra; one was a CPMAS spectrum at 3 ms contact time and a CPMAS/dipolar dephasing spectrum at the same contact time to attenuate the CH and CH2 intensity. NMR spectra were ^{1}H decoupled in order to enhance the carbon habitat. The dipolar dephasing was used to distinguish between protonated and non-protonated aromatic carbons (Kelemen et al., 2007). The contact time was determined after testing 1 ms, 2 ms, 3 ms, and 4 ms contact times as well. The 3 ms contact time was chosen based on how well it allowed for the comparison of the spectra from different samples to one another. Direct ^{13}C pulse experiment was conducted on the highly aromatic samples to confirm that all the carbons were cross polarizing and the aromaticity was accurate. Samples were loaded onto a 4 mm rotor and Bruker Avance II console hardware and Bruker Topspin 3.0 software were used for data reduction. Chemical shifts were referenced to glycine carbonyl defined at 176.46 ppm. All the NMR data was collected at Rice University by Dr. Lawrence Alemany.

Chapter 5: Results

5.1 Total Organic Carbon (TOC) Results

The TOC for the samples ranged from as high as 10.7% for the $Barnett_{imm}$ to 2.0% for the Haynesville. For the carbon, the values have an instrumental error margin of ±0.005% and for the sulfur the instrumental error margin is ±0.007%.

Sample	TOC (wt%)
Barnett (immature)	10.70
Monterey	6.08
Marcellus	10.10
Polish Shale	4.53
Haynesville	2.00

Table 5.1.1: TOC results for the whole-rock samples given in wt%.

5.2 RockEval Pyrolysis Results

RockEval Pyrolysis was conducted on the whole-rocks as well as the bitumen-free rocks. The results are shown in Table 5.2.1. The $Barnett_{imm}$ and Monterey shales in this study showed the highest THGP and HI values indicating a greater potential for hydrocarbons. The $Barnett_{imm}$ has a HI of 371 mg HC/g TOC and a THGP of 40.48 mg HC/g rock, which reflects the sample's thermal immaturity, being an outcrop with a large S2 and very rich in organic carbon content based on the TOC. The Monterey had a HI of 656 mg HC/g TOC and a THGP of 42.04 mg HC/g rock since it is a rich oil shale with relatively high TOC. The Haynesville shale and the Polish shale had much lower THGP and HI values since they are very high-maturity shales that most likely lost a large portion of their original TOC and organic hydrogen.

The largest drop in the S1 was seen in the values for the cuttings samples of the Marcellus Shale. This was due to the fact that the mature Marcellus was obtained from the subsurface by drilling down to the Marcellus Formation using an oil-based drilling mud. The Haynesville experienced a drop in the S1 values as well for the extracted rock which indicates a slight contamination of the whole-rock caused by the drilling and recovery of the sample using an oil-based drilling mud. For the Monterey there was a drop in the S1 values for the extracted rock versus the whole-rock which is a result of the Monterey being an oil shale with high bitumen content. For the $Barnett_{imm}$ and the Polish shale there was virtually no change in the S1, S2, and S3 values before and after bitumen extraction indicating either there was no oil contamination of the whole-rock samples, or the samples were completely devoid of any indigenous bitumen at their current state of thermal maturity.

Properties of native rocks									
Sample	**TOC (wt%)**	**S1 (mg HC/ g rock)**	**S2 (mg HC/ g rock)**	**S3 (mg CO_2/ g rock)**	**THGP S1+S2 (mg HC/ g rock)**	**HI S2/TOC (mg HC/ g TOC)**	**OI S3/TOC (mg CO_2/g TOC)**	**KTR (S1/(S1+S2))**	**Tmax (°C)**
Barnett (immature)	10.70	0.78	39.70	1.07	40.48	371	10	0.02	418
Monterey	6.08	2.17	39.87	1.13	42.04	656	19	0.05	408
Marcellus	10.10	23.49	3.33	1.43	26.82	33	14	0.88	343
Polish Shale	4.53	0.09	0.21	0.12	0.30	5	3	0.30	455
Haynesville	2.00	0.47	0.35	0.07	0.82	18	4	0.57	463
Properties of bitumen extracted native rocks									
Sample	**TOC (wt%)**	**S1 (mg HC/ g rock)**	**S2 (mg HC/ g rock)**	**S3 (mg CO_2/ g rock)**	**THGP (mgHC/ grock)**	**HI (mgHC/ gTOC)**	**OI (mgCO_2/ gTOC)**	**KTR (S1/(S1+S2))**	**Tmax (°C)**
Barnett (immature)	10.30	0.30	40.85	1.30	41.15	382	12	0.007	418
Monterey	6.50	0.14	31.98	0.54	32.12	526	9	0.004	409
Marcellus	9.00	0.32	0.87	0.36	1.19	9	4	0.269	478
Polish Shale	4.60	0.09	0.12	0.07	0.21	3	2	0.429	385
Haynesville	2.00	0.09	0.17	0.26	0.26	9	13	0.346	420

Table 5.2.1: RockEval Pyrolysis results for the whole-rock (top) and the bitumen-free rocks (bottom).

5.3 Bitumen Extraction Results

The amount of bitumen extracted from the whole-rocks was quantified and is shown in Table 5.3.1. The Monterey shows significantly higher concentration shown in ppm of bitumen because of its maturity and because it is an oil shale. The Marcellus shows high ppm of bitumen as well, most likely due to the contamination from the oil-based drilling fluid.

Sample	Initial Ext. Rock Wt. (g)	Bitumen Wt. (g)	Bitumen (ppm)
Barnett (matured)	78.08	0.03	0.36
Barnett (immature)	129.63	0.57	4.43
Monterey	120.08	2.85	23.74
Marcellus	108.90	2.88	26.44
Polish Shale	251.73	0.05	0.20
Haynesville	121.06	0.09	0.70

Table 5.3.1: Quantified bitumen for whole-rock samples.

5.4 Sulfur Forms Results

Figure 5.4.1 shows the results of the sulfur forms on the whole-rock. The Marcellus shale had the highest total sulfur content followed by the Monterey, the Polish Shale, the $Barnett_{imm}$, and the Haynesville in order of decreasing sulfur wt%. The sulfur forms results are also displayed in Figure 5.4.2 as pie charts to highlight in which form the sulfur occurs for each of the samples. The Marcellus, the Polish Shale, and the Haynesville all have most of their sulfur in the form of pyritic sulfur (71-83%), whereas the $Barnett_{imm}$ and the Monterey samples contain less sulfur in the pyritic form (40%). The $Barnett_{imm}$ organic sulfur constitutes about 40% whereas only about 7% of the sulfur in the Polish shale and the Haynesville is organic and about 20% is organic for the Marcellus.

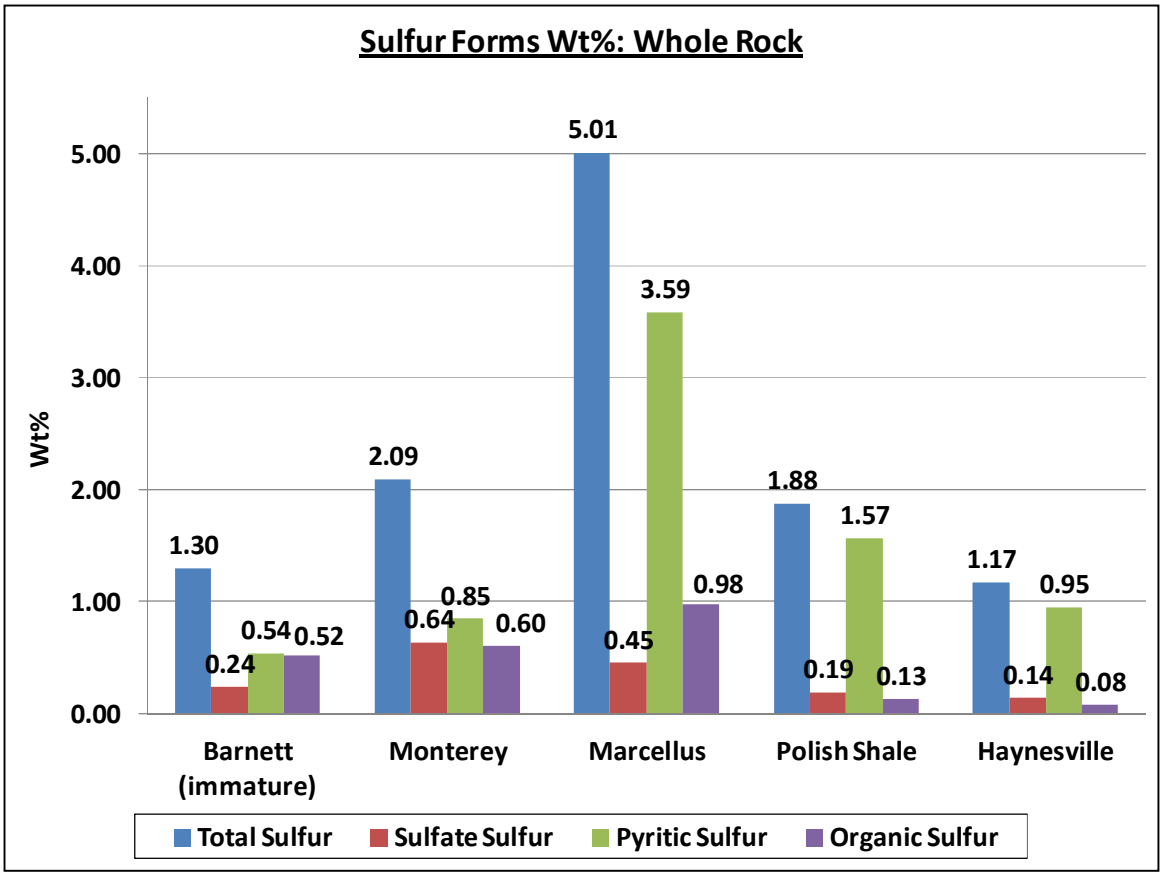

Figure 5.4.1: Bar graph showing the sulfur weight percentages (wt%) of the different sulfur forms from the whole-rock. From left to right: Total Sulfur, Sulfate Sulfur, Pyritic Sulfur, and Organic Sulfur.

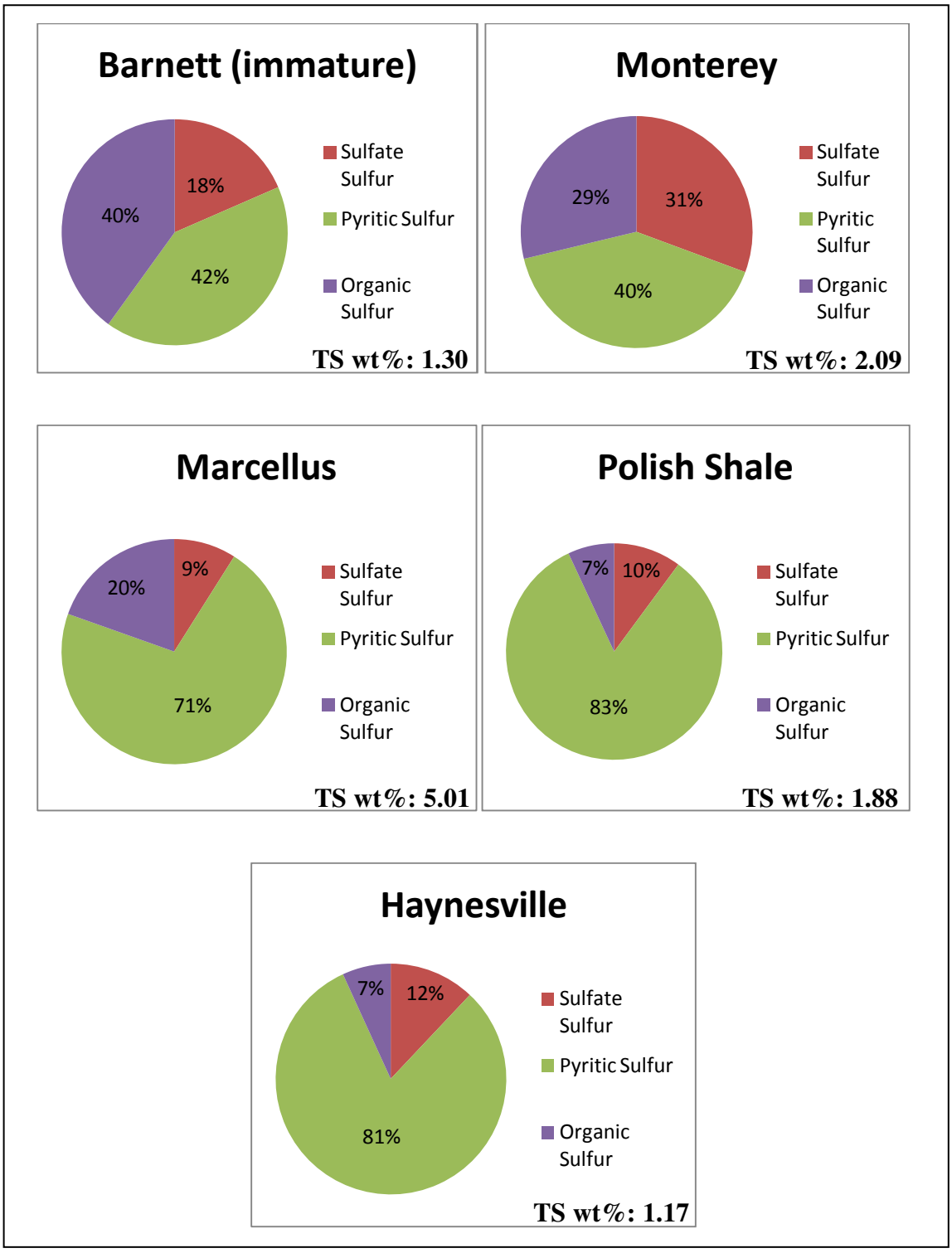

Figure 5.4.2: Pie charts showing the sulfur forms in terms of percentages of the total sulfur.

5.5 X-Ray Diffraction Results

The XRD results of the whole-rocks and the kerogens, show the presence of inorganics in the kerogen isolated via the two open-methods (OCM #1 and OCM #2). Figures 5.5.1 through 5.5.5 are the XRD patterns which summarize the results for each of the shales along with the corresponding traces for the kerogens. All of the diffraction patterns are shown with background subtracted. The whole-rock results, in black, have quartz as the main constituent for all the shales. The Haynesville shale is the only one with both quartz and calcite as the main constituents. Based on the diffraction patterns, the open-methods (OCM) kerogens show the presence of inorganic mineral phases after isolation while nearly all of the closed-method (CCM) kerogens lack these minerals. There was insufficient material to isolate the Haynesville sample via the OCM #1. In XRD, the intensity of the peaks depends on the detection limit of the instrument, so if a mineral present in the kerogen is below the detection limit it will not show in the XRD results. Yet, based on the XRD data it is clear that the CCM process yields much more pure kerogen.

Several of the OCM kerogen diffraction patterns show the presence of ralstonite, which is a neo-fluoride that can precipitate during kerogen isolation. This is a common problem when working with minerals rich in calcium and magnesium under a fluoride rich environment (i.e. HF). All of the OCM kerogens also show the presence of either quartz or pyrite, which as discussed previously is due to the inefficiency of the OCM process for kerogen isolation especially in the removal of pyrite. For the Haynesville and the Marcellus CCM kerogens (Figure 5.5.5), there appears to still be minor amounts of quartz present, but it most likely is the amorphous organic hump that was noted by

Ibrahimov and Bissada (2010) in their samples. For the same Haynesville kerogen from the CCM there is a distinct peak which is most likely a type of phyllosilicate. For several of the kerogen isolated via open-methods the presence of iron oxides was noted. According to Durand and Monin (1980), pyrite may be oxidized in water during kerogen isolation and form iron sulphates or oxides.

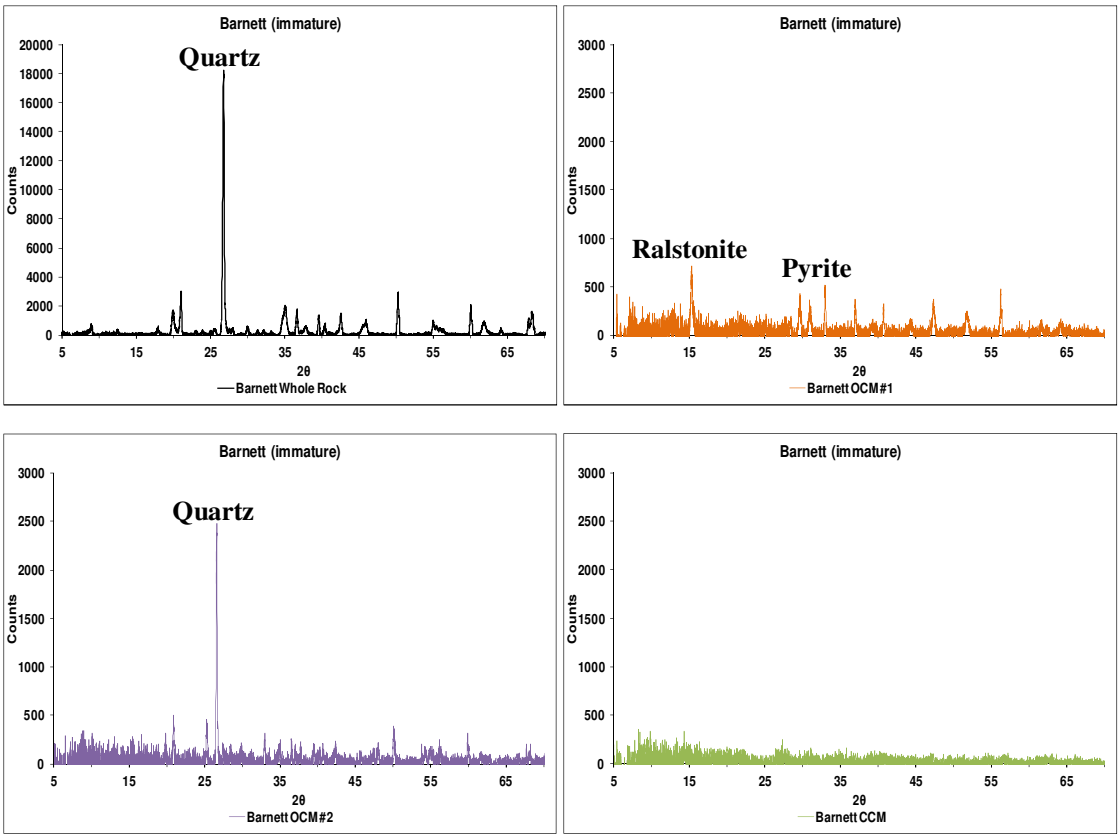

Figure 5.5.1: X-Ray diffractograms for the immature Barnett whole-rock in black, OCM #1 in purple, OCM #2 in orange, and CCM in green.

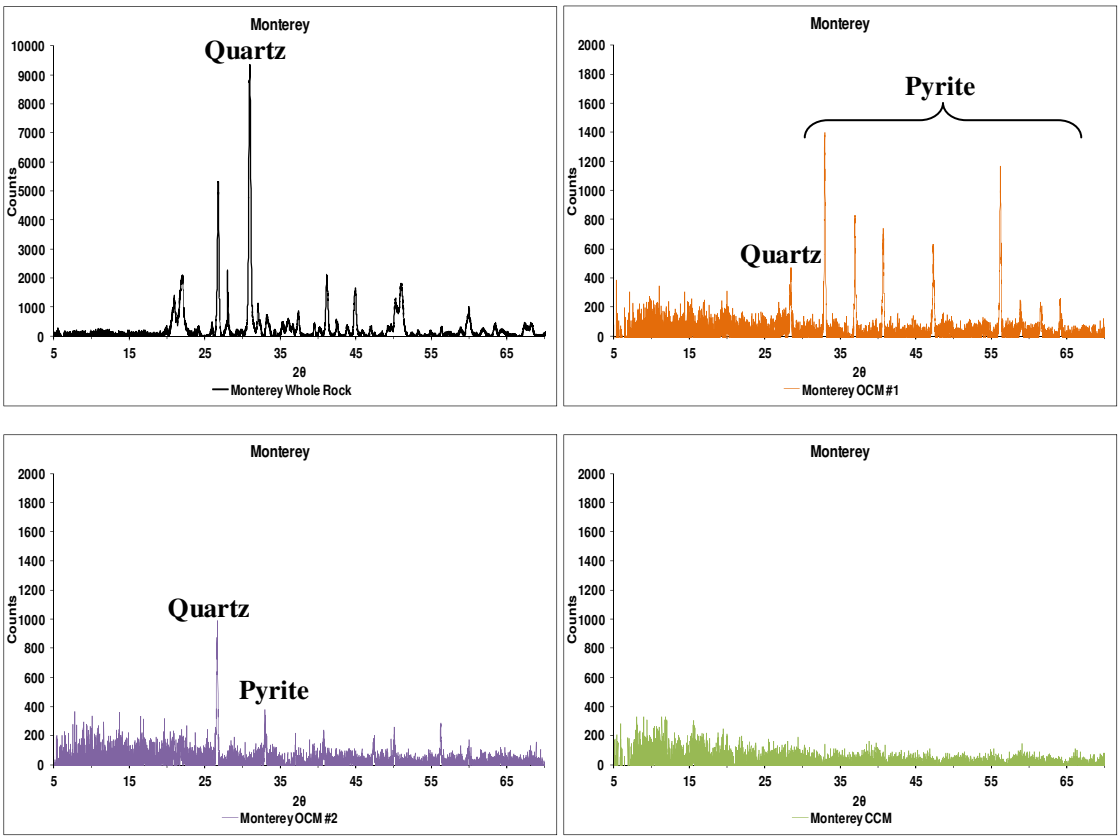

Figure 5.5.2: X-Ray diffractograms for the Monterey whole rock in black, OCM #1 in purple, OCM #2 in orange, and CCM in green.

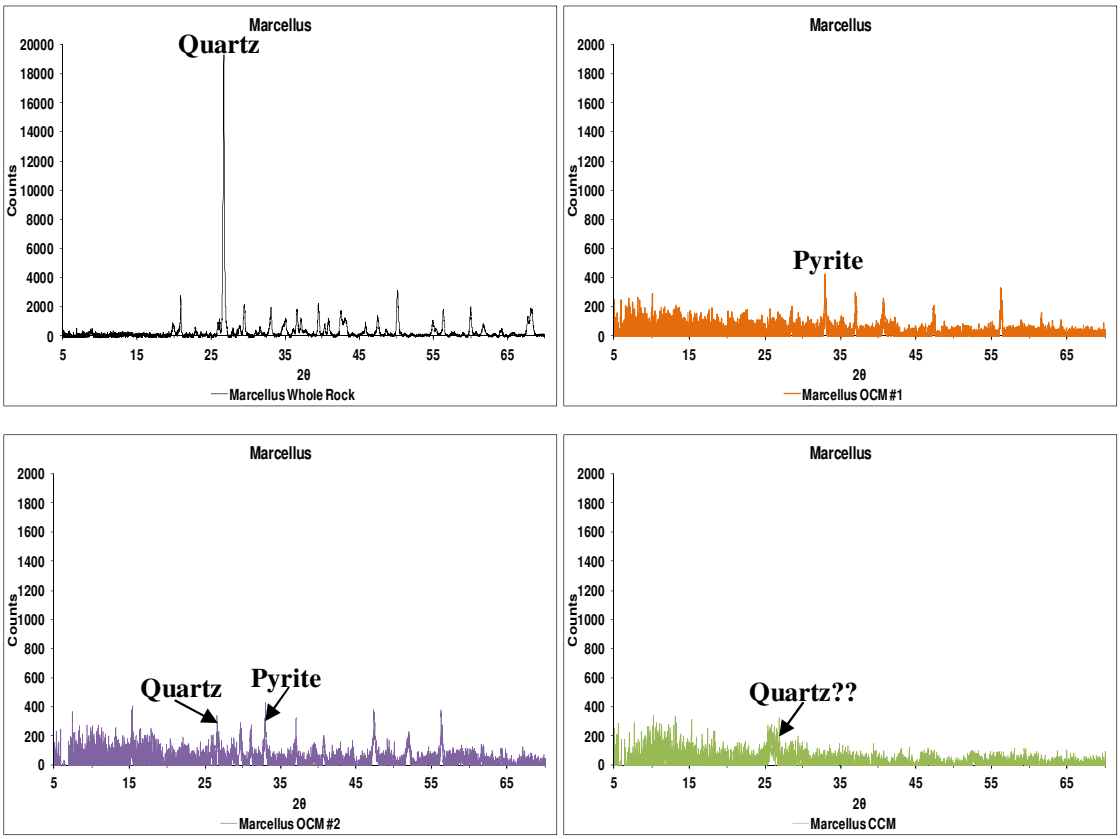

Figure 5.5.3: X-Ray diffractograms for the Marcellus whole rock in black, OCM #1 in purple, OCM #2 in orange, and CCM in green.

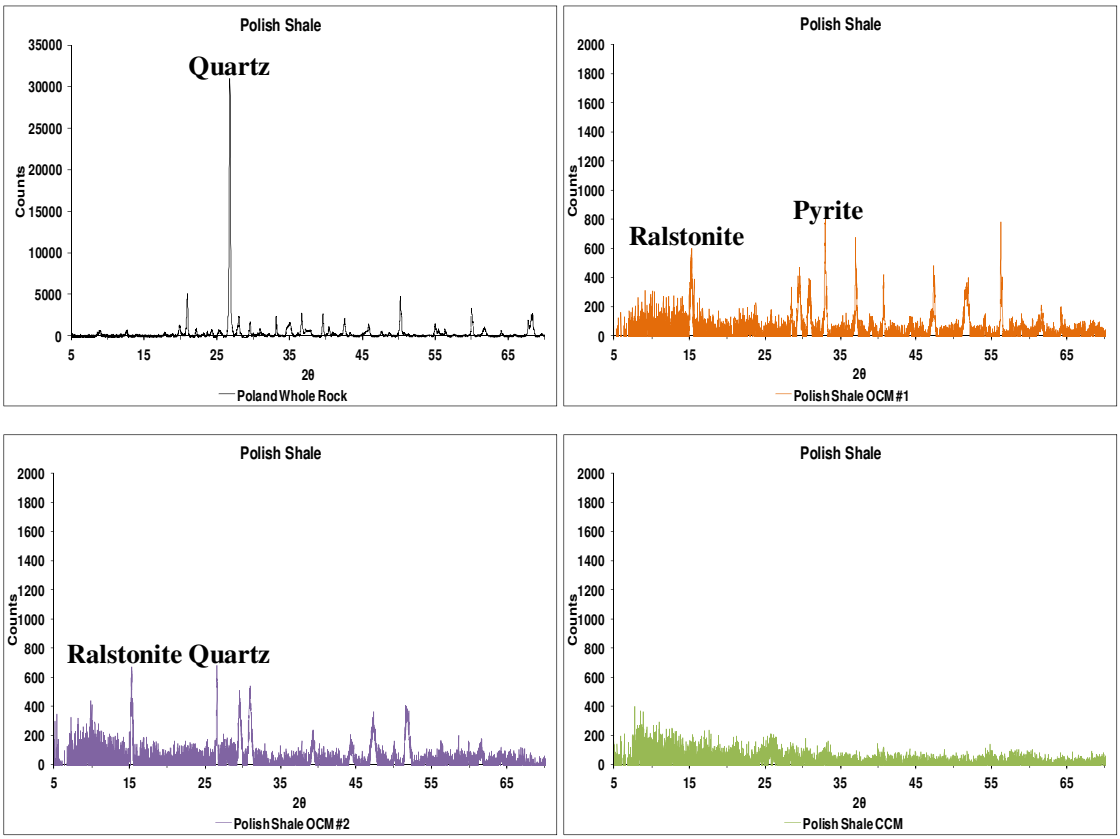

Figure 5.5.4: X-Ray diffractograms for the Polish Shale whole rock in black, OCM #1 in purple, OCM #2 in orange, and CCM in green.

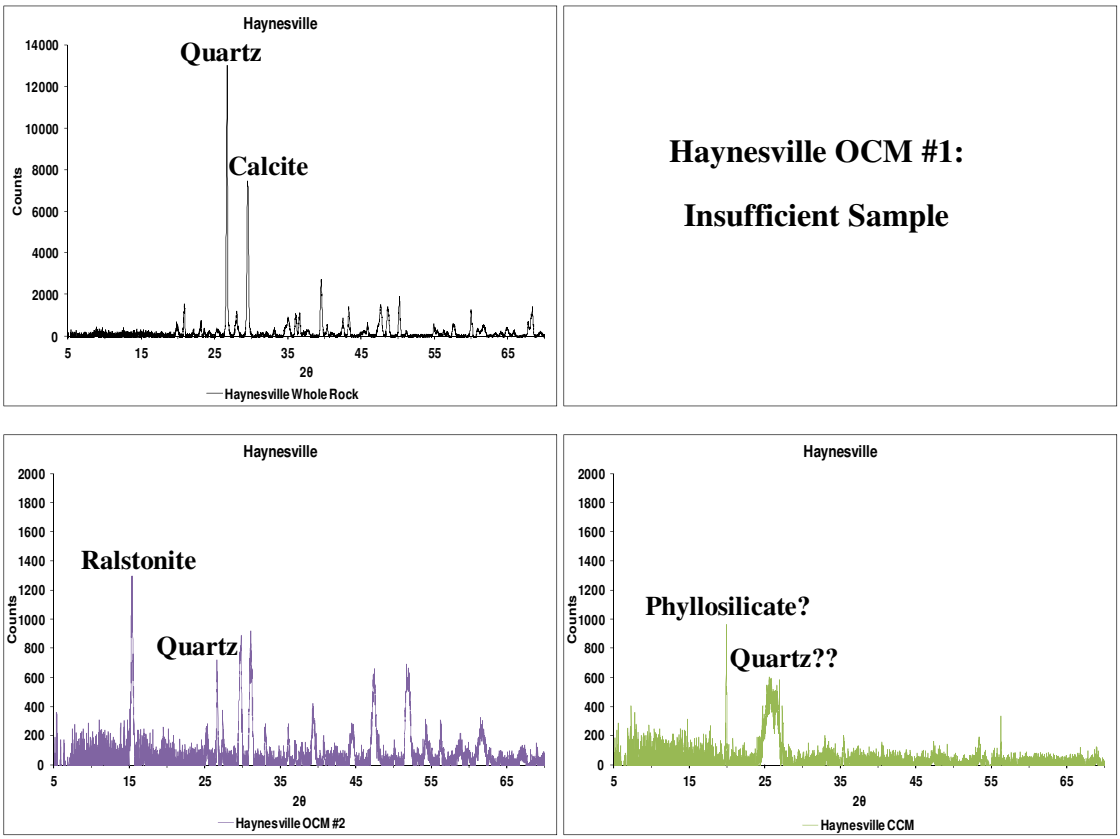

Figure 5.5.5: X-Ray diffractograms for the Haynesville whole rock in black, OCM #2 in orange, and CCM in green.

5.6 Ash Content Results

Ash content was determined for all the kerogen recovered and is displayed in Figure 5.6.1. Based on the results shown in Figure 5.6.1, the closed-method (CCM) resulted in significantly lower ash contents than those produced by either of the open-methods (OCM #1 or OCM #2). The open-methods yielded ash content as high as 34% meaning that 34% of what is thought to be organic matter is actually inorganic. In contrast, the CCM yielded ash content as low as 0.05 wt% and never higher than 4.3 wt%. There was insufficient material to isolate the Haynesville sample via the OCM #1. The ash content results support the XRD results showing the presence of significant amounts of inorganics in OCM kerogen.

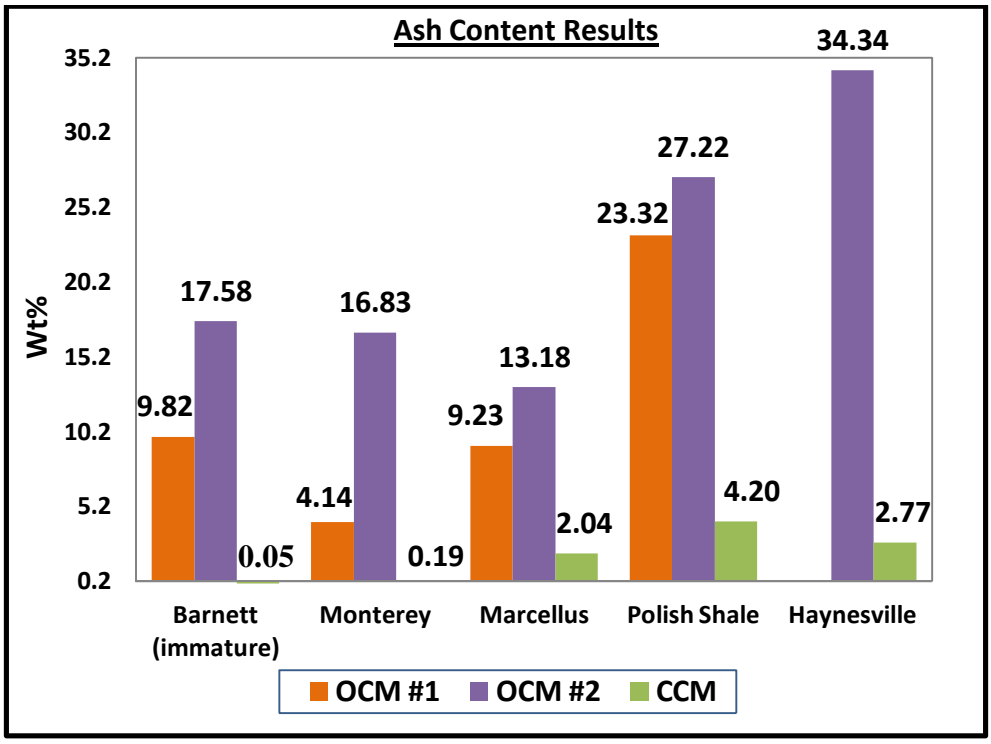

Figure 5.6.1: Bar graph comparing ash content results. The OCM kerogens have higher ash contents than the CCM.

5.7 Kerogen Recovery Efficiency Results

Kerogen recovery was determined for all the kerogen and is displayed in Figure 5.7.1. The closed-method (CCM) had recoveries ranging from 81-98%, whereas the OCM #1 recoveries ranged from 4-41% and the OCM #2 recoveries ranged from 10-75%. The CCM had significantly higher recovery efficiencies than those of either the OCM #1 or the OCM #2.

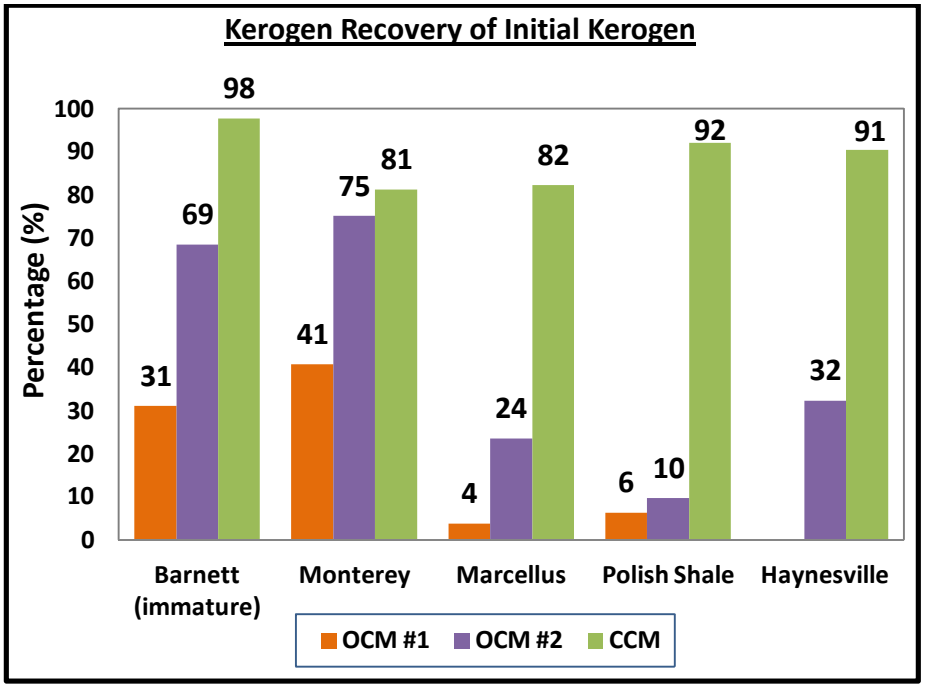

Figure 5.7.1: Bar graph comparing the results of kerogen recovery efficiency of initial kerogen of the three labs. The two OCM approaches show lower recovery compared to the CCM.

5.8 Visual Kerogen Assessment Results

5.8.1 Vitrinite Reflectance (R_o)

Vitrinite reflectance equivalent (R_o eq) is a maturity indicator based on the percent of white light reflected back from the surface of vitrinite particle identified in a polished surface of a sample of the organic matter under reflected light microscopy.

Vitrinite reflectance was acquired for all the kerogens isolated but one of the Haynesville kerogens which lacked sufficient material to prepare a vitrinite microscope mount (Table 5.8.1). Histograms were created for the vitrinite reflectance measurements to identify indigenous populations (in blue) versus non-indigenous (gray). The R_o eq values of the kerogen samples were the calculated mean from the indigenous populations (Figures 5.8.2 through 5.8.7).

Vitrinite reflectance values for the $Barnett_{imm}$ shale indicate that the Barnett at the sampling location was immature, entirely within hydrocarbon generation Zone I (see Figure 5.8.1). The $Barnett_{mat}$ R_o eq values indicate Zone V. The Monterey R_o eq values indicate Zone I/II. The R_o eq value for the Marcellus Shale indicates a Zone IV. The R_o eq value for the Polish Shale and the Haynesville Shale indicate Zone V. For the Polish Shale the maturity was based on vitrinite-like particles and graptolites that were present. Because the organic microscopist imparts a great deal of discretion and objectivity in selecting the measured population in the microscope mount, the isolation method used did not have a significant impact on the thermal maturity interpretations. One noteworthy observation is that the visual examination showed the presence of framboidal pyrite in all the samples, but the kerogen isolated via the open-methods had significantly higher pyrite contents.

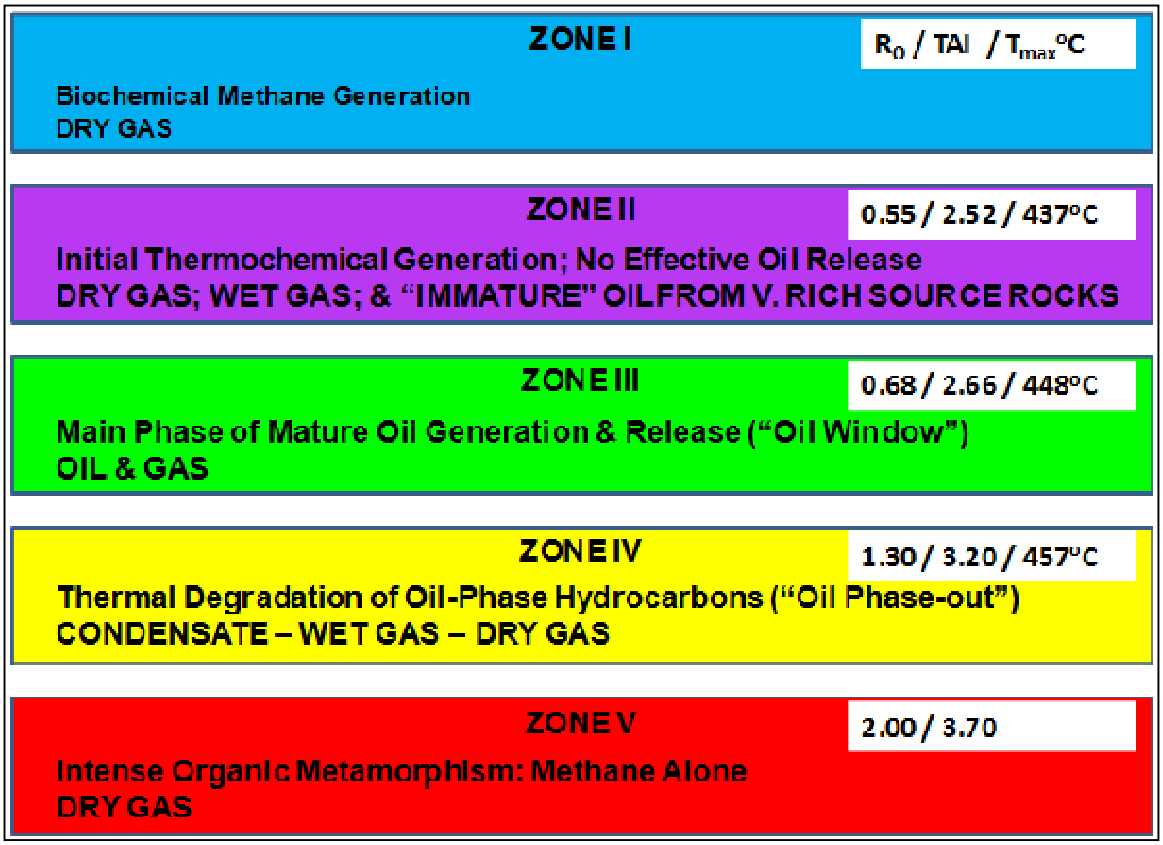

Figure 5.8.1: Zones of hydrocarbon generation, expulsion, and preservation. Modified from Bissada (1979).

	OCM #1	OCM #2	CCM
Sample	**Mean R_o eq**	**Mean R_o eq**	**Mean R_o eq**
Barnett (immature)	0.37	0.41	0.44
Barnett (matured)	Insufficient Sample	Insufficient Sample	2.57
Monterey	0.41	0.45	0.35
Marcellus	1.94	2.02	2.00
Polish Shale	2.38	2.39	2.49
Haynesville	Insufficient Sample	1.94	Not analyzed

Table 5.8.1: Summary table of the vitrinite reflectance work. Mean R_o eq is based on the representative kerogen seen in blue in the histograms shown in Figures 5.8.2-5.8.4. Note the very little variance in thermal maturity results across methods used.

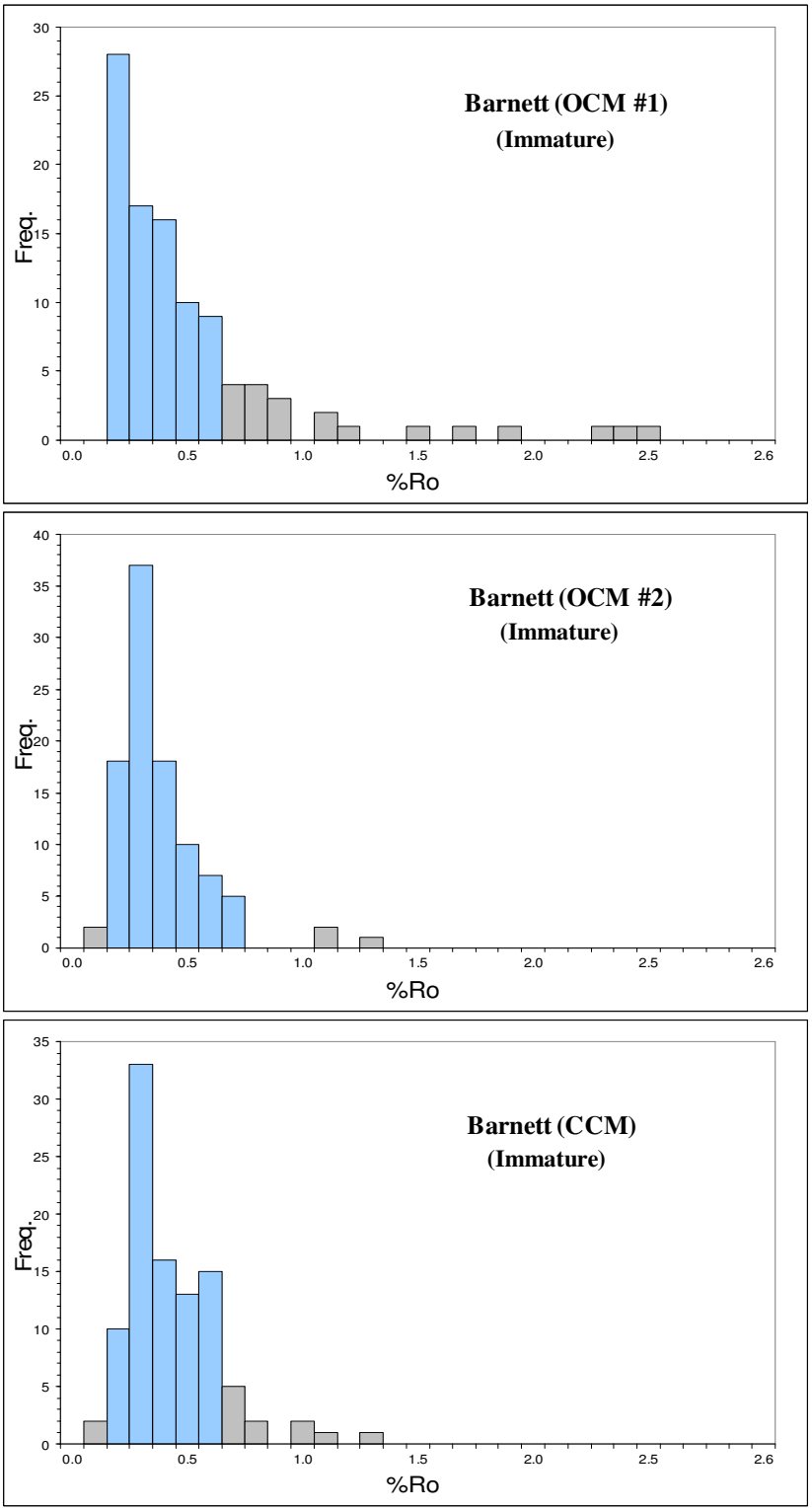

Figure 5.8.2: Histograms for the immature Barnett based on the vitrinite reflectance values of the kerogens.

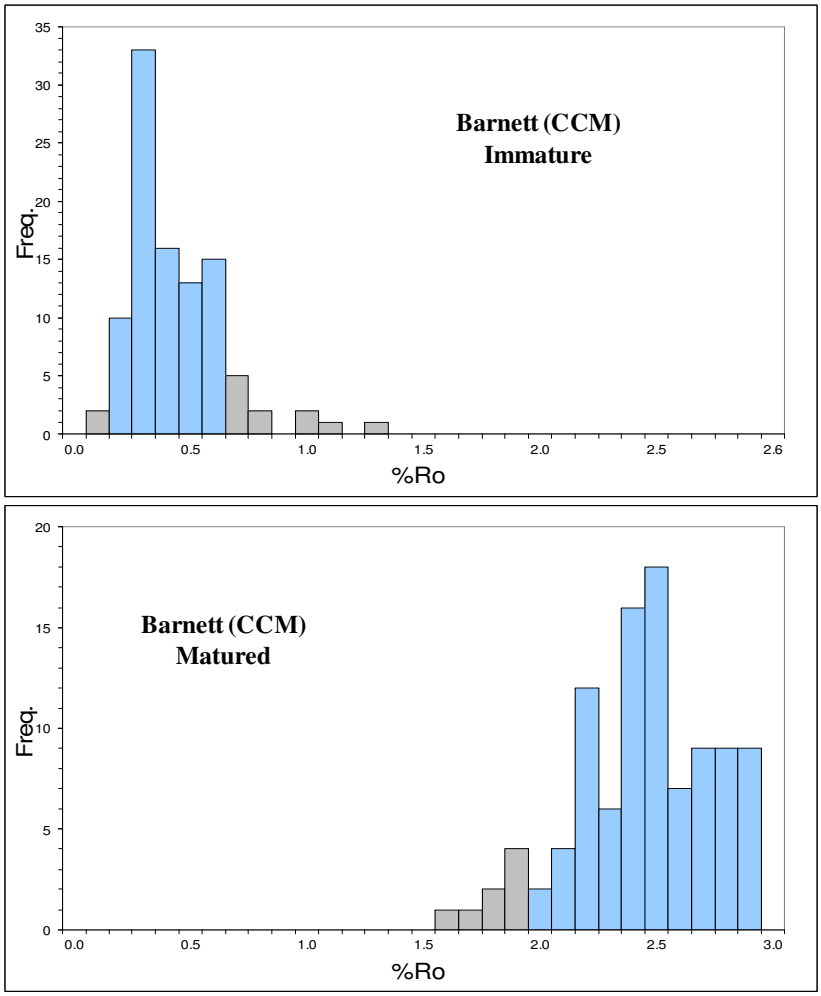

Figure 5.8.3: Histograms for the immature Barnett and matured Barnett based on the vitrinite reflectance values of the kerogens.

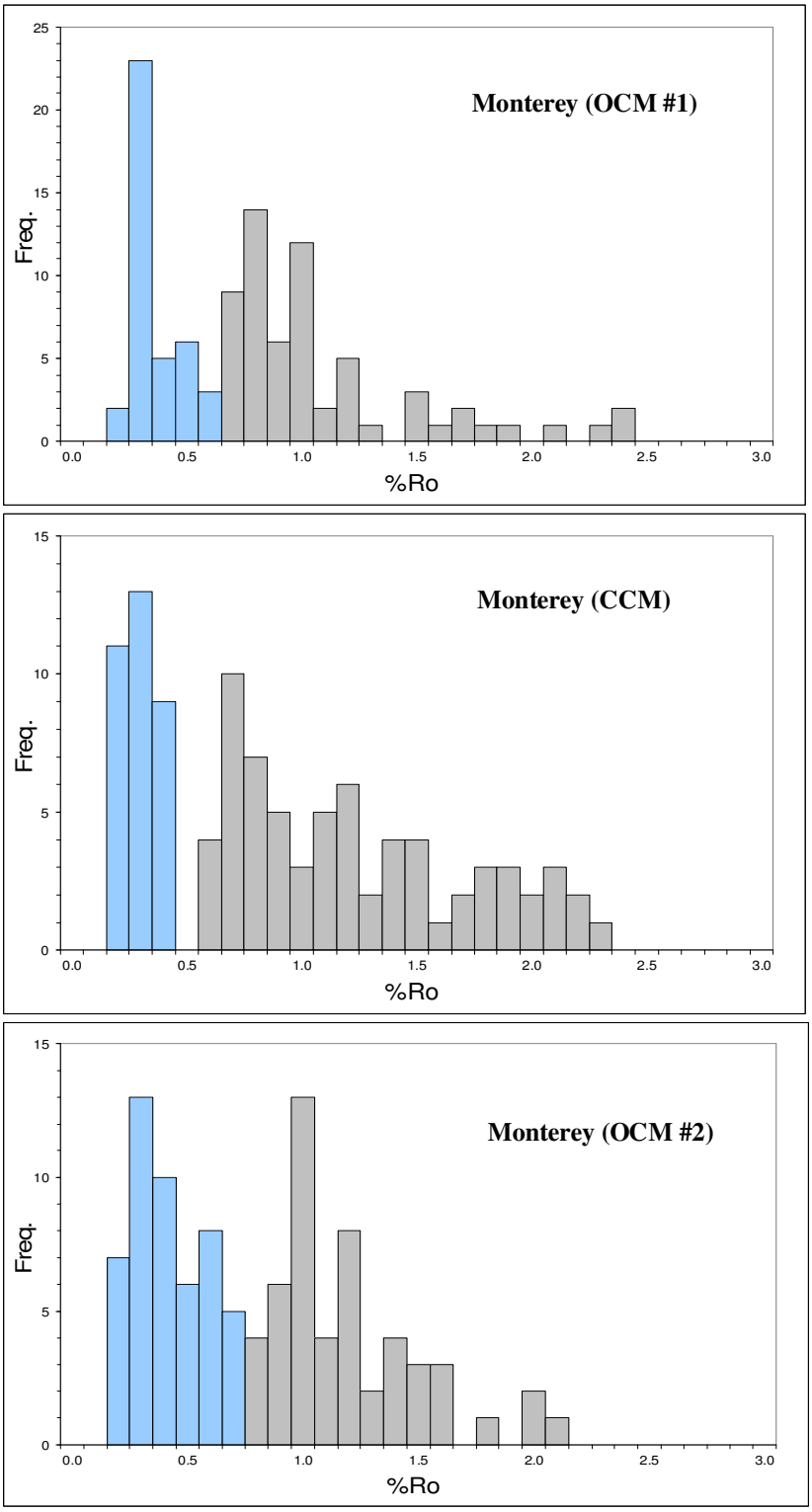

Figure 5.8.4: Histograms for the Monterey based on the vitrinite reflectance values of the kerogens.

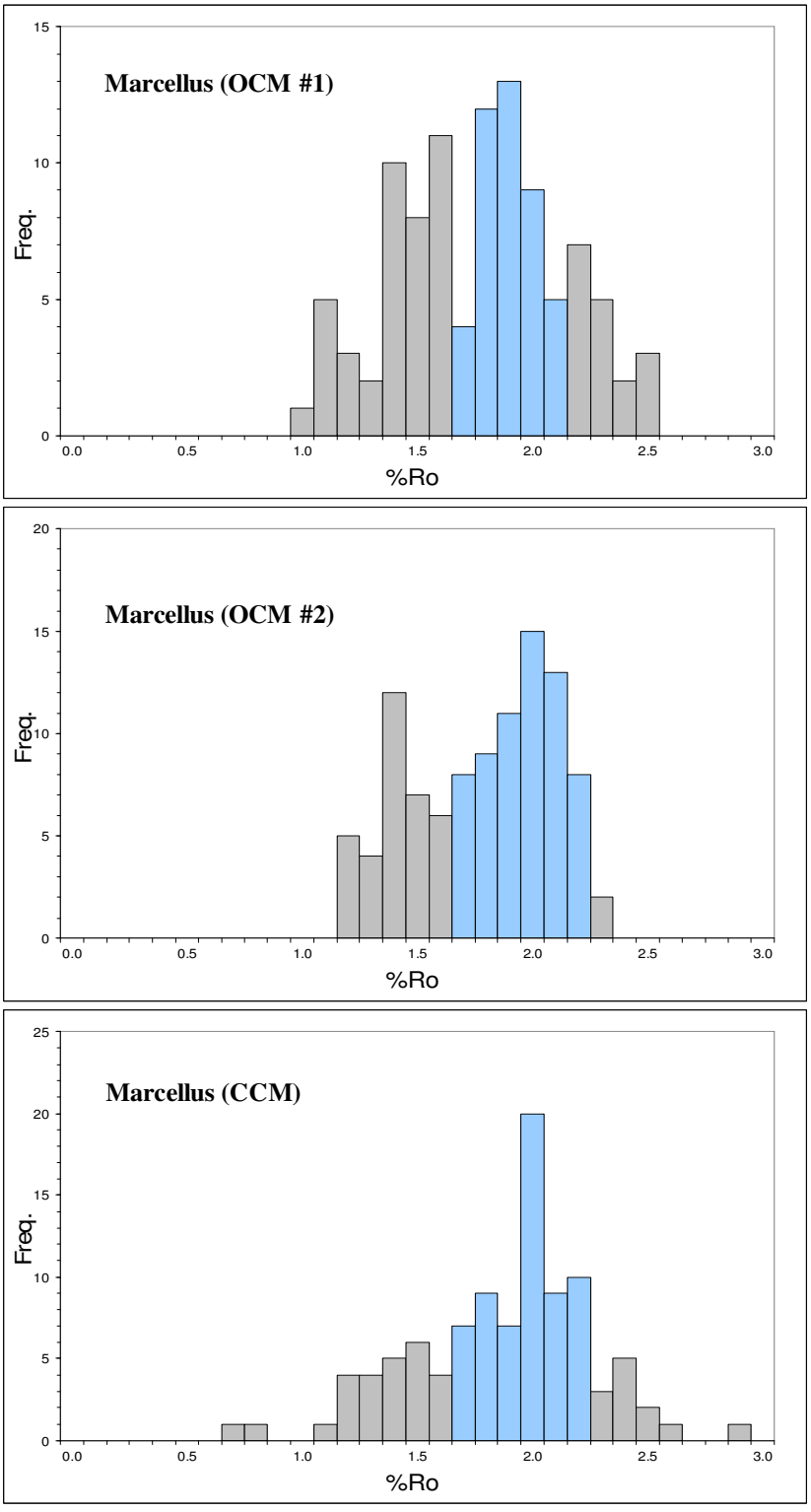

Figure 5.8.5: Histograms for the Marcellus based on the vitrinite reflectance values of the kerogens.

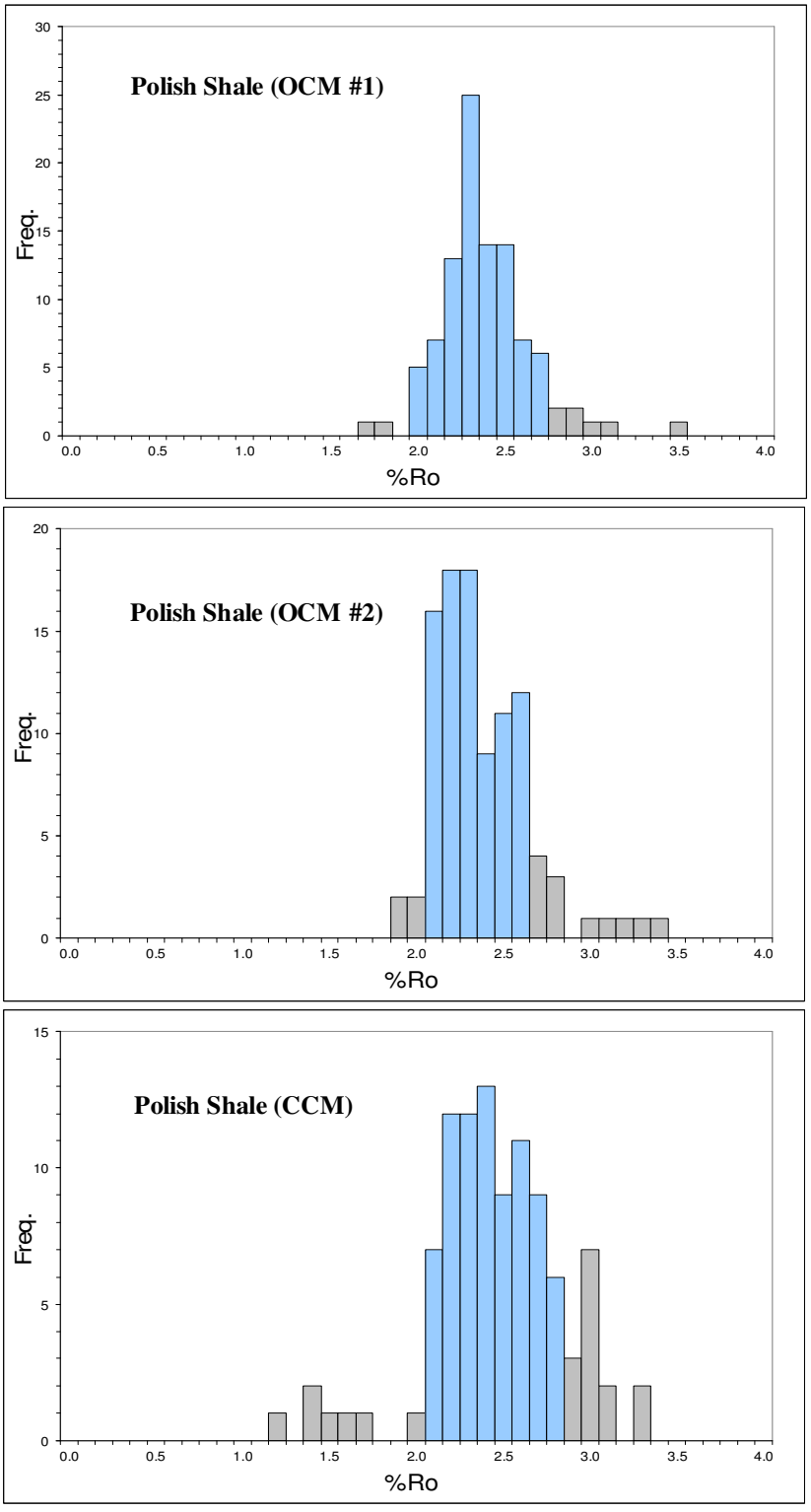

Figure 5.8.6: Histograms for the Polish Shale based on the vitrinite reflectance values of the kerogens.

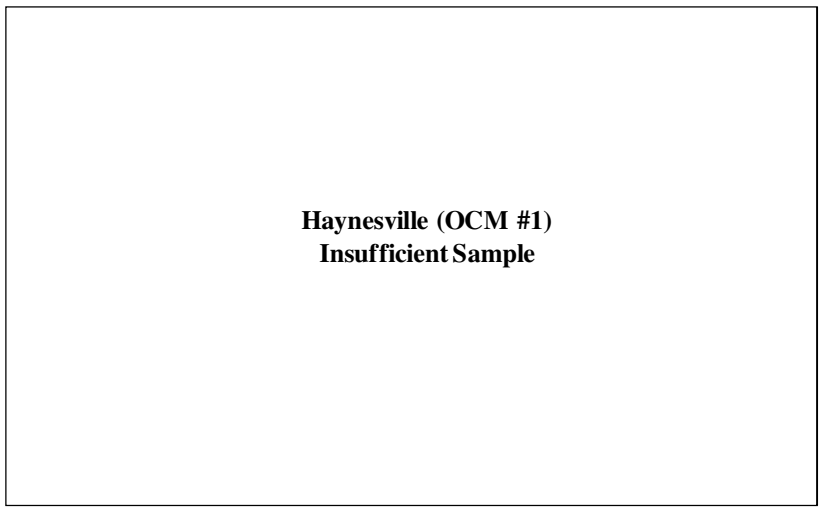

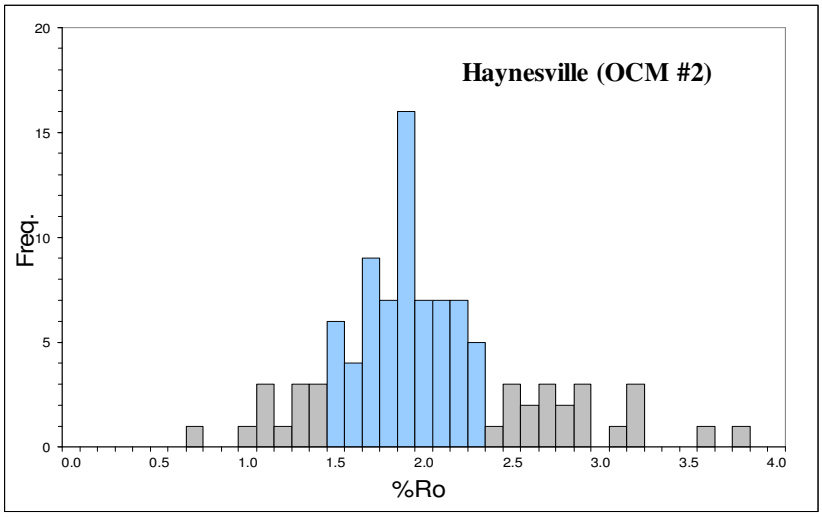

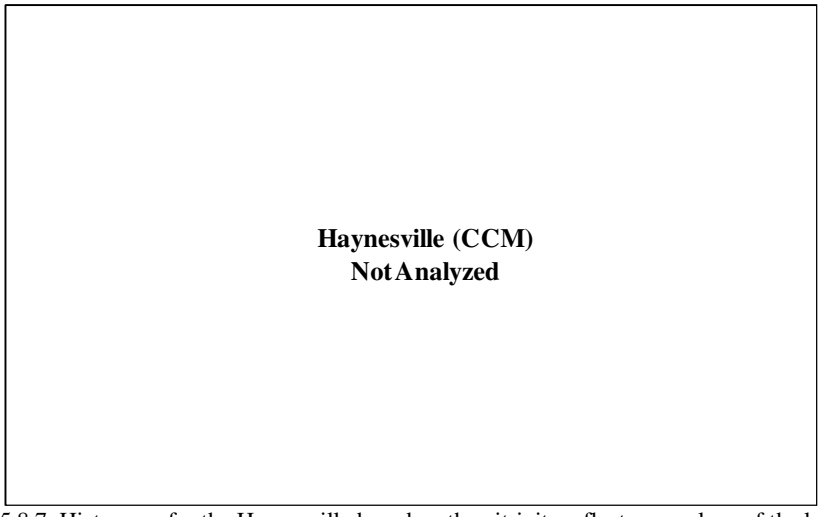

Figure 5.8.7: Histogram for the Haynesville based on the vitrinite reflectance values of the kerogen.

5.8.2 Thermal Alteration Index (TAI)

Thermal alteration index (TAI) is a thermal maturity indicator based on the color of spores, pollens, and cuticle material in a transmitted-light microscope slide. Again, because the organic microscopist imparts a great deal of discretion and objectivity in selecting the measured particles in the microscope slide, the isolation method did not have a significant impact on the thermal maturity interpretations (refer to Table 5.8.1). For the Marcellus, the Polish Shale, and the Haynesville samples no spores were found for TAI measurements (see Table 5.8.2). For these three samples the appearance of the kerogen was 100% non-fluorescing under UV light and black in color under transmitted light (see Table 5.8.2). For the Monterey and $Barnett_{imm}$ samples the kerogen appeared as amorphous and dark-brown in color under transmitted light (see Table 5.8.2). Most of the macerals in the kerogen in this study were non-fluorescing but have high reflectance which is indicative of highly altered (thermally overmature) organic matter (see Table 5.8.2).

Sample	Isolation Method	TAI	FL. AMOR	NFL. AMOR.	Alginite (%)	Exinite (%)	Vitrinite (%)	Inertinite (%)
Barnett (immature)	OCM #1	2.0-2.4	10-15	85-90	70-79	1-5	15-20	~5
	OCM #2	2.0-2.4	1-5	95-99	74-84	~1	15-20	~5
	CCM	2.0-2.4	5-10	90-95	74-84	~1	15-20	~5
Barnett (mature)	**Not Analyzed**							
Monterey	OCM #1	2.6-3.0	1-5	95-99	79-84	1-5	15-20	~5
	OCM #2	2.6-3.0	1-5	95-99	74-84	~1	15-20	~5
	CCM	2.6-3.0	~5	~95	74-84	~1	15-20	~5
Marcellus	OCM #1	**Not Analyzed**						
	OCM #2	No spores		100				
	CCM	No spores		100				
Polish Shale	OCM #1	**Not Analyzed**						
	OCM #2	No spores		100				
	CCM	No spores		100				
Haynesville	OCM #1	**Not Analyzed**						
	OCM #2	No spores	1-5	95-99				
	CCM	No spores	1-5	95-99				

Table 5.8.2: Summary table of TAI results for the samples.

5.9 Stable Isotope Analysis Results

5.9.1 Stable Carbon Isotope Analysis ($\delta^{13}C$) Results

Before samples were analyzed the stable-isotope mass spectrometer was checked by running a reference gas standard. All carbon isotope values are reported against the Pee Dee Belemnite (PDB) standard. Stable carbon isotope values are within ±0.5‰. The results from the stable carbon isotope analysis are used as one of the tools to assess if the different isolation methods cause any isotopic fractionation. Based on the results displayed in Figure 5.9.1 below there seems to be no fractionation of the carbon isotopes. There appears to be little or no difference in the carbon isotope values of each of the kerogens isolated by either the open-methods or the closed-method. The error bars in Figure 5.9.1 are based on two times the standard deviation (2SD).

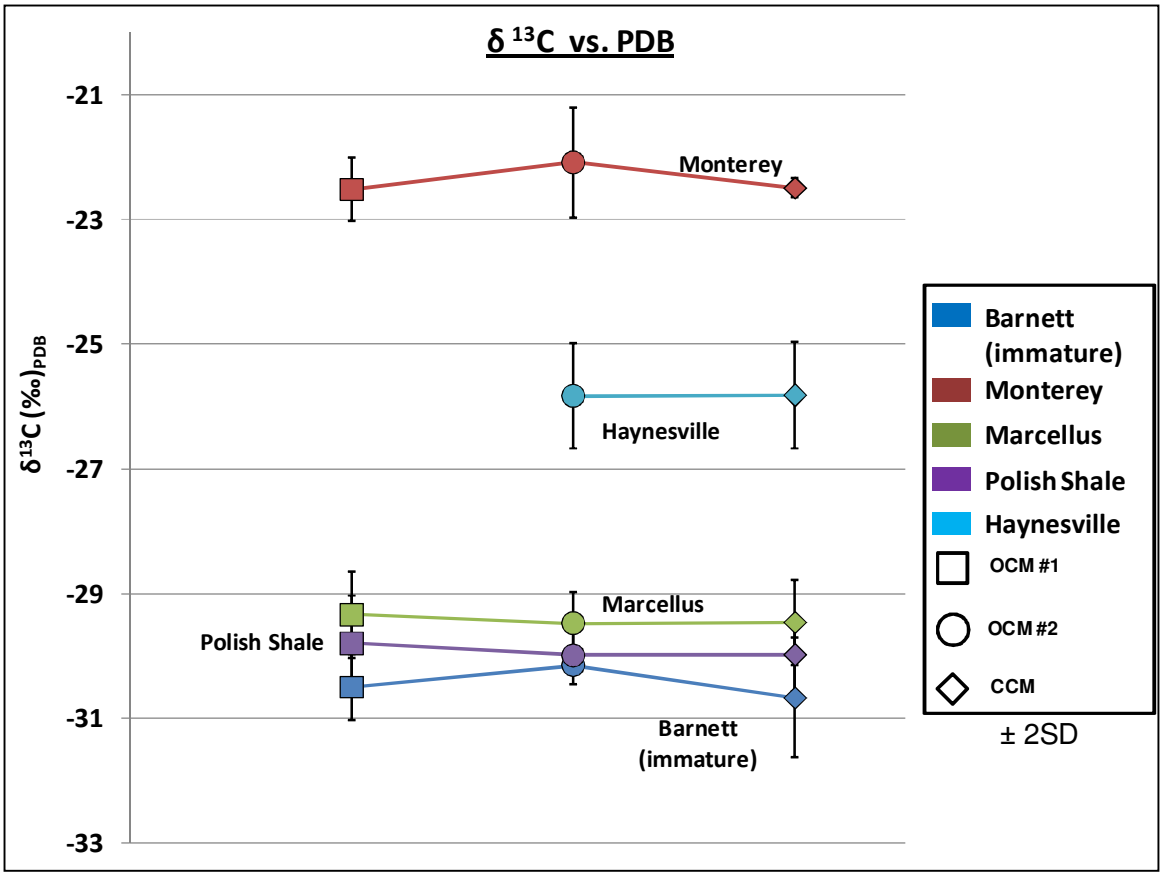

Figure 5.9.1: Carbon isotopic composition of the various kerogens isolated by the three approaches (error bars based on twice the standard deviation).

5.9.2 Stable Sulfur Isotope Analysis ($\delta^{34}S$) Results

The stable sulfur-isotope analyses conducted by Isotech have a standard error of ±0.3‰, which falls within the symbols in the plot (Figure 5.9.2). Based on the results plotted on Figure 5.9.2 there is significant difference in the values of the sulfur isotopes of the kerogens isolated via the different methods. The UH closed-method (CCM) yielded heavier sulfur isotopes than the other two commercial open-methods (OCM). The source of this variance in the sulfur is most likely due to the presence of significant pyrite in the OCM-separated kerogens. Clearly, the isotopically lighter pyritic sulfur is interfering with the isotopically heavier organic sulfur.

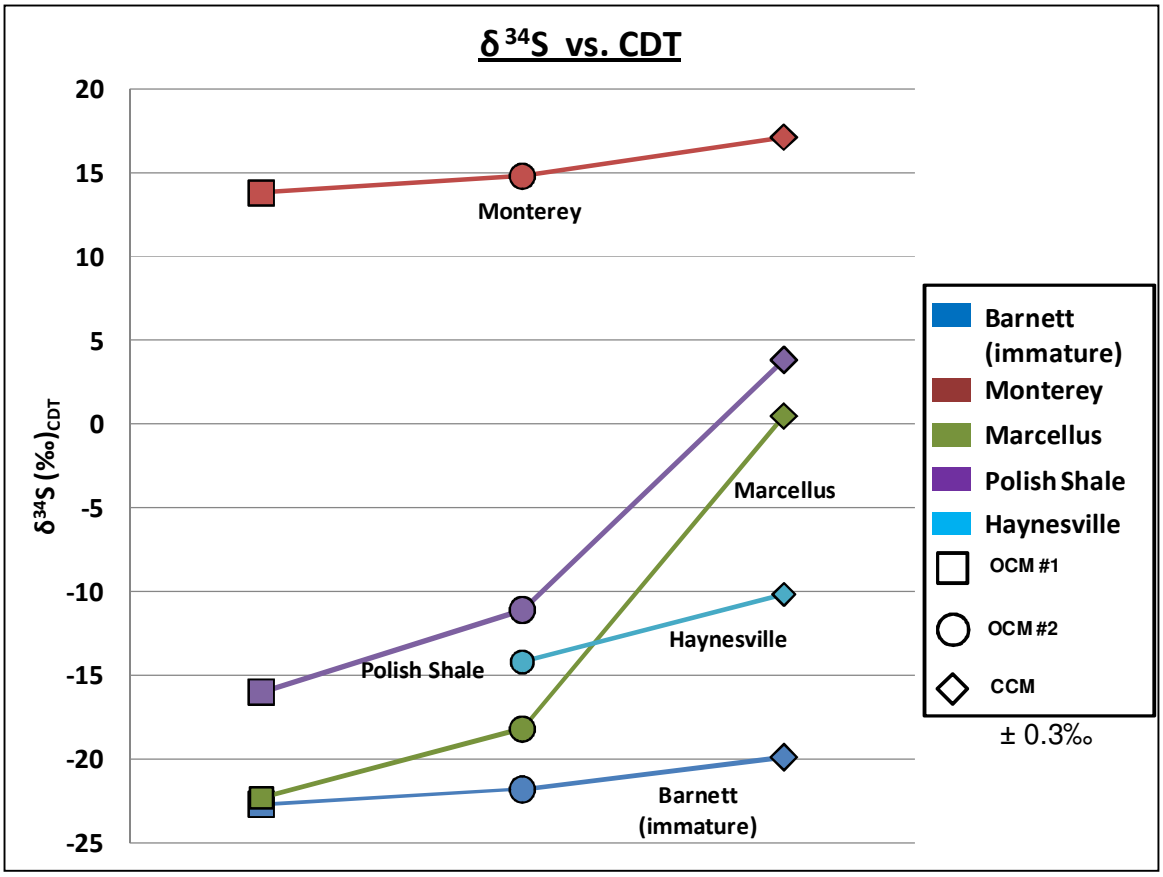

Figure 5.9.2: Sulfur isotopic composition of the various kerogens isolated by the three approaches (values are within ± 0.3‰).

5.10 Elemental Analysis Results

Elemental analysis results for C, H, N, S, and O are typically reported in wt% values. The first step was to normalize the elemental composition values for the ash content. Once normalized to 100%, the wt% values were converted into atomic values for characterization of the samples. For the C, H, N, and S values QTI claims an accuracy of ±0.3 to 0.4% (absolute). For the oxygen values they state an accuracy of ±2% to 5%. Figure 5.10.1 shows the normalized elemental analysis results for the kerogen. Generally the kerogen isolated via the CCM had higher carbon weight percentages and lower sulfur weight percentages than those from the open-methods (OCM).

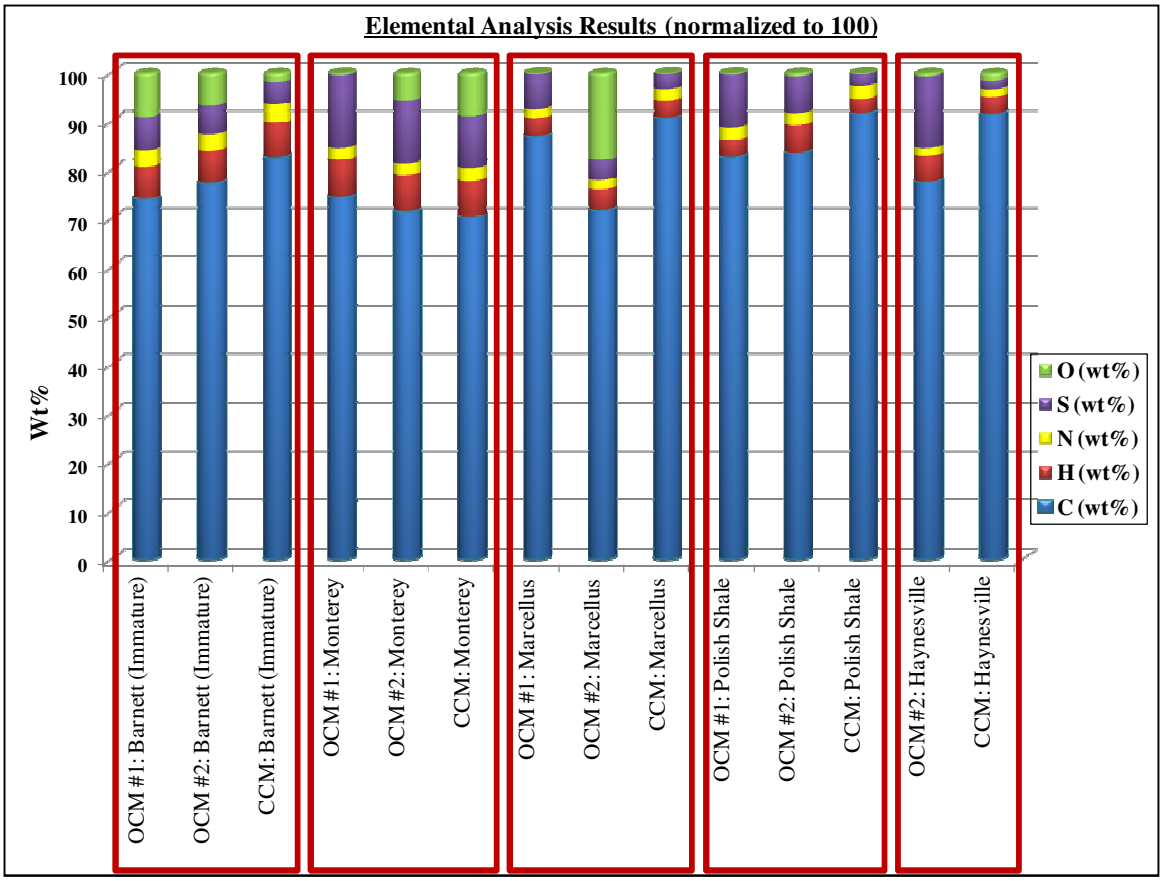

Figure 5.10.1: Elemental analysis results of the kerogens. Note variance in the values across the isolation methods.

Figure 5.10.2 shows the elemental analysis results for kerogens of the Barnett comparing the thermally mature versus the immature (outcrop) sample. The $Barnett_{imm}$ kerogen has lower carbon content (wt%) and more nitrogen, sulfur, hydrogen, and oxygen than the thermally mature sample. This is because as the shale is buried and heated the kerogen goes through carbonization, increasing in carbon content. Figure 5.10.2 also shows the elemental analysis for the kerogen from the Monterey, comparing the solvent-extracted kerogen to the non-extracted kerogens. The Monterey kerogen was analyzed before and after it was bitumen extracted once again after isolation. The results do not show much change in the kerogen elemental composition.

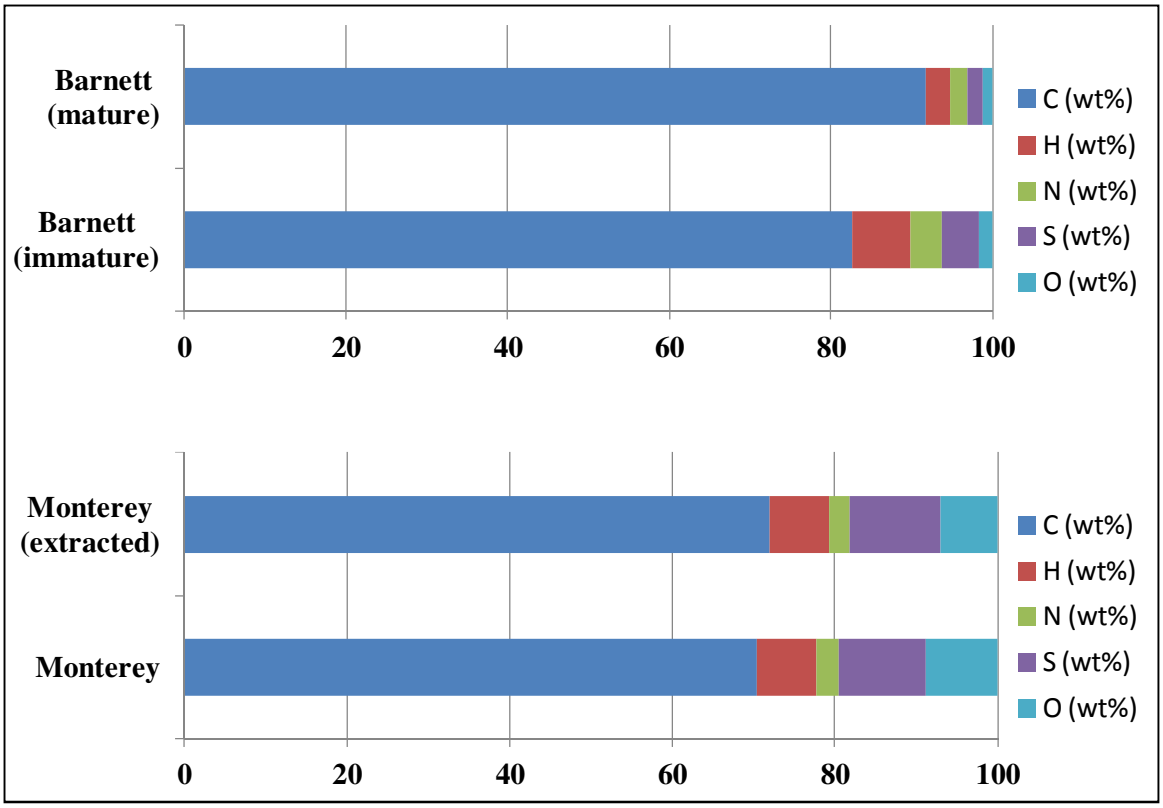

Figure 5.10.2: Comparative analysis of the elemental compositions (normalized to 100 %) for the Barnett immature (outcrop) kerogen versus the Barnett matured kerogen and the solvent-extracted versus the non solvent-extracted Monterey kerogens.

5.11 Pyrolysis-GC Results

The degradation products of the kerogen were studied using Py-GC. The pyrograms are shown in Figures 5.11.6 through 5.11.10 and the aromaticities of the kerogens is given in Table 5.11.1. Aromaticity is defined as the percentage of aromatic compounds out of all the compounds generated from pyrolysis. Alkanes are compounds with saturated bonds (single bonds) while alkenes (olefins) are compounds with unsaturated bonds (double bonds).

Sample	Isolation Method	Aromaticity (%)
Barnett (immature)	OCM #1	4.78
	OCM#2	4.68
	CCM	6.04
Monterey	OCM #1	5.74
	OCM#2	4.93
	CCM	5.36
Marcellus	OCM #1	6.87
	OCM#2	8.53
	CCM	6.91
Polish Shale	OCM #1	2.88
	OCM#2	8.48
	CCM	7.45
Haynesville	OCM#2	5.75
	CCM	5.51

Table 5.11.1: Table showing the aromaticity of the kerogen from the Py-GC results. Aromaticity was determined from the percent of aromatics out of all the measured compounds.

Whereas aromaticity of the kerogens derived via the various methods did not vary more than ~2% across isolation methods, the alkane/alkene ratios of the pyrolysis products varied significantly. In Figures 5.11.1 through 5.11.5, the n-alkene/n-alkane ratios were calculated over the whole range of carbon numbers from C_1 through C_{36}, as well as for the group-fractions from C_1 to C_5 (light), C_6 to C_{10}, C_{11} to C_{14}, and C_{15+} (heavy) and plotted. For the Marcellus kerogens, the n-alkene/n-alkane ratio showed significant variability in the C1-C5 range where the OCM #1 plotted much twice as high as that of the closed-method and six times as high as that of the OCM #1 (see Figure 5.11.3). Similarly, the Monterey and Haynesville kerogens showed the greatest difference in the OCM #2, where the kerogen ratios plot higher than that of the other two methods

(see Figures 5.11.2 and 5.11.5). For the Monterey kerogens the greatest variability was seen in the C6-C10, the C11-C15, and in C15+ whereas for the Haynesville the variability was seen in all the carbon number ranges. The Polish shale showed the greatest variability in the OCM #1 versus the other two methods whose ratios were close to each other across the carbon number ranges (see Figure 5.11.4). The Barnett kerogens showed little significant change in the ratios across isolation methods (Figure 5.11.1).

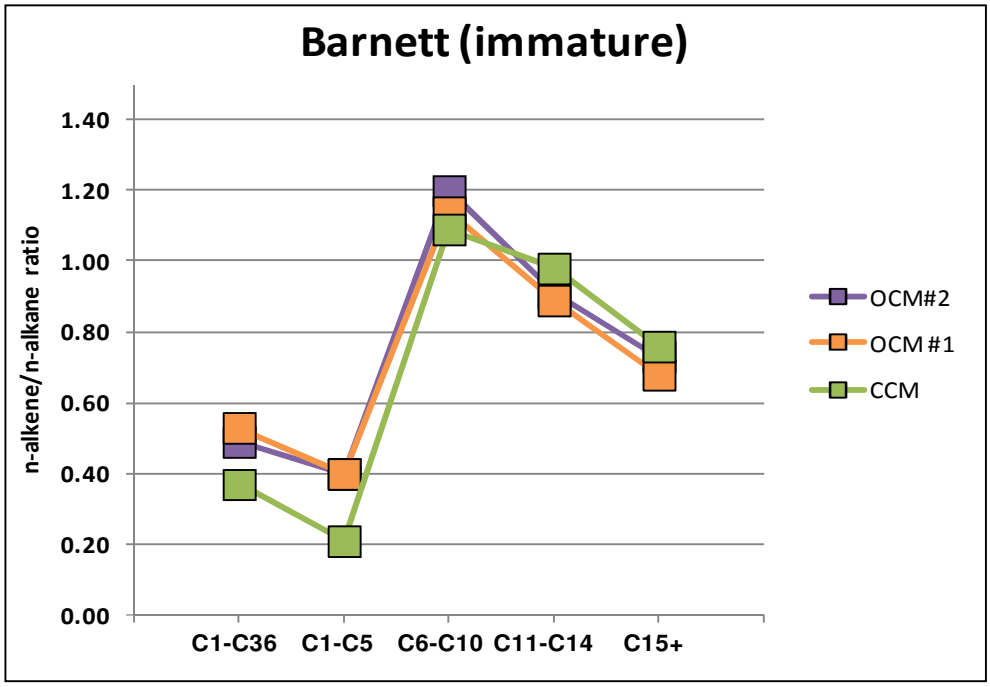

Figure 5.11.1: N-alkene/n-alkane ratios for the immature Barnett kerogens. Note the variability in the ratios across methods. Greatest variability in the ratios was seen in the C1 to C5 range.

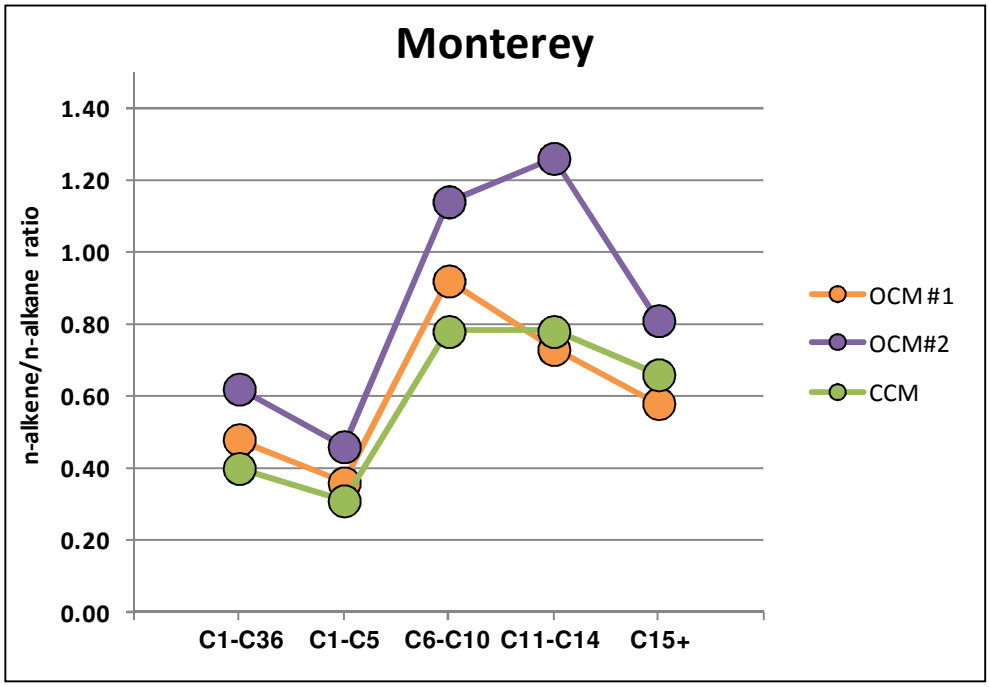

Figure 5.11.2: N-alkene/n-alkane ratios for the Monterey kerogens. Note the variability in the ratios across methods. The open-method #2 (OCM #2) kerogen significantly varies in the ratios from the other two methods.

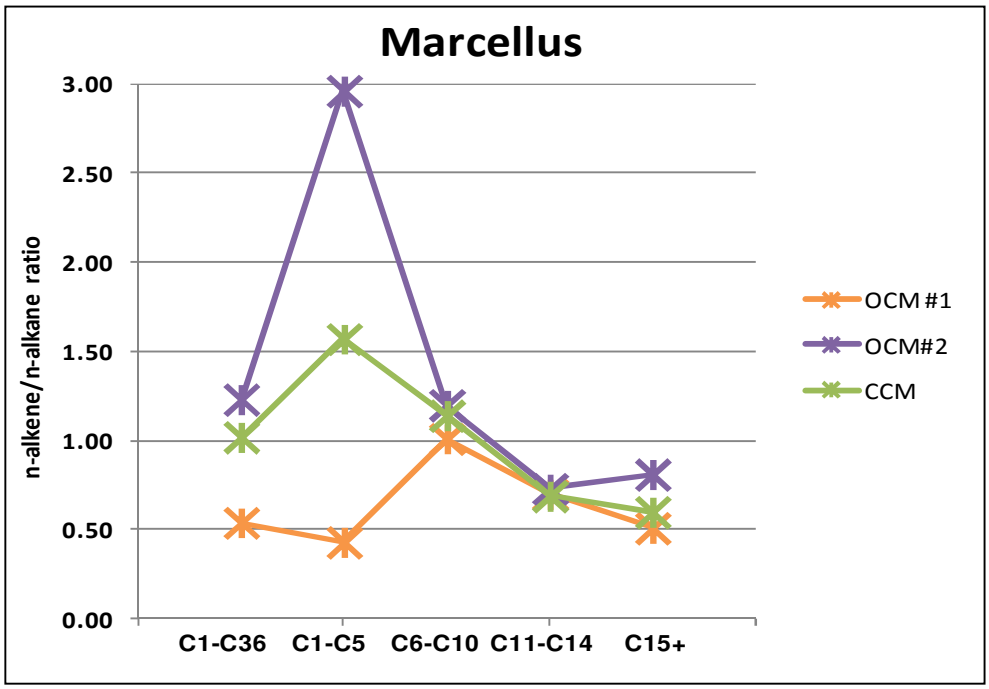

Figure 5.11.3: N-alkene/n-alkane ratios for the Marcellus kerogens. Note the variability in the ratios across methods. The most significant variability was seen in the C1-C5 range.

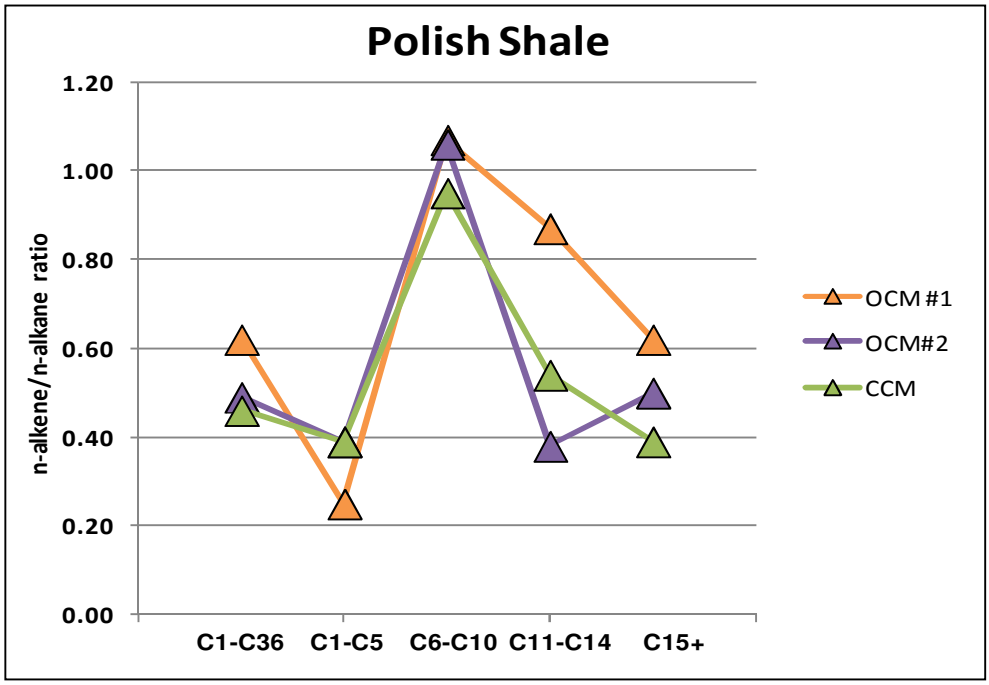

Figure 5.11.4: N-alkene/n-alkane ratios for the Polish Shale kerogens. Note the variability in the ratios across methods. The most significant variability was seen in the C1-C5, C11-C14, and C15+ ranges.

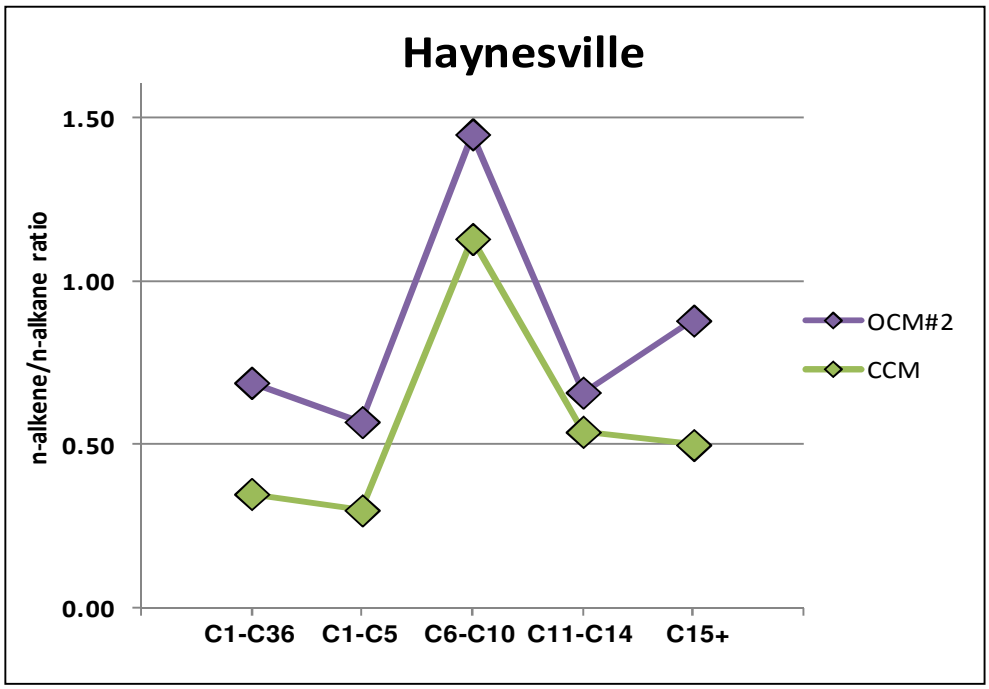

Figure 5.11.5: N-alkene/n-alkane ratios for the Haynesville kerogens. Note the variability in the ratios across methods. There was significant variability in all the ranges.

The Marcellus kerogen pyrograms (see Figure 5.11.8) showed a significant difference in the intensity of the products being measured. Similarly, the Polish shale kerogen pyrograms (Figure 5.11.9) show a significant variability in the intensity of the peaks. The Haynesville kerogen pyrograms (Figure 5.11.10) also showed significant variance in the intensities of the peaks. The pyrograms of the $Barnett_{imm}$ kerogens (Figure 5.11.6), showed minor variability with varying isolation methods. Similarly, the Monterey kerogen pyrograms (Figure 5.11.7) show little significant variability across the kerogen samples, other than a large unidentified peak between n-alkane 28 and n-alkane 29 in the OCM #1 kerogen.

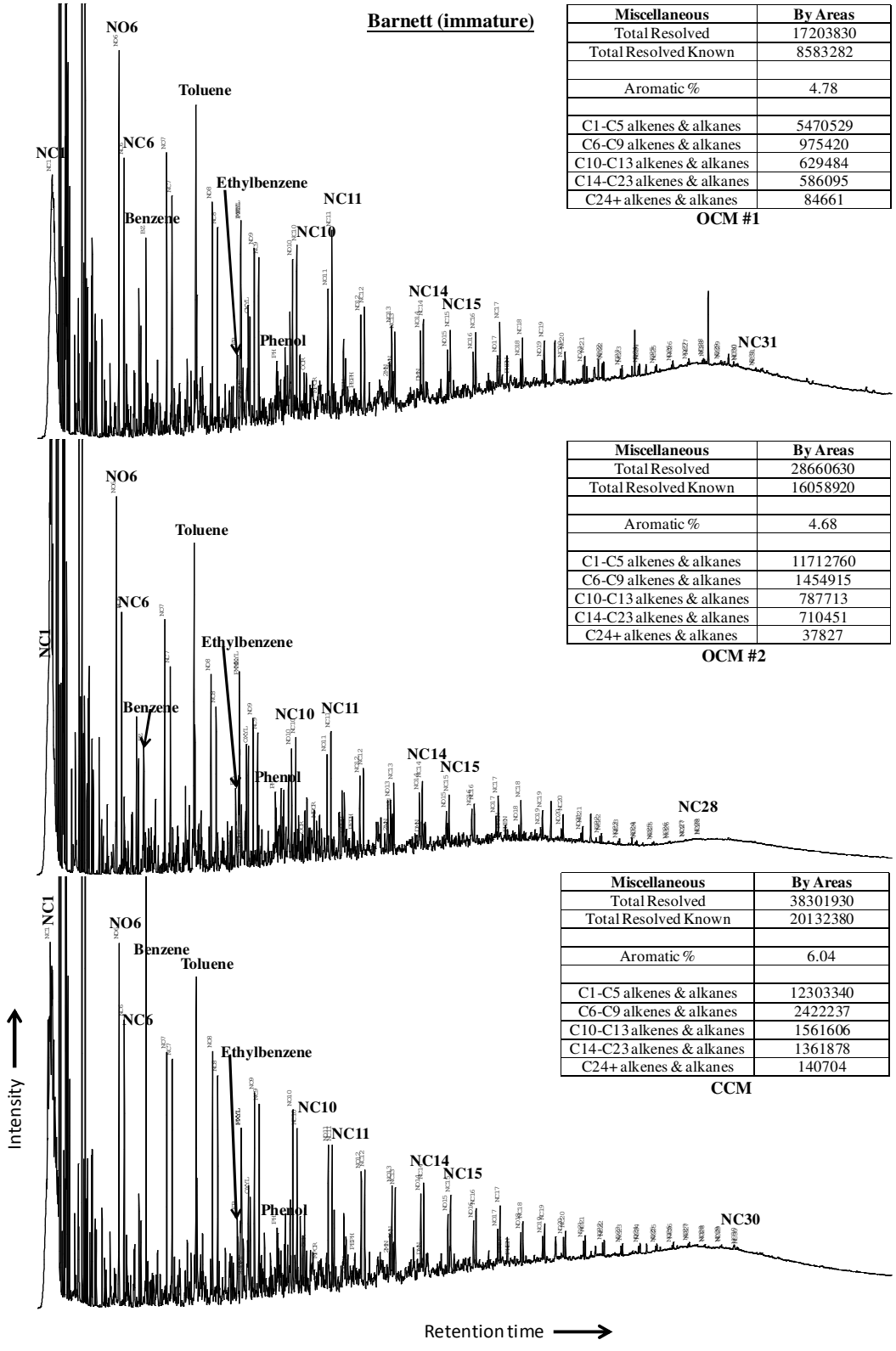

Miscellaneous	By Areas
Total Resolved	17203830
Total Resolved Known	8583282
Aromatic %	4.78
C1-C5 alkenes & alkanes	5470529
C6-C9 alkenes & alkanes	975420
C10-C13 alkenes & alkanes	629484
C14-C23 alkenes & alkanes	586095
C24+ alkenes & alkanes	84661

OCM #1

Miscellaneous	By Areas
Total Resolved	28660630
Total Resolved Known	16058920
Aromatic %	4.68
C1-C5 alkenes & alkanes	11712760
C6-C9 alkenes & alkanes	1454915
C10-C13 alkenes & alkanes	787713
C14-C23 alkenes & alkanes	710451
C24+ alkenes & alkanes	37827

OCM #2

Miscellaneous	By Areas
Total Resolved	38301930
Total Resolved Known	20132380
Aromatic %	6.04
C1-C5 alkenes & alkanes	12303340
C6-C9 alkenes & alkanes	2422237
C10-C13 alkenes & alkanes	1561606
C14-C23 alkenes & alkanes	1361878
C24+ alkenes & alkanes	140704

CCM

Figure 5.11.6: Pyrograms for the three Barnett (immature) kerogens with a summary table for each result.

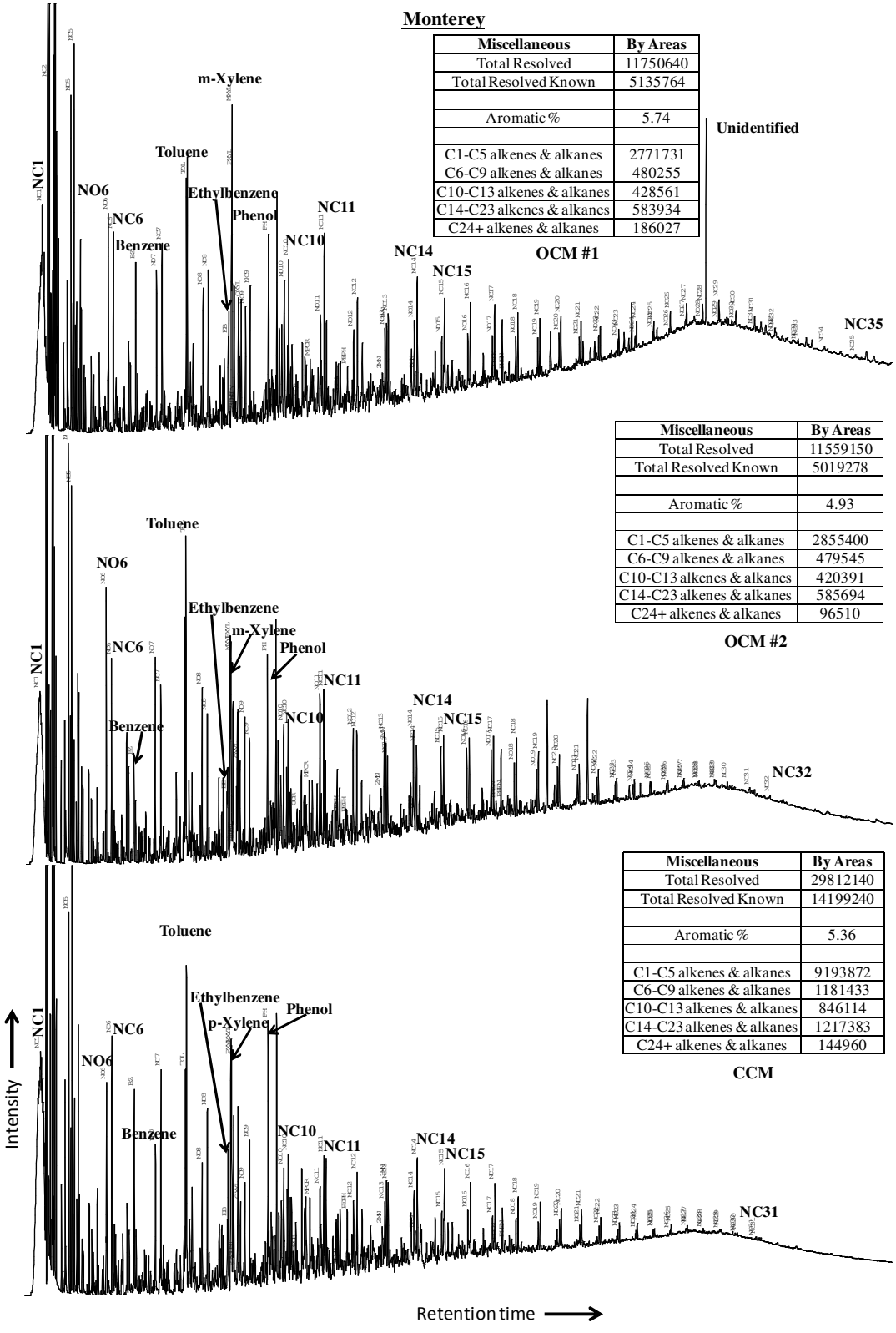

Figure 5.11.7: Pyrograms for the three Monterey kerogens with a summary table for each result.

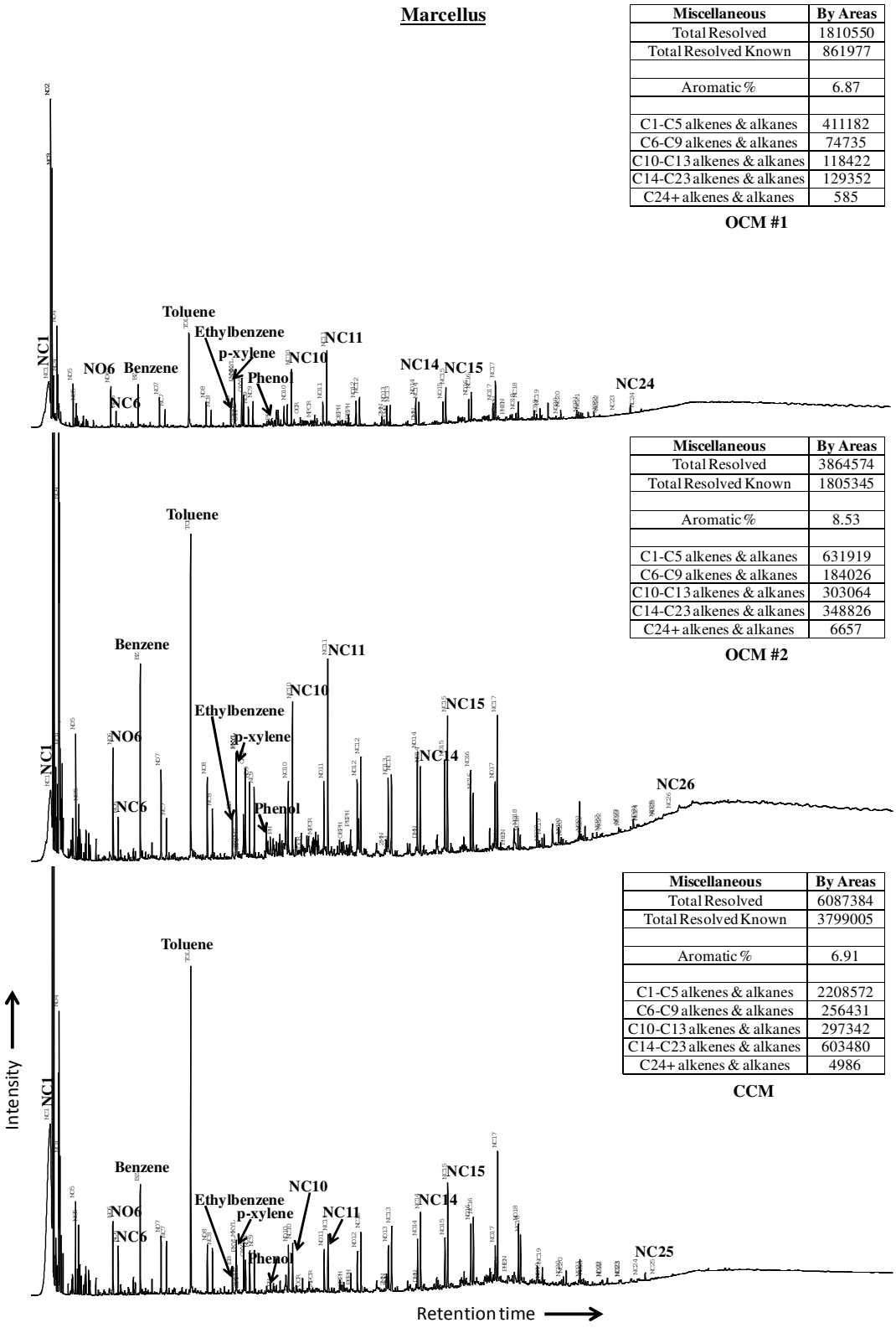

Figure 5.11.8: Pyrograms for the three Marcellus kerogens with a summary table for each result.

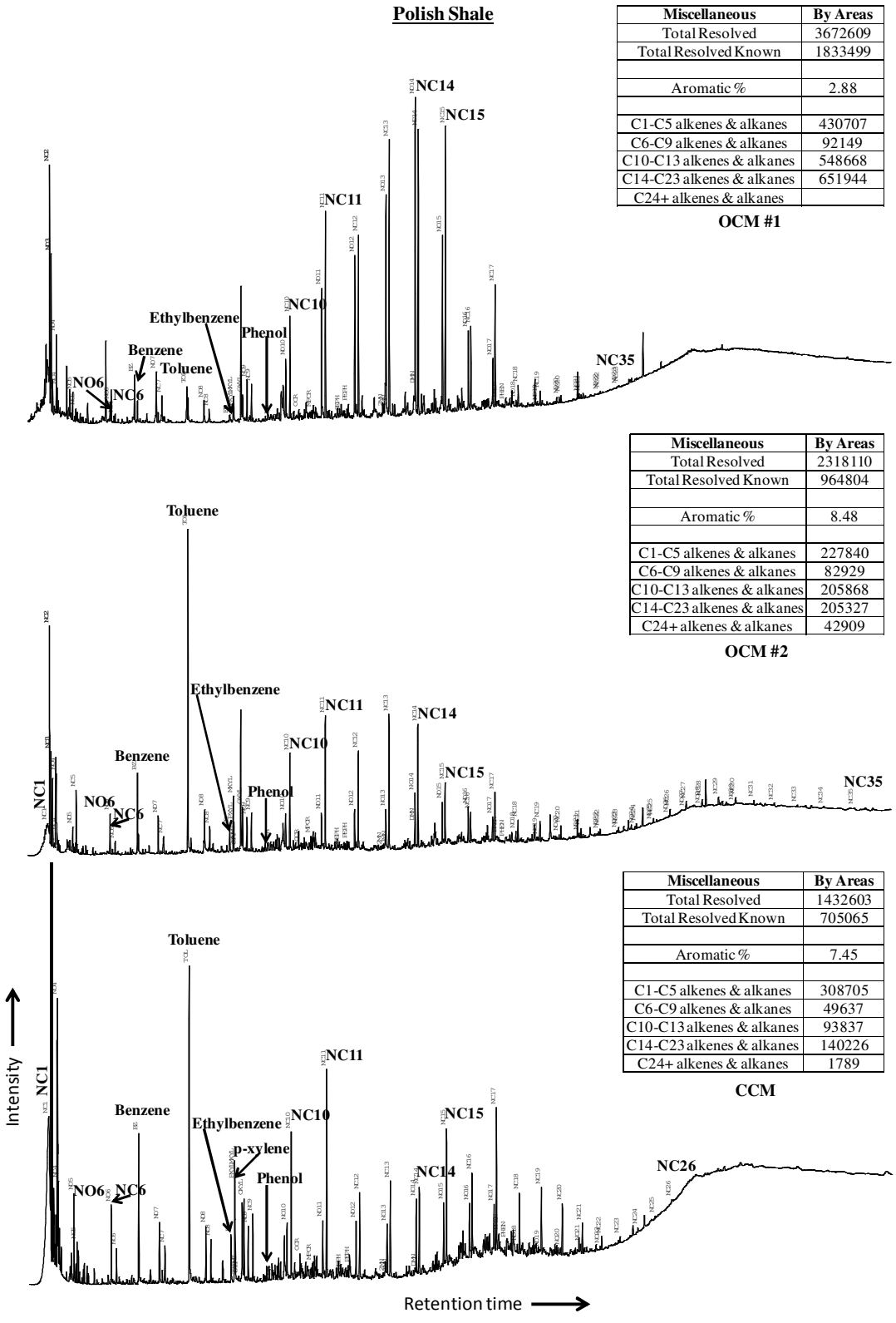

Miscellaneous	By Areas
Total Resolved	3672609
Total Resolved Known	1833499
Aromatic %	2.88
C1-C5 alkenes & alkanes	430707
C6-C9 alkenes & alkanes	92149
C10-C13 alkenes & alkanes	548668
C14-C23 alkenes & alkanes	651944
C24+ alkenes & alkanes	

Miscellaneous	By Areas
Total Resolved	2318110
Total Resolved Known	964804
Aromatic %	8.48
C1-C5 alkenes & alkanes	227840
C6-C9 alkenes & alkanes	82929
C10-C13 alkenes & alkanes	205868
C14-C23 alkenes & alkanes	205327
C24+ alkenes & alkanes	42909

Miscellaneous	By Areas
Total Resolved	1432603
Total Resolved Known	705065
Aromatic %	7.45
C1-C5 alkenes & alkanes	308705
C6-C9 alkenes & alkanes	49637
C10-C13 alkenes & alkanes	93837
C14-C23 alkenes & alkanes	140226
C24+ alkenes & alkanes	1789

Figure 5.11.9:Pyrograms for the three Polish Shale kerogens with a summary table for each result.

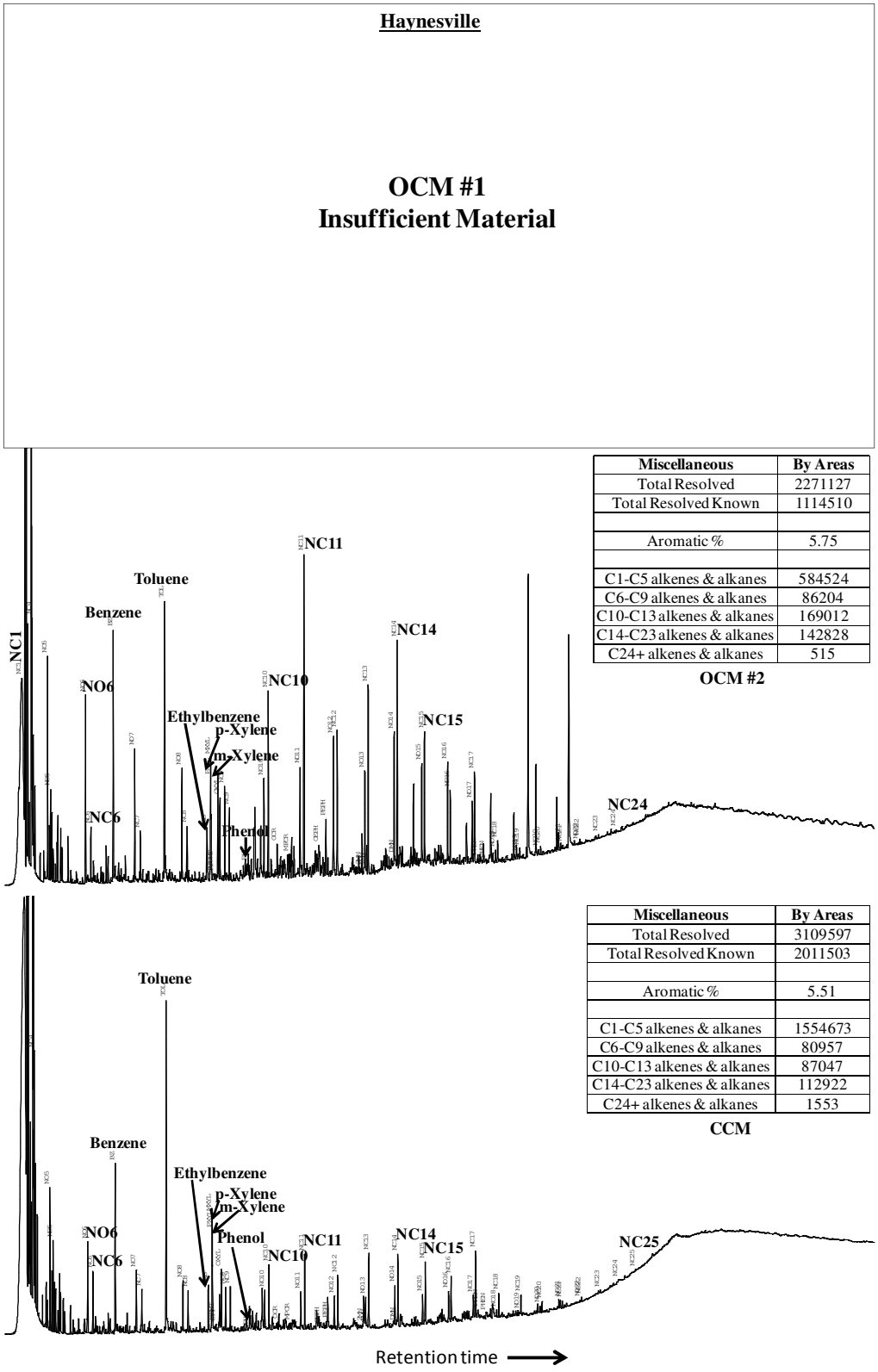

Figure 5.11.10: Pyrograms for the three Haynesville kerogens with a summary table for each result.

5.12 Solid-State ^{13}C Nuclear Magnetic Resonance (NMR) Results

Chemical shifts were referenced to glycine carbonyl defined at 176.46 ppm. This standard was chosen since it is a very well-known standard in solid-state NMR. There is currently no set standard for all solid-state NMR like in liquid NMR so the chemical shifts do vary slightly across the literature. This is not considered to be an issue with the results shown here because of the broadness in the spectra's signals meaning some small variance ($1/10^{th}$ of a decimal place) is not of concern.

The $Barnett_{imm}$ NMR spectra show higher aliphaticity than aromaticity. Similarly, the Monterey NMR spectra show more aliphaticity versus aromaticity. In contrast, the Marcellus, the Haynesville, and the Polish Shale NMR spectra all have high aromaticities. Aromaticity was calculated by adding together the integrated area for the aromatic centerband and for the two associated spinning sidebands to either side. The sum was then divided by the total area. The data showed that the $Barnett_{imm}$ aromaticity is merely 47-48%, whereas the $Barnett_{mat}$ has an aromaticity of 87%. The Monterey showed an aromaticity of 35-37%. Aromaticity of the Marcellus was estimated at 87%, the Polish Shale at 89-90%, and the Haynesville at 83%-85% (Figure 5.12.1 through 5.12.6).

Based on the dipolar dephasing NMR of the $Barnett_{mat}$, the Marcellus, the Polish Shale, and the Haynesville Shale, the very high aromaticity is indicative of a structure composed of relatively small aromatic ring-systems (7 benzene rings) with a significant number of aromatic CH groups and a few methyl groups which are most likely connected by short aliphatic chains. The Monterey and the Barnett have much more complicated

structures. Overall there was no significant difference were observed among kerogen samples separated by the diverse methods.

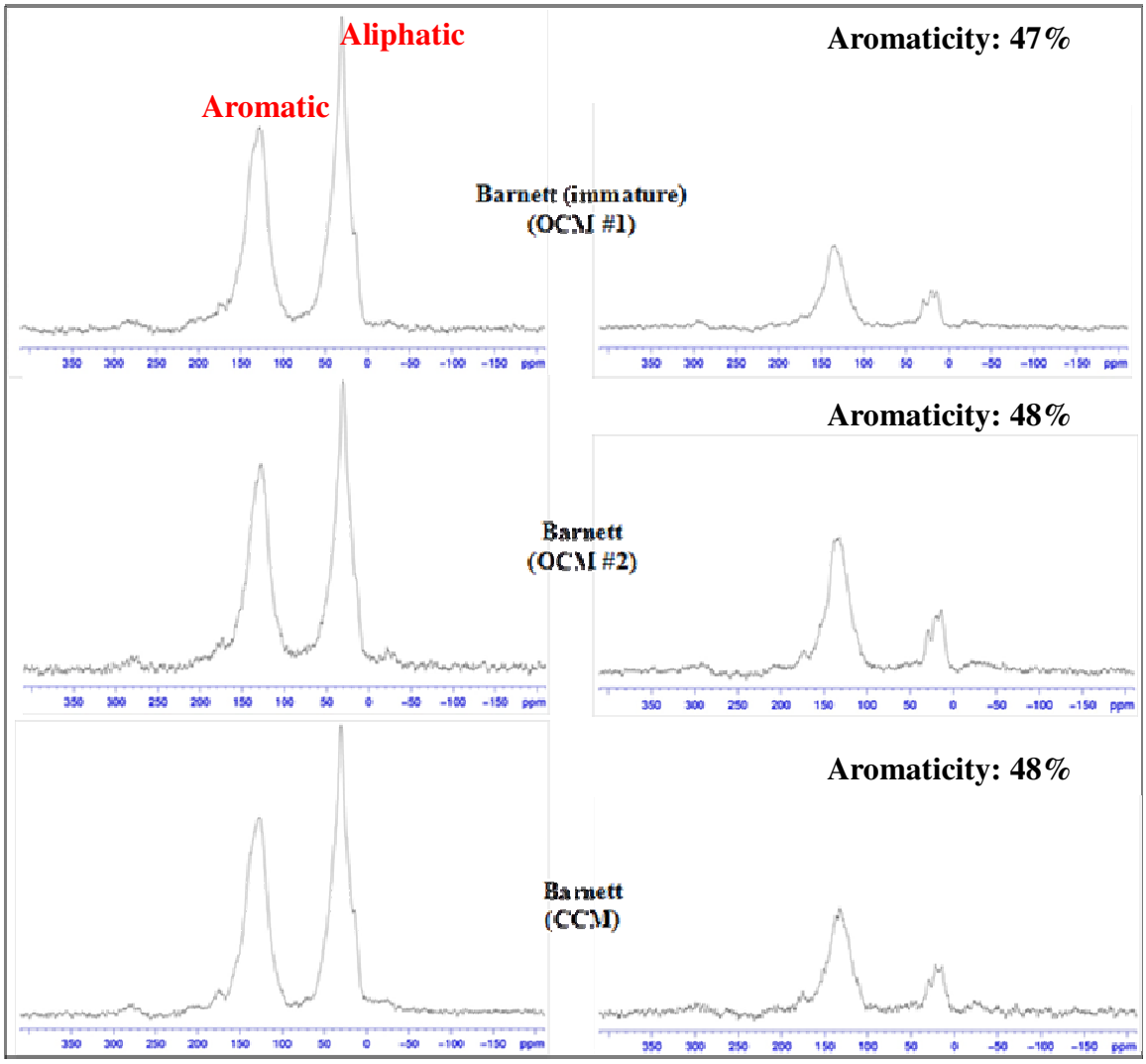

Figure 5.12.1: Solid-state 13C NMR results for the immature Barnett kerogen. On the left are the cross-polarization results and on the right are the dipolar dephasing results.

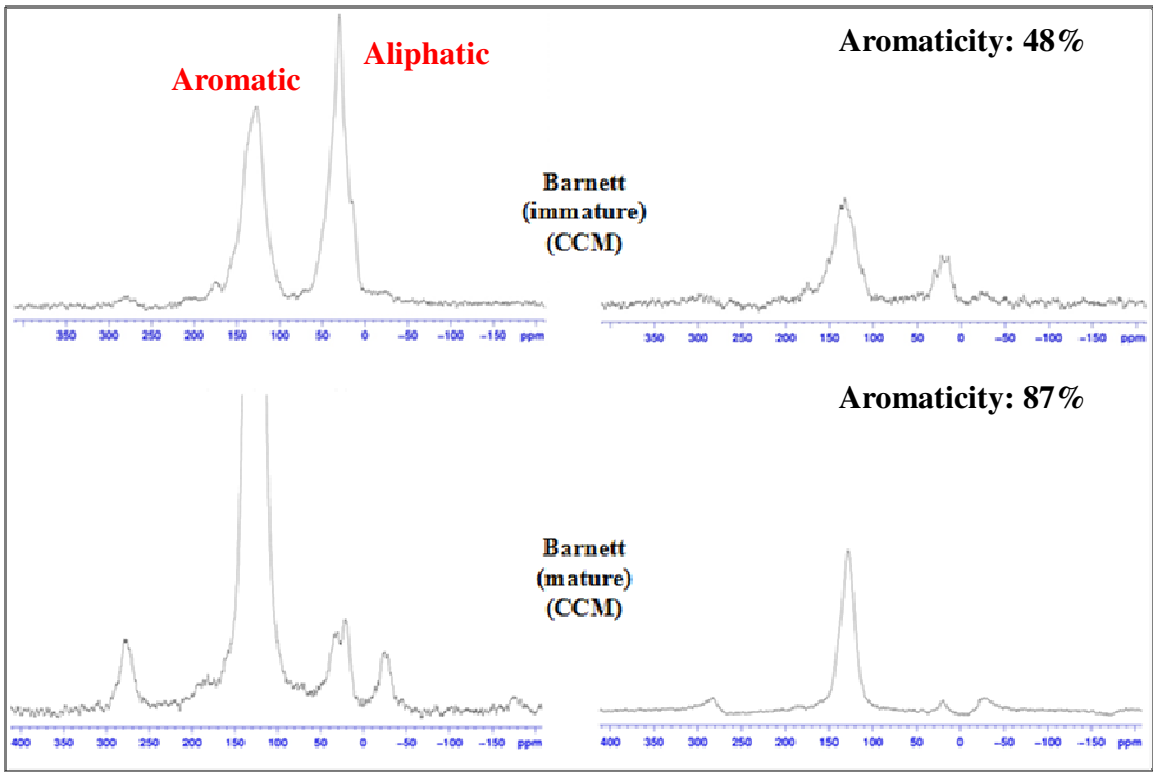

Figure 5.12. 2: Solid-state 13C NMR results for the Barnett kerogen comparing the thermally immature and the mature Barnett samples. On the left are the cross-polarization results and on the right are the dipolar dephasing results.

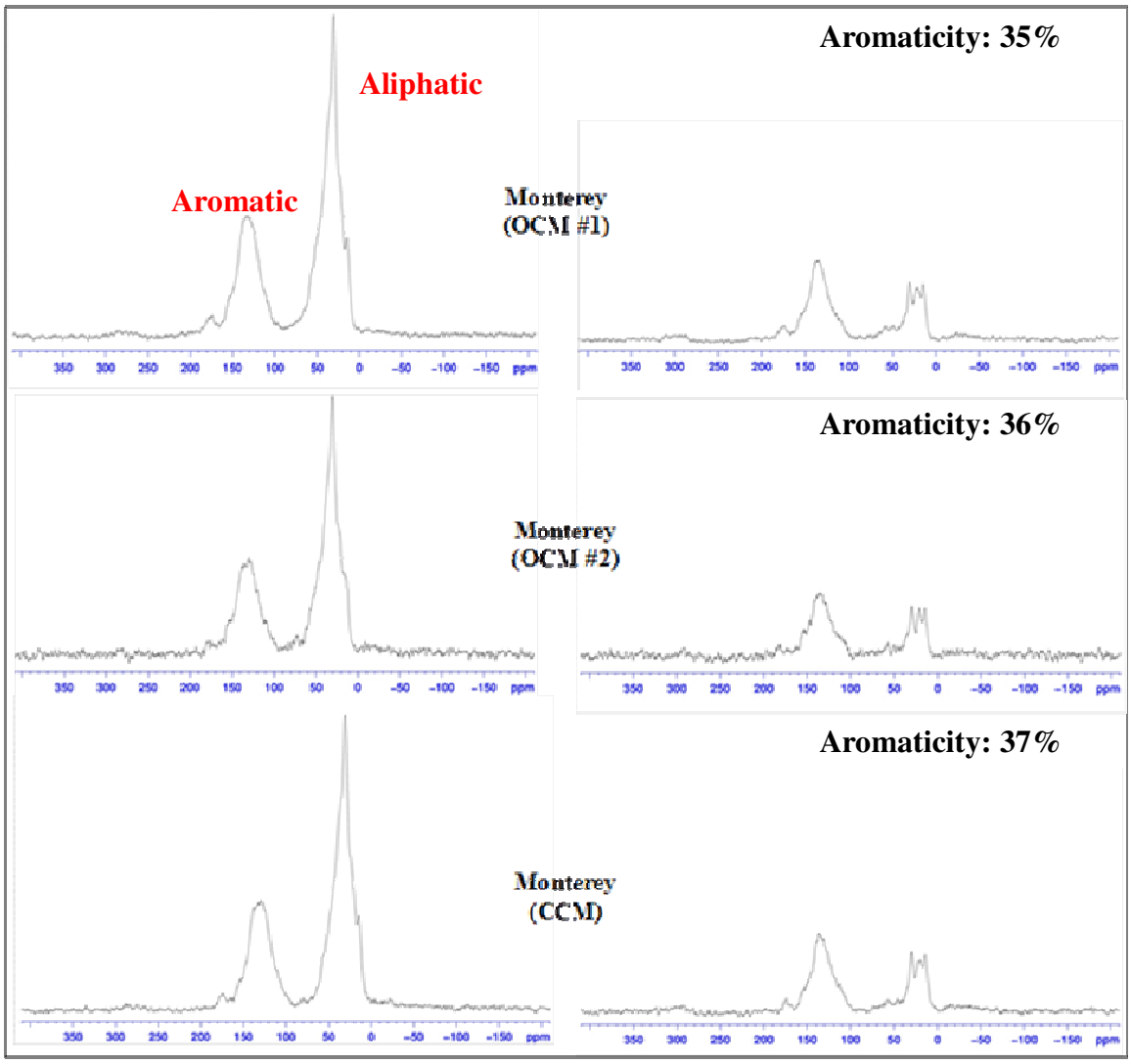

Figure 5.12.3: Solid-state 13C NMR results for the Monterey kerogen. On the left are the cross-polarization results and on the right are the dipolar dephasing results.

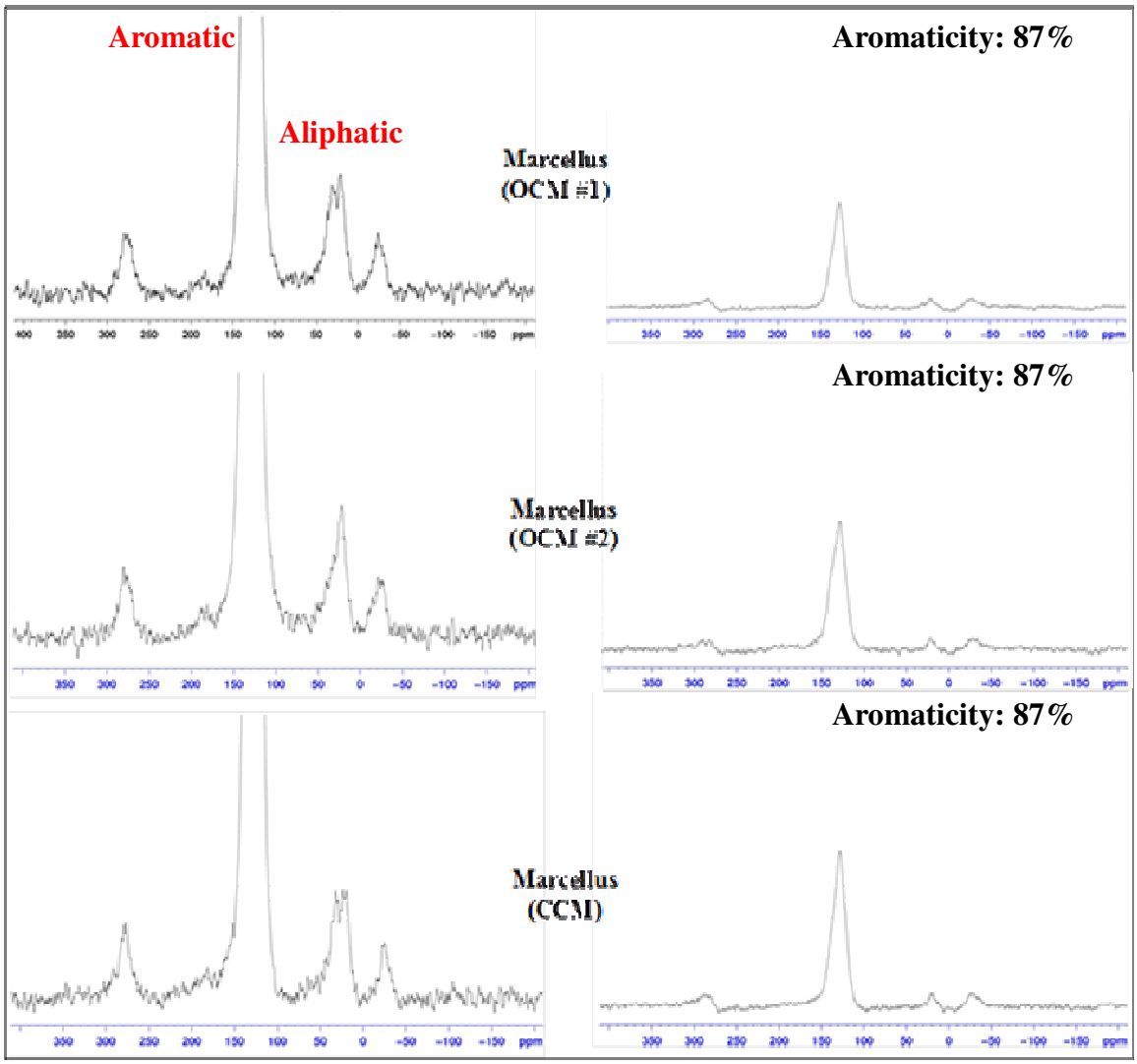

Figure 5.12.4: Solid-state 13C NMR results for the Marcellus kerogen. On the left are the cross-polarization results and on the right are the dipolar dephasing results.

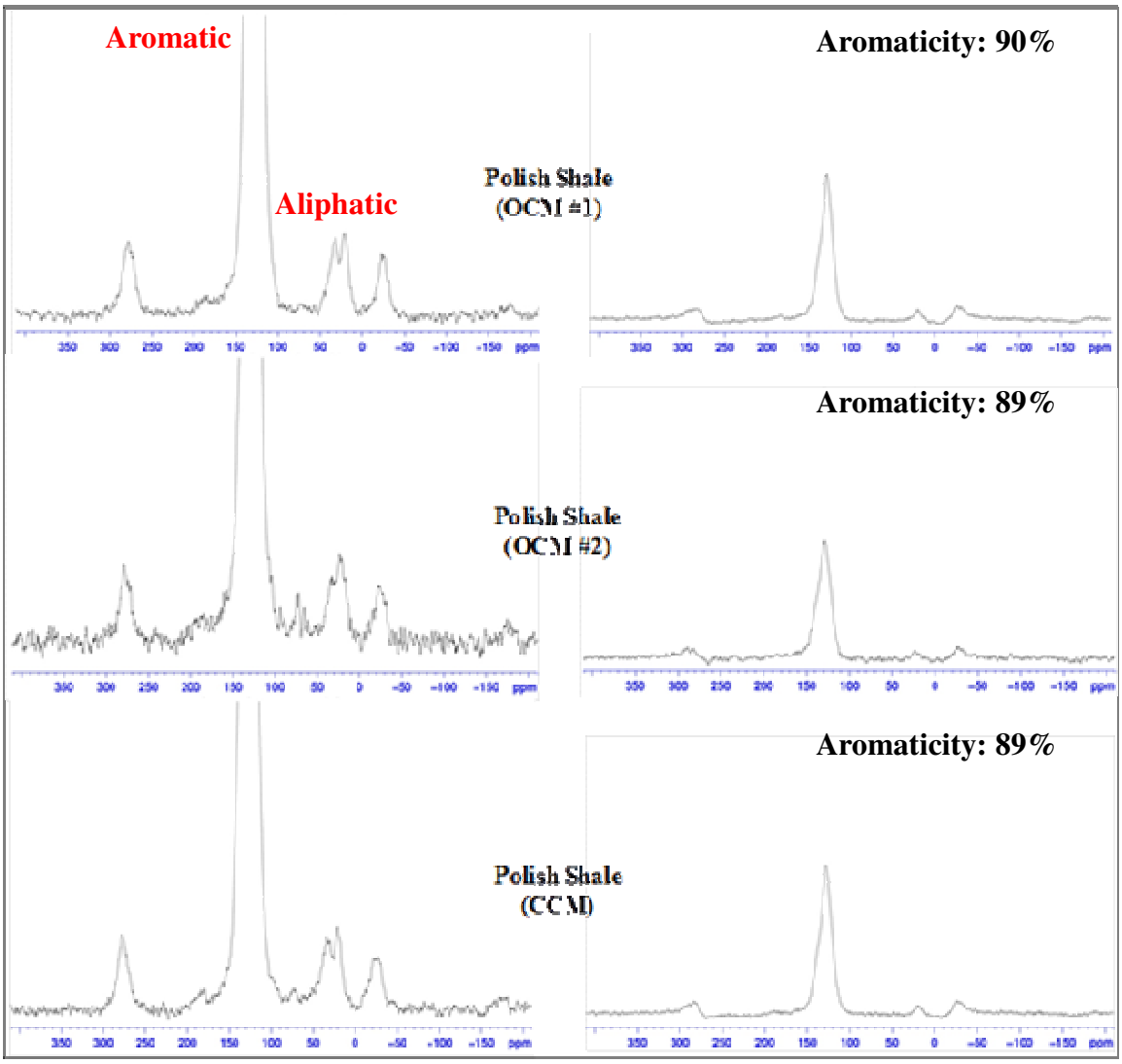

Figure 5.12 5:Solid-state 13C NMR results for the Polish Shale kerogen. On the left are the cross-polarization results and on the right are the dipolar dephasing results.

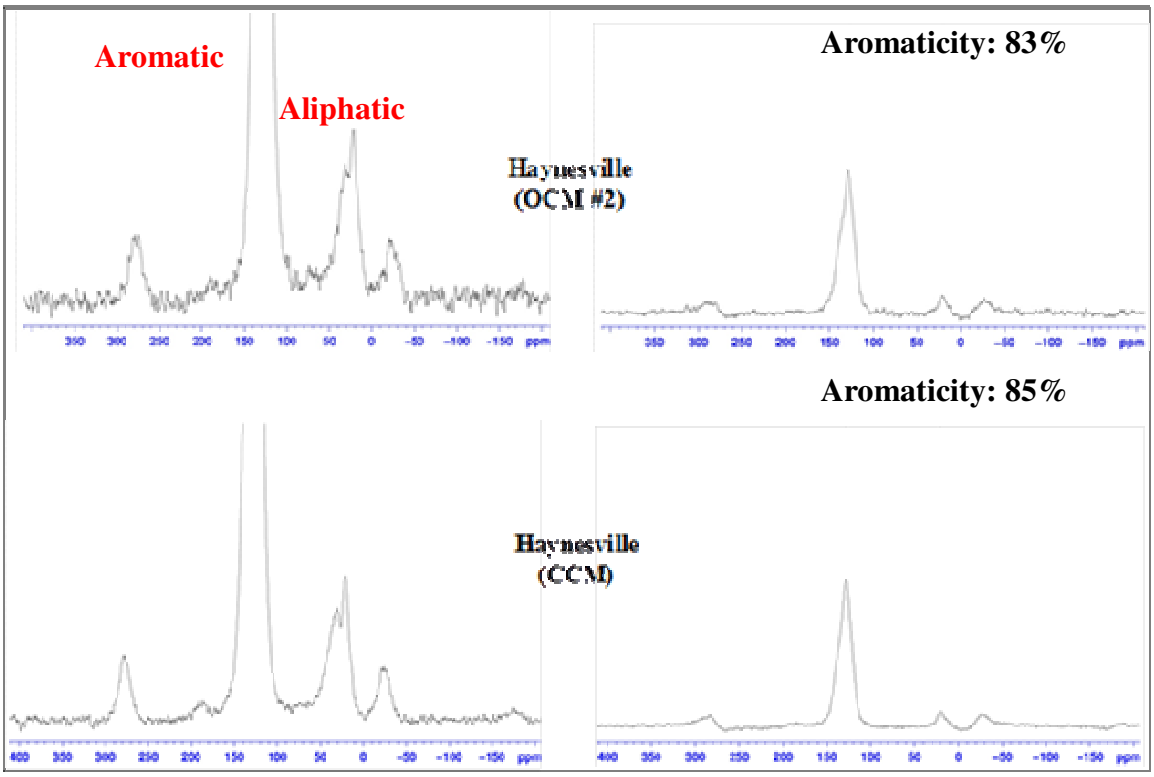

Figure 5.12.6:Solid-state 13C NMR results for the Haynesville kerogen. On the left are the cross-polarization results and on the right are the dipolar dephasing results.

Chapter 6: Discussion

6.1 Whole-Rock Properties

RockEval results for the whole-rock and the bitumen-free (solvent-extracted) rock were plotted on a modified van Krevelen Diagram (Figure 6.1.1). Based on the location of the samples in the plot the Monterey is an oil- and gas-prone source rock with Type II kerogen. The $Barnett_{imm}$ is also an oil- and gas-prone source rock with Type II kerogen. The hydrogen and oxygen indices of the Marcellus, the Haynesville, and Polish shales fall in the indeterminate area of the diagram where all three trends merge, reflecting their severe level of thermal alteration. At this stage of thermal maturity, it is virtually impossible to determine the original kerogen types in these shales.

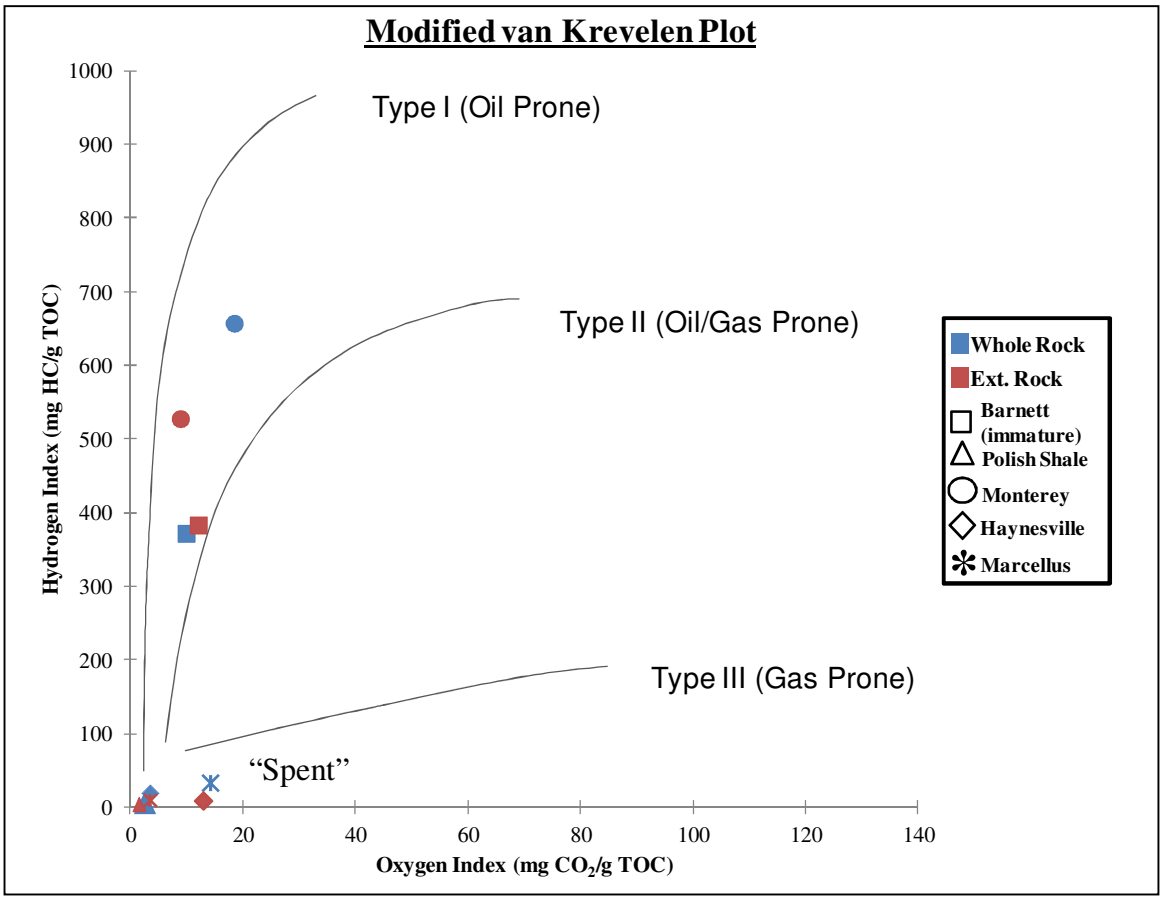

Figure 6.1.1: Modified van Krevelen Plot of RockEval Pyrolysis results. Plot from Ibrahimov and Bissada (2010).

Figure 6.1.2 is a diagram used for characterizing the samples based on TOC wt% versus THGP mg HC/g rock. Plots of the data for the native shales also show the Monterey and $Barnett_{imm}$ as mixed oil- and gas-prone, whereas the Marcellus, the Haynesville, and the Polish shales plot below the gas-prone area of the diagram where "spent" shales (dead carbon) normally plot. The Marcellus was the only sample where the non-extracted whole-rock falls in a different category from that of the extracted whole-rock. The reason for this is that the Marcellus sample used in this study was drilled with an oil-based drilling fluid and as a result the S1 was contaminated causing the non-extracted rock to plot in the gas/oil range when in fact it should be in the gas-prone area. The Haynesville shale shows a slight sign of contamination from the oil-based drilling fluid that was used to recover it. Table 6.1.1 summarizes the organic-matter richness of the whole-rock based on TOC.

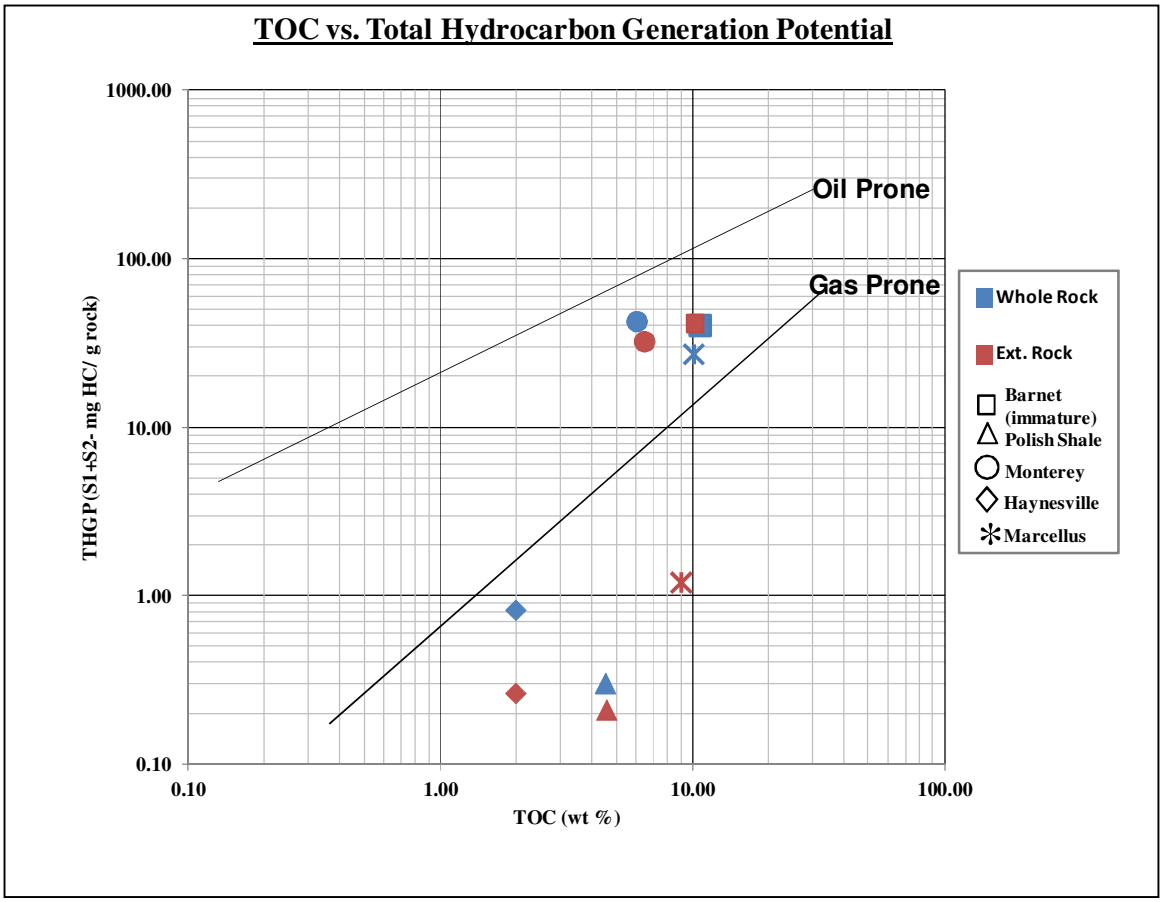

Figure 6.1.2: Plot of TOC vs. THGP to determine oil- vs. gas-proneness of samples. Plot from Ibrahimov and Bissada (2010).

Quantity of Organic Matter	Wt% TOC	Sample
Poor	<0.5	
Fair	0.5-1.0	
Good	1.0-2.0	
Very Good	2.0-4.0	Haynesville
Excellent	>4.0	Polish Shale, Monterey, Marcellus, Barnett (immature)

Table 6.1.1: Organic richness of the native shale samples (Richness scale modified from Baskin, 1997).

For only one of the sample suite, the Marcellus, the porosity and gas and liquid permeabilities were measured at different confining pressures and the results are given in Table 6.1.2. These measurements were carried out on core plugs 1" in diameter by 1 ½" in length. The porosity for the Marcellus ranges from 1.53 to 8.63 %, liquid permeability ranges from 0.043 to 3.199 µ Darcy, and gas permeability ranges from 0.013 to 9.049 µ Darcy.

(500 psi used as mean pore pressure; 200 psi as differential pressure; all measurements at 28˚C ± 0.1 constant temperature)										
Sample Marcellus	Density (gm/cm³)	1000 psi confining pressures			2000 psi confining pressures			3000 psi confining pressures		
		Gas Permeability k_g (µ Darcy)	*Liquid Permeability* k_l (µ Darcy)	*Porosity* ϕ_e (%)	*Gas Permeability* k_g (µ Darcy)	*Liquid Permeability* k_l (µ Darcy)	*Porosity* ϕ_e (%)	*Gas Permeability* k_g (µ Darcy)	*Liquid Permeability* k_l (µ Darcy)	*Porosity* ϕ_e (%)
Depth A	2.47	0.293	0.210	8.63	0.059	_	5.09	0.022	_	4.56
Depth B	2.45	0.196	0.120	6.11	0.079	_	4.16	0.038	_	3.91
Depth C	2.53	9.049	3.199	6.09	3.341	2.239	5.49	1.882	0.842	4.46
Depth D	2.55	0.089	0.043	4.35	0.041	_	3.01	0.020	_	2.37
Depth E	2.69	0.218	0.102	5.45	0.054	_	3.89	0.043	_	2.79
Depth F	2.93	0.027	_	3.48	0.019	_	1.71	0.013	_	1.53
Notes: k_g is gas permeability measured using Nitrogen (in micro Darcy) k_l is liquid permeability calculated from Klinkinberg effect (in micro Darcy) ϕ_e is porosity measured using corrected Boyle's Law The permeability error bar is 4%.										

Table 6.1.2: Permeability and porosity calculations for the Marcellus shale in this study. Increasing depth from A to F.

6.2 Kerogen Recovery and Purity

Based on the kerogen-recovery results (Figure 5.7.1), the CCM for kerogen isolation typically has much higher recoveries especially for source rocks with less richness (lower TOC) and higher maturity. This is most likely due to the significant loss of material during the open-methods (OCM #1 and OCM #2) for kerogen isolation caused by decanting.

Recovery is also affected by the purity of the samples which is based on the ash content of the kerogen. For the samples isolated via OCM #1 and OCM #2, the ash content was much higher than the closed-method (CCM) meaning there is more inorganics still present in the kerogen. This is related to the much more rigorous treatment the samples undergo in the CCM. The purity of the samples from the CCM is much higher than those of the OCM which were supported by the XRD (Figure 5.5.1 through 5.5.5) carried out on all the kerogens. The kerogen samples recovered from the OCM approaches had multiple minerals that appeared in the XRD including quartz, pyrite, and a neo-fluoride called ralstonite. Neo-fluorides are not native minerals in the samples. Instead they form during the kerogen isolation process under a warm, fluorine rich environment. As was discussed earlier this is one of the risks with the OCM for kerogen isolation.

6.3 Kerogen Elemental Properties

The elemental analysis results were converted into atomic ratios in order to plot the samples on a modified van Krevelen diagram (Figure 6.3.1). This allows for determination of kerogen type and maturity based on well established interpretation schemes in coal science. Based on Figure 6.3.1, the notable differences are in the O/C ratios which are most likely caused by the presence of inorganics and fluorine (i.e. ralstonite) in the open-method kerogens. The Polish shale kerogen, the Haynesville kerogen, and the Marcellus kerogen all plot in the thermally matured region of the diagram. There is one Marcellus kerogen from the OCM #2 which falls very far outside of the group. This could be due to the presence of the inorganics in the kerogen resulting in erroneous oxygen values. For the Haynesville and Polish shale kerogens from OCM #2

the values do not fall in the thermally mature range that the other corresponding kerogens plotted in (see Figure 6.3.1). Similar to the Marcellus kerogen from OCM #2, the presence of inorganics and also fluorine is interfering with the results. Clearly the open-methods inefficiency in removing inorganic mineralogy and the introduction of fluorides, such as the ralstonite, are resulting in incorrect maturity information for some of the Haynesville and Polish Shale kerogens. As far as the H/C atomic ratios are concerned, there is no significant influence from the methodology used for isolation.

The S/C ratio of the Monterey shale fits Orr's (1986) condition for a sulfur-rich sample with a S/C greater than 0.04. Also when you compare the S/C of the kerogen isolated via the open-methods, they are higher than those isolated via the closed-method (see Appendix for S/C values). This is most likely caused by the presence of the pyritic sulfur in the samples isolated via the OCM.

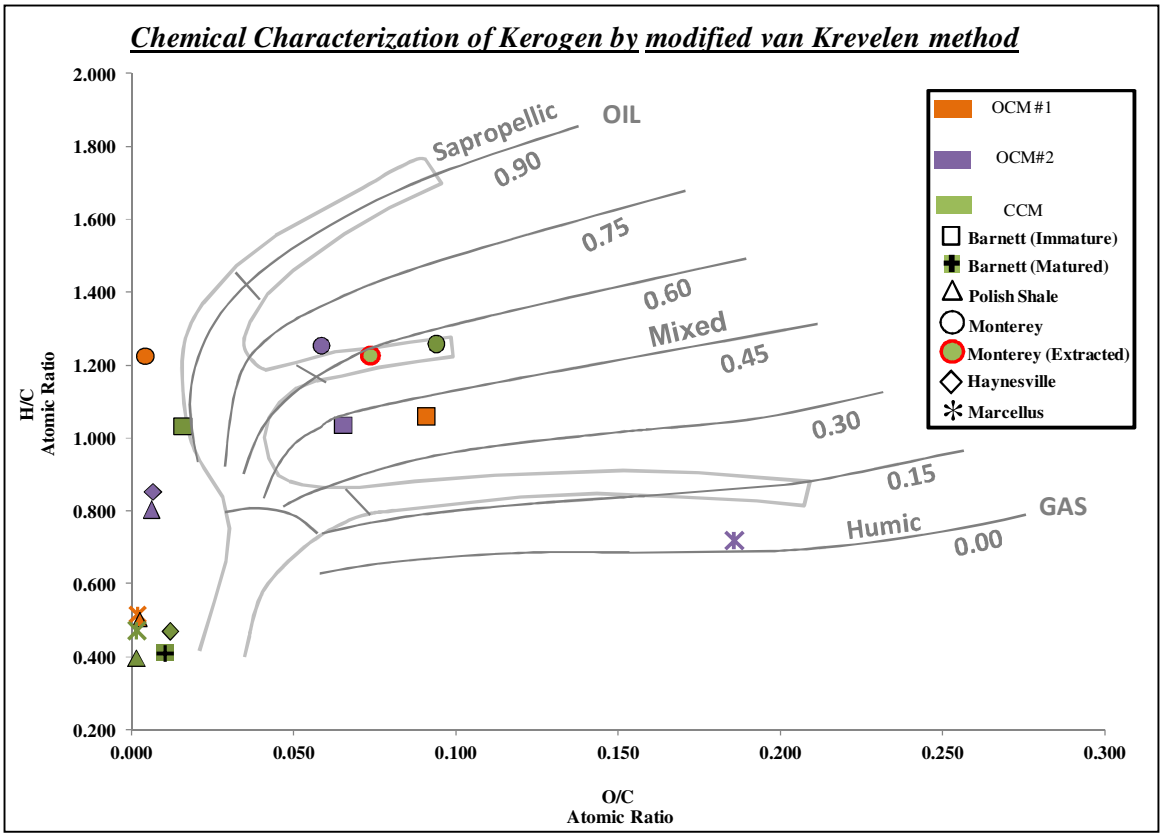

Figure 6.3.1: Chemical characterization of kerogen by van Krevelen method. Plot from Ibrahimov an d Bissada (2010).

6.4 Kerogen Structural (Physical) Properties

The physical properties of the kerogen show no evidence of alteration by any of the methods used for isolation. The vitrinite reflectance readings across the methods were reasonably close to each other. The only notable difference was the significantly larger amount of pyrite in the open-method kerogens unlike the closed-method kerogens.

6.5 Kerogen Isotopic Properties

The isotopic properties of the kerogen were studied to assess if any fractionation was taking place during kerogen isolation via the open-method (OCM #1 and OCM #2) versus the closed-method (CCM). The bulk carbon isotopes had no significant change in the values across the methods as seen in Figure 5.9.1. The fact that there is almost no

variation in the carbon isotope values for the kerogens isolated by either method could be explained by two possibilities. One is that the organic carbon in the whole-rock was homogeneous to begin with, such that there would be no observed isotope fractionation of the kerogen's carbon in spite of losses in the overall kerogen amounts during decantation of the samples in the open-methods. A second possibility is that the carbon in the macerals was homogenized during the isolation process, such that there would also be no difference in the isotope values.

Sulfur isotopes had notable variance in the values across the labs as seen in Figure 5.9.2. The whole-rock sulfur forms results were integrated with the kerogen sulfur values and their relationship is shown in Figure 6.5.1. The pie charts show the amount of sulfate sulfur, pyritic sulfur and organic sulfur. The samples with the most variance in the isotope values across methods are the ones which have majority of their sulfur in the pyritic sulfur form. For the Monterey and the $Barnett_{imm}$ shales, pyritic sulfur makes up about 40% of the sulfur in the whole-rock and their corresponding kerogens showed the least variance in their sulfur isotope values. For the Polish shale, the Haynesville shale, and the Marcellus shale pyritic sulfur makes up between 71-83% of the sulfur in the whole-rock and their corresponding kerogens had the greatest variations in their sulfur isotope values. One explanation for the apparent link between pyritic sulfur and the isotopes is related to the effectiveness of the OCM in removing pyrite from the samples.

From XRD data and the visual kerogen assessment the presence of pyrite was noted in the kerogen isolated via OCM #1 and OCM #2. Thus, the pyrite which still remains in the kerogen isolated via the OCM give incorrect sulfur isotope values as seen in Figure 6.5.1.

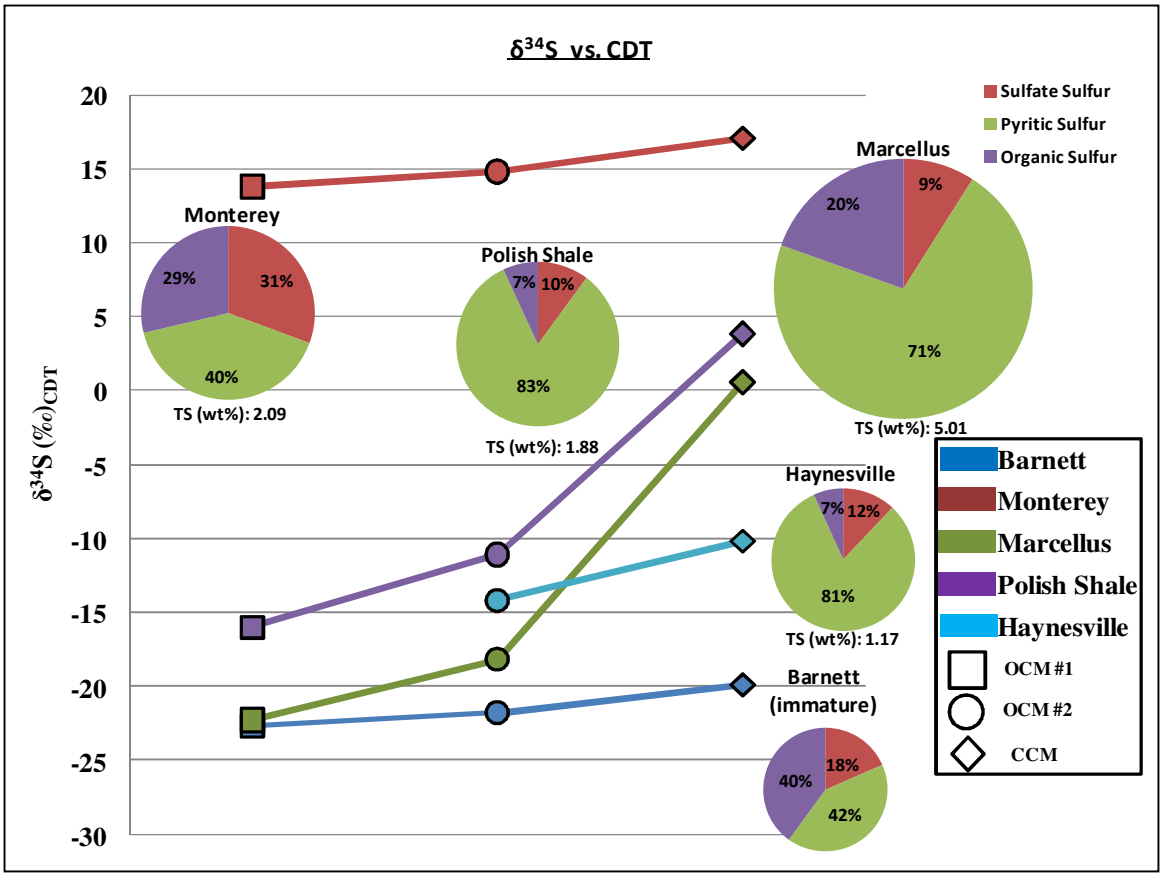

Figure 6.5.1: Results of the sulfur isotopes (±0.3‰) of the kerogens showing the sulfur form results for the whole-rock with the percentages of sulfate, pyritic, and organic sulfur. Note the relationship between high amounts of pyritic sulfur and greater variance in the sulfur isotopes.

6.6 Kerogen Molecular Properties

Pyrolysis-GC was contracted to Weatherford Laboratories to study the molecular properties of the kerogen. Figure 6.6.1 plots compare the alkanes, alkenes, and aromatics for the samples based on the Py-GC of the kerogens. Note the variability in the values. Overall the values follow the same pattern but with varying intensities based on the isolation method used.

The Polish and the Haynesville sample both show larger differences in the alkenes. Presence of impurities (inorganic mineralogy) in the open-method (OCM)

kerogen may help explain the different cracking behaviors of the kerogen seen in the Py-GC results. As mentioned above, the n-alkene/n-alkane ratios show much variability across samples isolated by the three methods, as though the same sample's kerogen has been structurally altered in varying degrees or the kerogen mix has been fractionated to various extents during processing. This is of concern to those who deal with kerogen retorting.

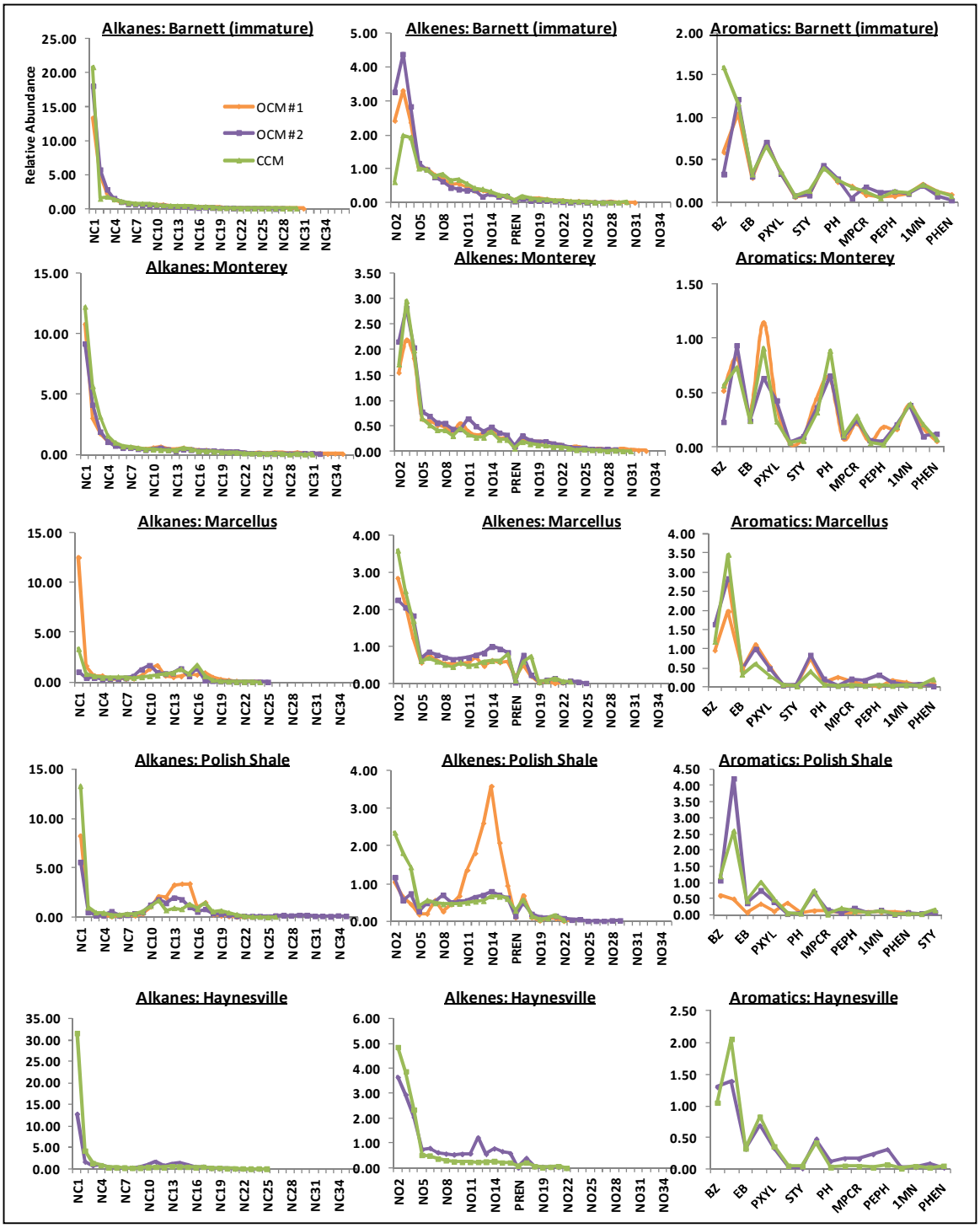

Figure 6.6.1: The above plots compare the alkanes, alkenes, and aromatics for the samples based on the Py-GC of the kerogens. Overall the values follow the same pattern but with varying intensities based on the isolation method used. Presence of impurities (inorganic mineralogy) in the OCM kerogen may help explain the different cracking behaviors of the kerogen.

6.7 Kerogen Spectroscopic Properties

Elucidation of the structure of kerogen has been a challenge and has been attempted through the integration of various techniques like pyrolysis, IR and NMR spectroscopy, elemental analysis, study of degradation products, functional group studies, and computer structure modeling (Rullkotter and Michaelis, 1989; Vandenbroucke and Largeau, 2007). See Vandenbroucke and Largeau (2007) for a history on kerogen structure studies and Vandenbroucke (2003) for structural models for different kerogen types.

The preliminary results given in this study show there were no notable differences in the ^{13}C NMR of the kerogen in this study. The spectra for the Monterey and the $Barnett_{imm}$ showed much more complexity in the structure of the kerogens versus the highly aromatic structures of the $Barnett_{mat}$, the Marcellus, the Polish, and the Haynesville samples. One possibility for not seeing changes in the structure of the kerogens, even though there are distinct changes in the elemental, isotopic, and molecular structure, could be that the ^{13}C NMR singles out only the carbon structure and cannot image the periphery structures. Much like when a petrographer does vitrinite reflectance, they look down a microscope and only pick certain vitrinite particles and they ignore the rest of slide, even though it is part of the entire structure. Kelemen et al. (2007) acknowledged that the weakness of the solid-state NMR analysis is that the results are to be viewed as an averaged composition. Furthermore, since no change was noted in the kerogen $\delta^{13}C$, this could relate to not being able to note any differences in the kerogen structure using a ^{13}C based NMR.

To truly address the structure aspect of the kerogen then integrated with this approach should be other NMR techniques which specifically focus on the other functional groups present in the kerogen. Maybe then any variability in the structure of the kerogen will become visible.

Chapter 7: Summary and Conclusions

This work has documented the effects of isolation methods on the elemental, isotropic, spectroscopic, and structural (physical) properties of kerogen. Table 7.1 summarizes most of these properties for the kerogens in the five gas and oil shales studied here. Also documented are the characteristics of the bulk (whole-rock) shales. Careful review of the data sets and interpretations gathered, lead to the following conclusions:

1. The closed-conservative method (CCM) for quantitative isolation and recovery of kerogen from the rock matrix in which it is intimately imbedded has been shown to yield ultra-pure kerogen that is of research quality, whereas the open-conventional method (OCM) yielded ash-rich, altered and fractionated kerogen. Based on the findings in this study and those of Ibrahimov and Bissada (2010), the CCM yields kerogen that allows more accurate interpretation of kerogen origin, thermal maturity, and depositional environment. It is important to note that the effective porosity in gas shales is now thought by some to lie mostly within the organic micro structure of the kerogen. If this is a critical element in assessing storage capacity of gas shales, then it will be important to recover kerogen that is the best representative of the system.
2. Based on the kerogen-purity assessment parameters (ash content and XRD analysis), the kerogens isolated via the OCM had large amounts of impurities including quartz, pyrite, and ralstonite. For the kerogen samples isolated via OCM #1 and OCM #2, the ash content was much higher than the ash content in the CCM-separated kerogen. There is more inorganics still present in the OCM-separated kerogen. This is related to the much more rigorous treatment the

samples undergo in the CCM. The purity of the samples from the CCM is supported by the XRD analysis of the kerogens

3. Quantitative mass balance calculations for kerogen recovery showed higher recovery efficiencies for the CCM-separated kerogen: Greater than 81%, while the OCM were less than 75%. The CCM for kerogen isolation typically yields much higher recoveries especially for carbon-lean source rocks (lower TOC) with higher maturity. This is most likely due to the significant loss of material during the OCM #1 and OCM #2 during the decanting steps of the methods.
4. Kerogen chemical integrity was assessed via elemental analysis and stable carbon and sulfur isotope analysis. Kerogen isolated via the CCM had higher carbon wt% than those isolated via the OCM Stable carbon isotope analysis did not show any significant difference in the $\delta^{13}C$ values of the kerogens. Stable sulfur isotope analysis showed significant differences in the $\delta^{34}S$ for the kerogens separated by the various methods. Integration of the whole-rock sulfur-forms information, the XRD mineralogy information, and sulfur isotope data helped explain the differences in the $\delta^{34}S$ values. The kerogens showing the greatest differences in the $\delta^{34}S$ compositions were the kerogens with the largest amount of pyrite measured in the XRD data, and those whose parent rocks showed the highest proportions of pyritic sulfur in the sulfur-forms data.
5. Microscopic analysis of vitrinite reflectivity did not show significant differences in the R_o eq of the kerogens, but it showed that the kerogen isolated via OCM #1 and OCM #2 had much higher pyrite content.

6. Molecular properties of the pyrolysis products of kerogens isolated by the various methods, as studied by Py-GC, showed differences in the alkene/alkane ratios and in the amounts of pyrolytically generated aromatic compounds
7. Spectroscopic analysis conducted with solid-state ^{13}C NMR showed no significant differences in the structure of the kerogens isolated via OCM versus CCM. One possible reason for not seeing differences in the structure of the kerogens might be that the ^{13}C NMR focuses only on the carbon structure and cannot image the periphery structures. The immature Barnett NMR spectra show high aliphaticity (low aromaticity). Similarly, the Monterey NMR spectra show high-aliphaticity versus aromaticity. The Marcellus, the Haynesville, and the Polish Shale NMR spectra all show much higher aromaticities. The immature Barnett has an aromaticity of 47-48%, whereas the mature Barnett has an aromaticity of 87%. The low-maturity Monterey kerogen shows aromaticities of only of 35-37% whereas the highly altered Marcellus kerogen shows aromaticities of 87%. Similarly, the highly metamorphosed Polish Shale and Haynesville shale show aromaticities of 89-90%, and 83%-85%, respectively.

	OCM #1	OCM #2	CCM	OCM #1	OCM #2	CCM	OCM #1	OCM #2	CCM	OCM #1	OCM #2	CCM	OCM #2	CCM
Sample	Barnett	Barnett	Barnett	Monterey	Monterey	Monterey	Marcellus	Marcellus	Marcellus	Polish Shale	Polish Shale	Polish Shale	Haynesville	Haynesville
Elemental Analysis (normalized)														
Carbon wt%	74.16	77.32	82.69	74.59	71.61	70.37	87.04	71.83	90.80	82.79	83.62	91.71	77.53	91.57
Hydrogen wt%	6.59	6.72	7.16	7.66	7.53	7.43	3.77	4.34	3.59	3.49	5.64	3.05	5.55	3.61
Nitrogen wt%	3.36	3.46	3.76	2.34	2.26	2.69	1.77	1.83	2.29	2.48	2.51	2.55	1.50	1.47
Sulfur wt%	6.90	5.78	4.66	14.97	13.00	10.71	7.19	4.22	3.11	10.94	7.54	2.48	14.73	1.89
Oxygen wt%	8.98	6.72	1.73	0.43	5.59	8.81	0.23	17.78	0.21	0.30	0.68	0.21	0.68	1.46
H/C Atomic Ratio	1.059	1.035	1.031	1.224	1.253	1.258	0.517	0.720	0.471	0.502	0.804	0.397	0.854	0.469
O/C Atomic Ratio	0.091	0.065	0.016	0.004	0.059	0.094	0.002	0.186	0.002	0.003	0.006	0.002	0.007	0.012
Aromaticty-Pyrolysis-GC (%)	4.78	4.68	6.04	5.74	4.93	5.36	6.87	8.53	6.91	2.88	8.48	7.45	5.75	5.51
Aromaticity-NMR (%)	47	48	48	35	36	37	87	87	87	90	89	89	83	N/A
Sulfur Isotopes (‰)	-22.7	-21.8	-19.9	13.8	14.8	17.1	-22.3	-18.2	0.5	-16	-11.1	3.8	-14.2	-10.2
Carbon Isotopes (‰)	-30.5	-30.2	-30.7	-22.5	-22.1	-22.5	-29.3	-29.5	-29.5	-29.8	-30.0	-30.0	-25.8	-25.8

Table 7. 1: Summary table of the elemental, isotopic, molecular, and spectroscopic results. Note the variance in the results. Aromaticity is given from the Py-GC and the NMR which differ greatly.

Chapter 8: Recommendations

To address the many questions that this research study has raised much more work must be done. Below are some recommendations for future work.

1. The question of what causes the differences in sulfur isotopic compositions, can be addressed with sulfur isotope analyses on the three sulfur forms (sulfate, pyritic, and organic sulfur).
2. To address the effects of the kerogen isolation methods on kerogen gas-retention and storage capacity, SEM/FIB can be a helpful tool for imaging the nano-pores of the kerogen and seeing if any changes have occurred.
3. To constrain the molecular structure of the kerogen from the five shales, a more in depth study of the NMR is needed. The first step will be to run NMR on simple highly aromatic compounds with relatively few small ring systems (anthracene, pyrene, and biphenyl). The purpose is to see if the reference compounds' dipolar dephasing behavior in the CP and direct ^{13}C pulse versions of the experiment show the essentially complete decay that is expected for aromatic CH signal and any aliphatic CH and CH2 signals. The next step will be to test simple structures with methyl and methylene groups. These spectra will lend support to the spectra from the kerogen.
4. An interesting aspect of the kerogen that would be helpful to study given the results shown in this study, is measuring the "grain density" of the kerogens isolated by the various methods.
5. Another concern to address is reproducibility of the CCM and OCM methods in this study. The next step would be to take a random shale and isolate it using both

methods several times in order to assess whether the isolation methods influence the precision of the analysis of the kerogen products.

References

Acholla, F.V. and Orr, W.L., 1993. Pyrite removal from kerogen without altering organic matter: The chromous chloride method. *Energy and Fuels*, Volume 7, pp. 406–410.

Australian Oil Company, 2010. Monterey Shale Play Map. [Online] Available at: http://www.australianoilcompany.com/los-alamos.html [Accessed July 2012].

Barwise, A.J.G., Mann, A.L, Eglinton, G., Gowar, A.P., Wardroper, A.M.K., and Gutteridge, C.S., 1984. Kerogen characterisation by ^{13}C NMR spectroscopy and pyrolysis-mass spectrometry. *Organic Geochemistry*, Volume 6, pp. 343-349.

Baskin, D.K., 1997. Atomic H/C ratio of kerogen as an estimate of thermal maturity and organic matter conversion. *AAPG Bulletin*, Volume 81, pp. 1437-1540.

Baskin, D.K. and Peters, K.E., 1992. Early generation characteristics of a sulfur-rich Monterey kerogen. *AAPG Bulletin*, Volume 76, pp. 1-13.

Bordenave, M.L., Espitalie, J., Leplat, P., Oudin, J.L., and Vandernbroucke, M., 1993. Screening techniques for source rock evaluation. In: Bordenave, M.L. (Ed), *Applied Petroleum Geochemistry*. Editions Technip, pp. 219-278.

Breeden, D and Shipman, J, 2004. Shale analysis for mud engineers. AADE-04-DF-HO-30 presented at the AADE 2004 Drilling Fluids Conference, pp. 1-17.

Curiale, J.A. and Odermatt, J.R., 1988. Short-term biomarker variability in the Monterey Formation, Santa Maria Basin. *Organic Geochemistry*, Volume 14, pp. 1-13.

Down, A.L., and Himus, G.W., 1941. A preliminary study of the chemical constitution of kerogen. *Journal of the Institute of Petroleum*, Volume 27, pp. 426-445.

Durand, B., 1980. Sedimentary organic matter and kerogen. definition and quantitative importance of kerogen. In: Durand, B. (Ed.), *Kerogen, Insoluble Organic Matter from Sedimentary Rocks*. Editions Technip, Paris, pp. 13–34.

Durand, B. and Espitalie, J., 1973. Evolution de la matiere organique au cours de l'enfouissement des sediments. *Compte rendus de l'Academeie des Sciences, Paris*, Volume 276, pp. 2253-2256.

Durand, B. and Nicaise, G., 1980. Procedures of kerogen isolation. In: Durand, B. (Ed.), *Kerogen, Insoluble Organic Matter from Sedimentary Rocks*. Editions Technip, pp. 35–53.

Ettensohn, F.R., 1992. Controls on the origin of the Devonian-Mississippian oil and gas shales, east-central United States. *Fuel*, Volume 71, pp. 1487-1492.

Forsman, J.P. and Hunt, J.M., 1958. Insoluble organic matter (kerogen) in sedimentary rocks. *Geochimica et Cosmochimica Acta*, Volume 15, pp. 170–182.

Hill, R.J., Jarvie, D.M., Pollastro, R.M., and Ruble, T.E., 2007. Unconventional shale-gas systems: The Mississippian Barnett Shale of north-central Texas as one model for thermogenic shale-gas assessment. *AAPG Bulletin*, Volume 91, pp. 475-499.

Hitchon, B., Holloway, L.R., Bayliss, P., 1976. Formation of ralstonite during low-temperature acid digestion of shales. *Canadian Mineralogist*, Volume 14, pp. 391–392.

Hoefs, J., 1997. *Stable Isotope Geochemistry-Fourth Completely Revised, Updated, and Enlarged Edition*. Springer-Verlag Berlin Heidelberg, Germany, pp. 5-61.

Hutton, A., Bharati, S., and Robl, T., 1994. Chemical and petrographic classification of kerogen/macerals. *Energy & Fuels*, Volume 8, pp. 1478-1488.

Ibrahimov, R.A. and Bissada, K.K., 2010 Comparative analysis and geological significance of kerogen isolated using open-system (palynological) versus chemically and volumetrically conservative closed-system methods. *Organic Geochemistry*, Volume 41, pp. 800-811.

Jacobsen, N.E., 2007. *NMR Spectroscopy Explained Simplified Theory, Applications and Examples For Organic Chemistry and Structural Biology*. John Wiley & Sons, Inc., Hoboken, New Jersey, pp. 1-8.

Kelemen, S.R., Afeworki, M., Gorbaty, M.L., Sansone, M., Kwiatek, P.J., Walters, C.C., Freund, H., and Siskin, M., 2007. Direct characterization of kerogen by x-ray and solid-state ^{13}C nuclear magnetic resonance methods. *Energy & Fuels*, Volume 21, pp. 1548-1561.

Lambert, J.B. and Mazzola, E.P., 2004. *Nuclear Magnetic Resonance Spectroscopy- An Introduction to Principles, Applications, and Experimental Methods*. Pearson Education Inc., Upper Saddle River, New Jersey, pp. 1-47.

LaPlante, R.E., 1974. Hydrocarbon generation in gulf coast tertiary sediments. *AAPG Bulletin*, Volume 58, pp. 1281-1289.

National Energy Technology Lab (NETL), 2009. Modern Shale Gas Development in The United States: A Primer. [Online] Available at: www.netl.doe.gov/technlogies/oil-gas/ [Accessed July 2012].

Orr, W. L., 1986. Kerogen/asphaltene/sulfur relationships in sulfur-rich Monterey oils. *Advances in Organic Geochemistry*, Volume 10, pp. 499-516.

Rullkotter, J. and Michaelis, W., 1990. The structure of kerogen and related materials. A review of recent progress and future trends. *Organic Geochemistry*, Volume 16, pp. 829-852.

Ruppel, S.C. and Kane, J., 2006, The Mississippian Barnett Formation: A source-rock, seal, and reservoir produced by early carboniferous flooding of the Texas craton, The University of Texas at Austin, Bureau of Economic Geology, pp. 1-41. http://www.beg.utexas.edu/resprog/permianbasin/PBGSP_members/writ_synth/Mississippian_chapter.pdf.

Saxby, J.D., 1970 (a). Isolation of kerogens in sediments by chemical methods. *Chemical Geology*, Volume 6, pp. 173–184.

Saxby, J.D., 1970 (b). Technique for isolation of kerogen from sulfide ores. *Geochemica et Cosmochimica Acta*, Volume 34, pp. 1317-1326.

Shoolery, J., 1972. *A Basic Guide to NMR*. Varian Associates. Palo Alto, California, pp. 1-5.

Tissot, B., Durand, B., Espitalie´, J., Combaz, A., 1974. Influence of nature and diagenesis of organic matter in formation of petroleum. *AAPG Bulletin*, Volume 58, pp. 499–506.

Tissot, B. and Welte, D.H., 1978. *Petroleum Formation and Occurrence: A New Approach to Oil and Gas Exploration*. Springer-Verlag Berlin Heidelberg, Germany, pp. 123-147.

U.S. Energy Information Administration (EIA), 2011. Review of Emerging Resources: U.S. Shale Gas and Shale Oil Plays. [Online] Available at: ftp://ftp.eia.doe.gov/natgas/usshaleplays.pdf [Accessed July 2012].

Vandenbroucke, M., 2003. Kerogen: From types to models of chemical structure. *Oil & Gas Science and Technology-Rev*, Volume 58, pp. 243-269.

Vandenbroucke, M. and Largeau, C., 2007. Kerogen origin, evolution and structure. *Organic Geochemistry*, Volume 38, pp. 719-833.

Van De Meent, D., Brown, S. C., Philp, R.P., and Simoneit, B.R.T., 1980. Pyrolysis-high resolution gas chromatography and pyrolysis gas chromatography-mass spectrometry of kerogens and kerogen precursors. *Geochimica et Cosmochimica Acta*, Volume 44, pp. 99-1013.

Appendix

Company	Address
Weatherford Laboratories	143 Vision Park Boulevard Shenandoah, TX 77384
Intertek QTI	291 Route 22 East Salem Industrial Park, Bldg. #5 Whitehouse, NJ 08888
Isotech Laboratories	1308 Parkland Court Champaign Illinois 61821
National Petrographic Service, Inc.	5933 Bellaire Blvd., Suite 108 Houston, TX 77081

Addresses for the laboratories which provided analnyitcal services for this thesis.

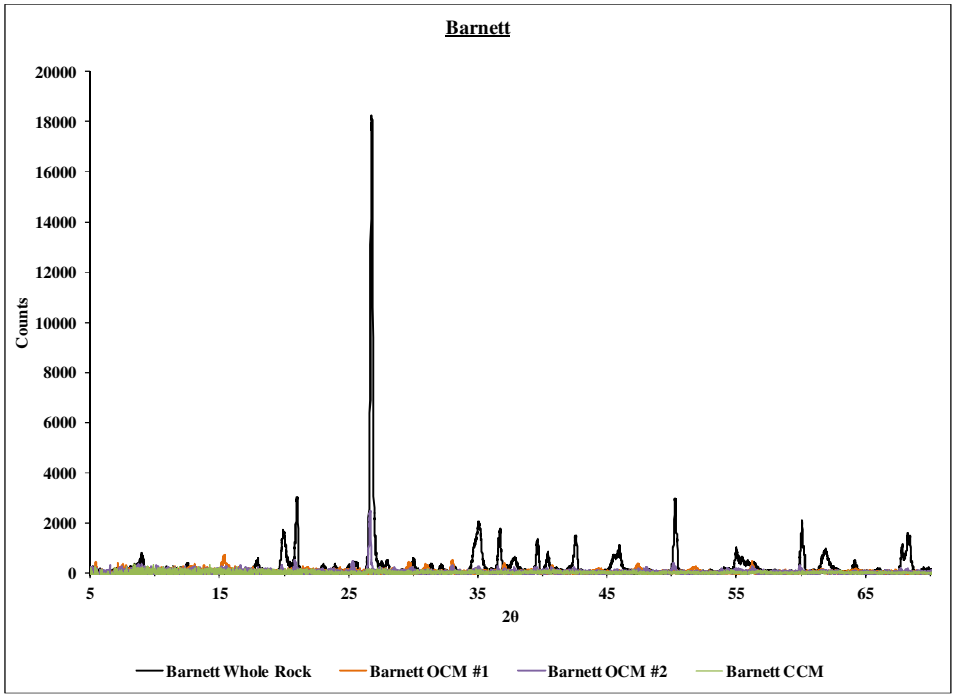

XRD diffractograms showing the whole-rock with corresponding kerogen overlapped for the immature Barnett.

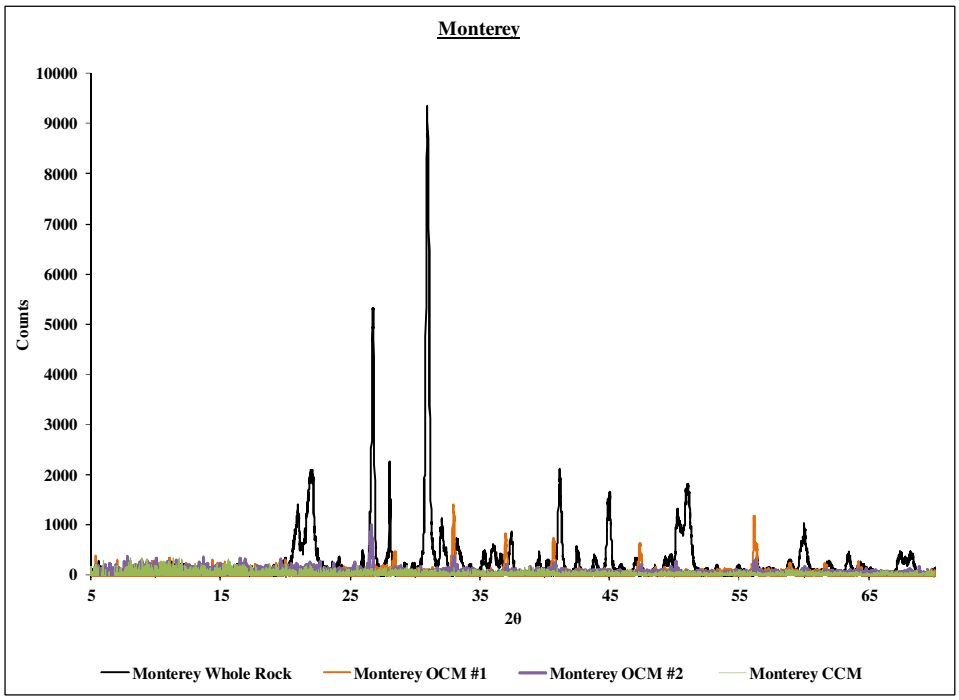

XRD diffractograms showing the whole-rock with corresponding kerogen for the Monterey.

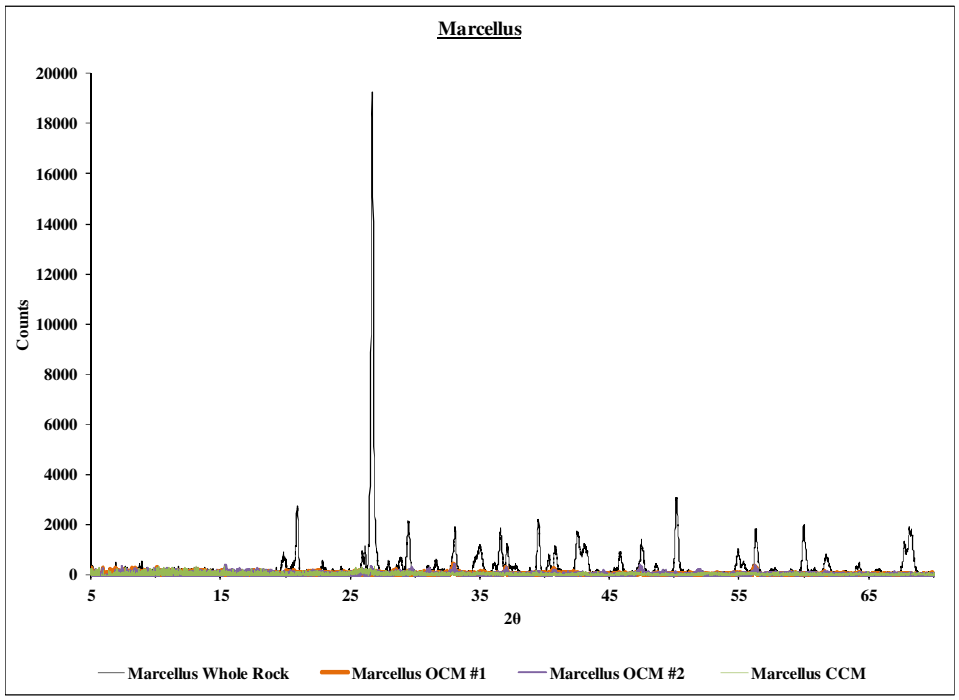

XRD diffractograms showing the whole-rock with corresponding kerogen for the Marcellus.

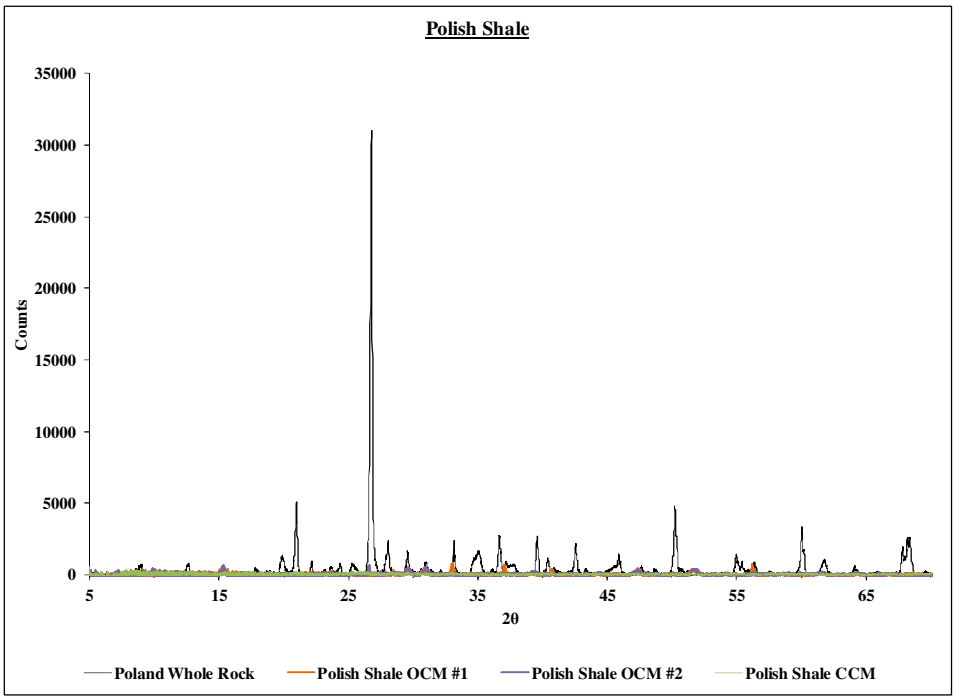

XRD diffractograms showing the whole-rock with corresponding kerogen for the Polish Shale.

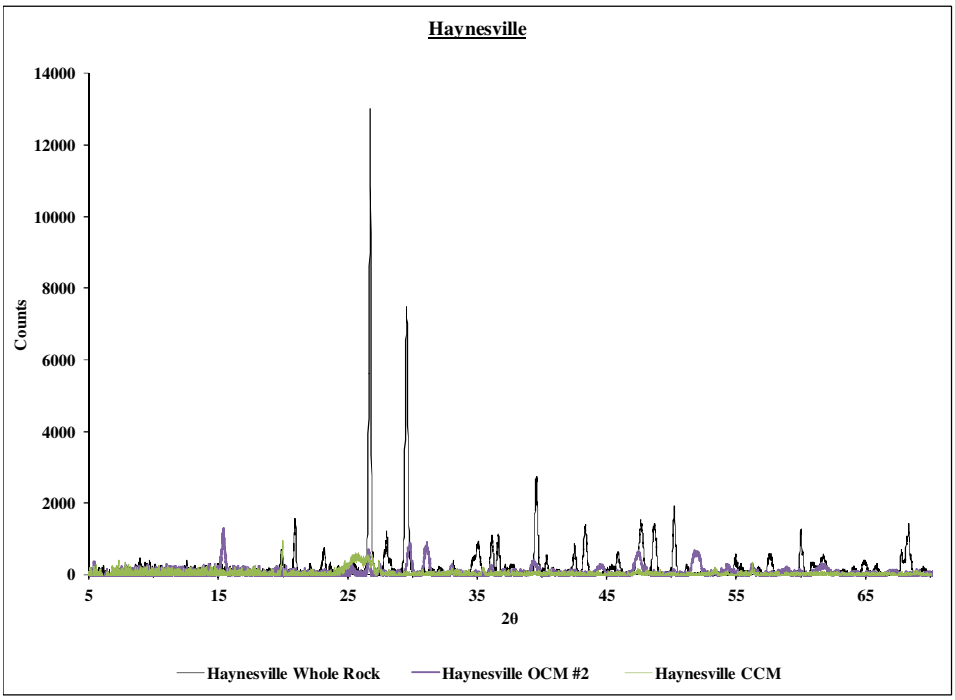

XRD diffractograms showing the whole-rock with corresponding kerogen for the Haynesville.

Elemental Analysis Results:

Measured values:

Sample ID	C (wt%)	H (wt%)	N (wt%)	S (wt%)	O (wt%)	Ash (wt%)	C (wt%)	H (wt%)	N (wt%)	S (wt%)	O (wt%)	Ash (wt%)	C (wt%)	H (wt%)	N (wt%)	S (wt%)	O (wt%)	Ash (wt%)
	Open-system						Open-system						Closed-system					
	Commercial Lab #1						Commercial Lab #2						UH Lab					
Barnett (immature)	59.53	5.29	2.70	5.54	7.21	9.82	41.33	3.59	1.85	3.09	3.59	17.58	71.53	6.19	3.25	4.03	1.50	0.05
Monterey	63.66	6.54	2.00	12.78	0.37	4.14	35.47	3.73	1.12	6.44	2.77	16.83	68.60	7.24	2.62	10.44	8.59	0.19
Marcellus	72.89	3.16	1.48	6.02	0.19	9.23	29.81	1.80	0.76	1.75	7.38	13.18	82.20	3.25	2.07	2.82	0.19	2.04
Narol PIG	51.76	2.18	1.55	6.84	0.19	23.32	23.28	1.57	0.70	2.10	0.19	27.22	81.07	2.70	2.25	2.19	0.19	4.20
Haynesville	Not Analyzed						21.64	1.55	0.42	4.11	0.19	34.34	82.01	3.23	1.32	1.69	1.31	2.77

Normalized values:

Sample ID	C (wt%)	H (wt%)	N (wt%)	S (wt%)	O (wt%)	C (wt%)	H (wt%)	N (wt%)	S (wt%)	O (wt%)	C (wt%)	H (wt%)	N (wt%)	S (wt%)	O (wt%)
	Open-system					Open-system					Closed-system				
	Commercial Lab #1					Commercial Lab #2					UH Lab				
Barnett (immature)	74.16	6.59	3.36	6.90	8.98	77.32	6.72	3.46	5.78	6.72	82.6936	7.156	3.75723	4.65896	1.7341
Monterey	74.59	7.66	2.34	14.97	0.43	71.61	7.53	2.26	13.00	5.59	70.3662	7.426	2.68746	10.70879	8.81116
Marcellus	87.04	3.77	1.77	7.19	0.23	71.83	4.34	1.83	4.22	17.78	90.7986	3.59	2.28653	3.11499	0.20988
Narol PIG	82.79	3.49	2.48	10.94	0.30	83.62	5.63937	2.51437	7.5431	0.68247	91.7081	3.054	2.54525	2.477376	0.21493
Haynesville	Not Analyzed					77.53	5.55357	1.50484	14.7259	0.68076	91.5699	3.607	1.47387	1.887003	1.46271

Atomic values:

Sample ID	Atomic H/C	Atomic O/C	Atomic S/C	Atomic N/C	Atomic H/C	Atomic O/C	Atomic S/C	Atomic N/C	Atomic H/C	Atomic O/C	Atomic S/C	Atomic N/C
	Open-system				Open-system				Closed-system			
	Commercial Lab #1				Commercial Lab #2				UH Lab			
Barnett (immature)	1.0589	0.09092	0.03486	0.03889	1.03505	0.06521	0.028	0.03838	1.03118	0.01574	0.0211	0.03896
Monterey	1.22418	0.00436	0.0752	0.02694	1.25309	0.05863	0.06801	0.02708	1.25762	0.094	0.05701	0.03275
Marcellus	0.5166	0.00196	0.03094	0.01741	0.71952	0.18585	0.02199	0.02186	0.47113	0.00174	0.01285	0.02159
Narol PIG	0.50188	0.00276	0.0495	0.02568	0.80362	0.00613	0.03379	0.02578	0.39686	0.00176	0.01012	0.0238
Haynesville	Not Analyzed				0.85351	0.00659	0.07114	0.01664	0.46932	0.01199	0.00772	0.0138

Kerogen Recovery Efficiency Results:

		C content of kerogen (wt%)			Theoretical Initial kerogen Content (wt%)			Total Initial Rk. Wt (g)			Acutal Kerogen Recovered (g)		
		Open-system		Closed-system	Open-system		Closed-system	Open-system		Closed-system	Open-system		Closed-system
Sample ID	TOC (wt%)	Commerical Lab #1	Commercial Lab #2	UH Lab	Commerical Lab #1	Commercial Lab #2	UH Lab	Commerical Lab #1	Commercial Lab #2	UH Lab	Commerical Lab #1	Commercial Lab #2	UH Lab
Barnett (immature)	10.70	74.16	77.32	82.69	14.43	13.84	12.94	39.90	35.02	30.09	1.98	4.03	3.81
Monterey	6.08	74.59	71.61	70.37	8.15	8.49	8.64	50.01	45.02	64.88	1.73	3.45	4.56
Marcellus	10.10	87.04	71.83	90.80	11.60	14.06	11.12	34.90	29.64	38.89	0.17	1.13	3.64
Narol PIG	4.53	82.79	83.62	91.71	5.47	5.42	4.94	71.16	65.14	81.79	0.32	0.47	3.88
Haynesville	2.00	N/A	77.53	91.57	N/A	2.58	2.18	N/A	45.11	48.51	N/A	0.57	0.96

	Theoretical Initial Kerogen (g)			Kerogen recovery of rock (%)			Kerogen recovery of initial kerogen (%)		
	Open-system		Closed-system	Open-system		Closed-system	Open-system		Closed-system
Sample ID	Commercial Lab #1	Commercial Lab #2	UH Lab	Commercial Lab #1	Commercial Lab #2	UH Lab	Commercial Lab #1	Commercial Lab #2	UH Lab
Barnett (immature)	5.76	4.85	3.89	4.96	11.51	12.66	34.39	83.17	97.83
Monterey	4.08	3.82	5.61	3.46	7.67	7.04	42.44	90.30	81.42
Marcellus	4.05	4.17	4.33	0.49	3.81	9.35	4.20	27.10	84.06
Narol PIG	3.89	3.53	4.04	0.45	0.72	4.74	8.22	13.28	96.05
Haynesville	N/A	1.16	1.06	N/A	1.27	1.98	N/A	49.23	90.50

Carbon Isotope Results:

Sample ID	$\delta^{13}C$ vs. PDB (‰)			δ13C vs. PDB (‰)			$\delta^{13}C$ vs. PDB (‰)		
	Open-system						Closed-system		
	Commercial Lab #1			Commercial Lab #2			UH Lab		
		SD	2SD		SD	2SD		SD	2SD
Barnett (immature)	-30.504	0.265	0.529	-30.151	0.040	0.079	-30.670	0.479	0.958
Monterey	-22.517	0.256	0.512	-22.085	0.440	0.880	-22.490	0.075	0.149
Marcellus	-29.337	0.348	0.696	-29.481	0.253	0.506	-29.459	0.342	0.684
Polish Shale	-29.797	0.378	0.755	-29.990	0.237	0.473	-29.981	0.295	0.589
Haynesville	Not Analyzed			-25.829	0.350	0.700	-25.820	0.426	0.852

Barnett Vitrinite Reflectance Readings:

Barnett Kerogen											
OCM #1				OCM #2				CCM			
Count	Ro	Count	Ro	Count	Ro	Count	Ro	Count	Ro	Count	Ro
1	0.211	51	0.422	1	0.162	51	0.375	1	0.152	51	0.416
2	0.211	52	0.432	2	0.162	52	0.375	2	0.152	52	0.426
3	0.221	53	0.442	3	0.203	53	0.375	3	0.203	53	0.436
4	0.231	54	0.442	4	0.223	54	0.375	4	0.203	54	0.436
5	0.231	55	0.442	5	0.254	55	0.386	5	0.254	55	0.436
6	0.231	56	0.452	6	0.254	56	0.386	6	0.264	56	0.447
7	0.231	57	0.452	7	0.254	57	0.396	7	0.264	57	0.457
8	0.241	58	0.470	8	0.254	58	0.406	8	0.264	58	0.457
9	0.241	59	0.472	9	0.264	59	0.406	9	0.274	59	0.477
10	0.241	60	0.472	10	0.274	60	0.406	10	0.274	60	0.497
11	0.241	61	0.492	11	0.274	61	0.406	11	0.284	61	0.497
12	0.251	62	0.502	12	0.274	62	0.416	12	0.294	62	0.507
13	0.251	63	0.513	13	0.284	63	0.416	13	0.304	63	0.518
14	0.251	64	0.533	14	0.284	64	0.416	14	0.315	64	0.518
15	0.251	65	0.543	15	0.284	65	0.416	15	0.325	65	0.518
16	0.251	66	0.553	16	0.294	66	0.426	16	0.325	66	0.518
17	0.261	67	0.553	17	0.294	67	0.426	17	0.325	67	0.558
18	0.261	68	0.563	18	0.294	68	0.426	18	0.335	68	0.568
19	0.261	69	0.580	19	0.294	69	0.426	19	0.335	69	0.589
20	0.261	70	0.583	20	0.294	70	0.447	20	0.345	70	0.589
21	0.261	71	0.593	21	0.304	71	0.447	21	0.345	71	0.589
22	0.281	72	0.613	22	0.304	72	0.457	22	0.345	72	0.589
23	0.281	73	0.613	23	0.304	73	0.467	23	0.345	73	0.599
24	0.281	74	0.613	24	0.304	74	0.467	24	0.345	74	0.599
25	0.281	75	0.623	25	0.315	75	0.467	25	0.355	75	0.609
26	0.291	76	0.633	26	0.315	76	0.507	26	0.355	76	0.619
27	0.291	77	0.633	27	0.315	77	0.518	27	0.355	77	0.629
28	0.291	78	0.673	28	0.315	78	0.538	28	0.355	78	0.639
29	0.301	79	0.683	29	0.325	79	0.538	29	0.355	79	0.639
30	0.301	80	0.693	30	0.325	80	0.538	30	0.365	80	0.650
31	0.312	81	0.713	31	0.325	81	0.558	31	0.365	81	0.660
32	0.312	82	0.744	32	0.325	82	0.568	32	0.365	82	0.660
33	0.312	83	0.754	33	0.325	83	0.589	33	0.365	83	0.670
34	0.322	84	0.784	34	0.325	84	0.589	34	0.365	84	0.670
35	0.332	85	0.834	35	0.335	85	0.589	35	0.365	85	0.670
36	0.332	86	0.884	36	0.335	86	0.609	36	0.375	86	0.670
37	0.332	87	0.894	37	0.345	87	0.629	37	0.375	87	0.680
38	0.332	88	0.894	38	0.345	88	0.639	38	0.375	88	0.690
39	0.342	89	0.935	39	0.345	89	0.650	39	0.386	89	0.690
40	0.342	90	0.945	40	0.345	90	0.660	40	0.386	90	0.721
41	0.342	91	0.995	41	0.355	91	0.660	41	0.386	91	0.741
42	0.352	92	1.115	42	0.355	92	0.680	42	0.396	92	0.741
43	0.352	93	1.166	43	0.355	93	0.721	43	0.396	93	0.751
44	0.362	94	1.286	44	0.365	94	0.721	44	0.396	94	0.751
45	0.362	95	1.568	45	0.365	95	0.741	45	0.396	95	0.812
46	0.402	96	1.789	46	0.375	96	0.741	46	0.406	96	0.812
47	0.412	97	1.909	47	0.375	97	0.792	47	0.406	97	1.015
48	0.412	98	2.392	48	0.375	98	1.116	48	0.406	98	1.086
49	0.412	99	2.402	49	0.375	99	1.126	49	0.406	99	1.157
50	0.422	100	2.542	50	0.375	100	1.390	50	0.406	100	1.319

Monterey Vitrinite Reflectance Readings:

Monterey Kerogen											
OCM #1				OCM #2				CCM			
Count	Ro	Count	Ro	Count	Ro	Count	Ro	Count	Ro	Count	Ro
1	0.275	51	0.802	1	0.246	51	0.830	1	0.244	51	0.873
2	0.294	52	0.802	2	0.267	52	0.841	2	0.254	52	0.883
3	0.304	53	0.812	3	0.277	53	0.871	3	0.264	53	0.885
4	0.304	54	0.822	4	0.277	54	0.912	4	0.264	54	0.893
5	0.304	55	0.822	5	0.297	55	0.923	5	0.274	55	0.905
6	0.315	56	0.822	6	0.297	56	0.933	6	0.274	56	0.924
7	0.325	57	0.832	7	0.297	57	0.974	7	0.274	57	0.934
8	0.325	58	0.832	8	0.318	58	0.974	8	0.284	58	0.995
9	0.325	59	0.842	9	0.318	59	0.994	9	0.284	59	0.995
10	0.325	60	0.852	10	0.328	60	1.015	10	0.284	60	1.035
11	0.335	61	0.873	11	0.349	61	1.015	11	0.294	61	1.055
12	0.345	62	0.883	12	0.349	62	1.035	12	0.315	62	1.055
13	0.345	63	0.903	13	0.359	63	1.035	13	0.315	63	1.116
14	0.355	64	0.903	14	0.369	64	1.035	14	0.325	64	1.137
15	0.355	65	0.934	15	0.369	65	1.046	15	0.335	65	1.137
16	0.355	66	0.944	16	0.379	66	1.046	16	0.335	66	1.157
17	0.365	67	0.964	17	0.379	67	1.046	17	0.345	67	1.198
18	0.365	68	0.995	18	0.379	68	1.066	18	0.345	68	1.218
19	0.375	69	1.005	19	0.390	69	1.066	19	0.345	69	1.228
20	0.375	70	1.005	20	0.390	70	1.076	20	0.375	70	1.248
21	0.386	71	1.025	21	0.410	71	1.076	21	0.375	71	1.258
22	0.386	72	1.035	22	0.420	72	1.087	22	0.375	72	1.299
23	0.386	73	1.045	23	0.441	73	1.105	23	0.375	73	1.299
24	0.396	74	1.055	24	0.451	74	1.117	24	0.386	74	1.329
25	0.396	75	1.055	25	0.461	75	1.148	25	0.406	75	1.360
26	0.447	76	1.066	26	0.475	76	1.169	26	0.406	76	1.421
27	0.465	77	1.096	27	0.482	77	1.220	27	0.426	77	1.425
28	0.467	78	1.096	28	0.482	78	1.220	28	0.447	78	1.472
29	0.487	79	1.096	29	0.482	79	1.230	29	0.467	79	1.492
30	0.497	80	1.096	30	0.495	80	1.230	30	0.467	80	1.505
31	0.507	81	1.187	31	0.533	81	1.251	31	0.477	81	1.543
32	0.518	82	1.198	32	0.533	82	1.281	32	0.477	82	1.563
33	0.528	83	1.235	33	0.543	83	1.281	33	0.487	83	1.593
34	0.535	84	1.238	34	0.554	84	1.292	34	0.619	84	1.634
35	0.578	85	1.238	35	0.584	85	1.363	35	0.650	85	1.766
36	0.589	86	1.248	36	0.584	86	1.394	36	0.670	86	1.776
37	0.609	87	1.299	37	0.615	87	1.404	37	0.670	87	1.817
38	0.619	88	1.350	38	0.636	88	1.415	38	0.710	88	1.847
39	0.660	89	1.512	39	0.646	89	1.415	39	0.731	89	1.857
40	0.721	90	1.532	40	0.656	90	1.497	40	0.745	90	1.949
41	0.721	91	1.563	41	0.677	91	1.527	41	0.751	91	1.979
42	0.731	92	1.664	42	0.697	92	1.595	42	0.751	92	1.999
43	0.731	93	1.735	43	0.697	93	1.599	43	0.761	93	2.060
44	0.731	94	1.776	44	0.697	94	1.609	44	0.761	94	2.070
45	0.741	95	1.837	45	0.748	95	1.640	45	0.765	95	2.101
46	0.761	96	1.969	46	0.759	96	1.671	46	0.781	96	2.131
47	0.771	97	2.162	47	0.759	97	1.855	47	0.781	97	2.151
48	0.792	98	2.334	48	0.779	98	2.015	48	0.812	98	2.202
49	0.802	99	2.405	49	0.789	99	2.040	49	0.822	99	2.273
50	0.802	100	2.436	50	0.830	100	2.153	50	0.842	100	2.314

Marcellus Vitrinite Reflectance Readings:

Marcellus Kerogen											
OCM #1				OCM #2				CCM			
Count	Ro	Count	Ro	Count	Ro	Count	Ro	Count	Ro	Count	Ro
1	1.087	51	1.845	1	1.238	51	1.888	1	0.741	51	2.020
2	1.148	52	1.855	2	1.269	52	1.908	2	0.863	52	2.020
3	1.169	53	1.876	3	1.269	53	1.928	3	1.126	53	2.030
4	1.179	54	1.895	4	1.279	54	1.949	4	1.269	54	2.030
5	1.179	55	1.896	5	1.299	55	1.959	5	1.279	55	2.030
6	1.189	56	1.896	6	1.309	56	1.959	6	1.299	56	2.040
7	1.220	57	1.907	7	1.360	57	1.959	7	1.299	57	2.040
8	1.230	58	1.917	8	1.360	58	1.969	8	1.370	58	2.050
9	1.240	59	1.927	9	1.370	59	1.969	9	1.380	59	2.060
10	1.343	60	1.937	10	1.400	60	1.979	10	1.380	60	2.060
11	1.384	61	1.937	11	1.400	61	1.979	11	1.380	61	2.060
12	1.404	62	1.948	12	1.411	62	1.989	12	1.411	62	2.060
13	1.445	63	1.968	13	1.411	63	2.009	13	1.451	63	2.060
14	1.456	64	1.978	14	1.441	64	2.009	14	1.461	64	2.070
15	1.456	65	1.978	15	1.441	65	2.009	15	1.482	65	2.070
16	1.466	66	1.989	16	1.441	66	2.015	16	1.492	66	2.080
17	1.466	67	1.989	17	1.461	67	2.025	17	1.522	67	2.080
18	1.466	68	1.999	18	1.482	68	2.030	18	1.532	68	2.091
19	1.475	69	1.999	19	1.482	69	2.040	19	1.532	69	2.091
20	1.476	70	2.009	20	1.492	70	2.050	20	1.543	70	2.111
21	1.476	71	2.009	21	1.492	71	2.060	21	1.543	71	2.111
22	1.507	72	2.009	22	1.502	72	2.070	22	1.593	72	2.131
23	1.527	73	2.019	23	1.502	73	2.070	23	1.634	73	2.131
24	1.527	74	2.050	24	1.502	74	2.070	24	1.675	74	2.131
25	1.527	75	2.081	25	1.512	75	2.080	25	1.685	75	2.151
26	1.538	76	2.081	26	1.522	76	2.080	26	1.695	76	2.162
27	1.538	77	2.091	27	1.563	77	2.085	27	1.725	77	2.172
28	1.548	78	2.091	28	1.583	78	2.135	28	1.756	78	2.182
29	1.599	79	2.122	29	1.603	79	2.141	29	1.766	79	2.212
30	1.609	80	2.153	30	1.603	80	2.151	30	1.776	80	2.223
31	1.609	81	2.173	31	1.634	81	2.162	31	1.776	81	2.223
32	1.620	82	2.173	32	1.644	82	2.162	32	1.786	82	2.223
33	1.630	83	2.173	33	1.675	83	2.162	33	1.786	83	2.233
34	1.640	84	2.214	34	1.675	84	2.172	34	1.806	84	2.233
35	1.640	85	2.214	35	1.715	85	2.172	35	1.817	85	2.233
36	1.640	86	2.214	36	1.715	86	2.172	36	1.837	86	2.263
37	1.640	87	2.235	37	1.725	87	2.172	37	1.857	87	2.263
38	1.681	88	2.265	38	1.756	88	2.182	38	1.867	88	2.294
39	1.691	89	2.276	39	1.766	89	2.182	39	1.877	89	2.324
40	1.691	90	2.286	40	1.786	90	2.192	40	1.877	90	2.365
41	1.732	91	2.306	41	1.786	91	2.212	41	1.888	91	2.395
42	1.743	92	2.337	42	1.796	92	2.212	42	1.898	92	2.405
43	1.784	93	2.337	43	1.806	93	2.225	43	1.908	93	2.425
44	1.794	94	2.368	44	1.806	94	2.233	44	1.928	94	2.436
45	1.804	95	2.378	45	1.817	95	2.255	45	1.928	95	2.436
46	1.804	96	2.429	46	1.827	96	2.263	46	1.959	96	2.466
47	1.835	97	2.429	47	1.827	97	2.283	47	1.959	97	2.507
48	1.845	98	2.522	48	1.857	98	2.283	48	1.969	98	2.547
49	1.845	99	2.532	49	1.867	99	2.354	49	1.999	99	2.618
50	1.845	100	2.563	50	1.867	100	2.395	50	2.020	100	2.913

Polish Shale Vitrinite Reflectance Readings:

Polish Shale Kerogen											
OCM #1				OCM #2				CCM			
Count	Ro	Count	Ro	Count	Ro	Count	Ro	Count	Ro	Count	Ro
1	1.746	51	2.395	1	1.969	51	2.365	1	1.266	51	2.485
2	1.877	52	2.395	2	1.999	52	2.375	2	1.457	52	2.502
3	2.040	53	2.405	3	2.040	53	2.375	3	1.477	53	2.502
4	2.070	54	2.405	4	2.060	54	2.385	4	1.568	54	2.512
5	2.080	55	2.415	5	2.101	55	2.385	5	1.688	55	2.522
6	2.080	56	2.425	6	2.101	56	2.395	6	1.799	56	2.532
7	2.080	57	2.425	7	2.111	57	2.405	7	2.030	57	2.532
8	2.131	58	2.436	8	2.121	58	2.405	8	2.110	58	2.563
9	2.162	59	2.436	9	2.121	59	2.415	9	2.120	59	2.565
10	2.162	60	2.436	10	2.131	60	2.415	10	2.140	60	2.593
11	2.172	61	2.456	11	2.131	61	2.425	11	2.140	61	2.603
12	2.182	62	2.456	12	2.141	62	2.446	12	2.150	62	2.613
13	2.182	63	2.476	13	2.141	63	2.466	13	2.181	63	2.623
14	2.192	64	2.486	14	2.162	64	2.466	14	2.191	64	2.643
15	2.202	65	2.497	15	2.162	65	2.497	15	2.201	65	2.653
16	2.202	66	2.497	16	2.162	66	2.507	16	2.221	66	2.683
17	2.212	67	2.507	17	2.172	67	2.527	17	2.221	67	2.693
18	2.212	68	2.507	18	2.182	68	2.527	18	2.221	68	2.693
19	2.223	69	2.507	19	2.182	69	2.557	19	2.231	69	2.693
20	2.223	70	2.517	20	2.192	70	2.557	20	2.261	70	2.693
21	2.243	71	2.517	21	2.202	71	2.568	21	2.261	71	2.695
22	2.263	72	2.527	22	2.202	72	2.568	22	2.271	72	2.703
23	2.273	73	2.527	23	2.212	73	2.578	23	2.271	73	2.733
24	2.273	74	2.537	24	2.212	74	2.588	24	2.271	74	2.733
25	2.283	75	2.547	25	2.212	75	2.588	25	2.281	75	2.733
26	2.283	76	2.557	26	2.223	76	2.588	26	2.281	76	2.733
27	2.283	77	2.557	27	2.223	77	2.608	27	2.311	77	2.753
28	2.304	78	2.578	28	2.233	78	2.618	28	2.311	78	2.774
29	2.304	79	2.578	29	2.243	79	2.628	29	2.321	79	2.784
30	2.304	80	2.598	30	2.243	80	2.628	30	2.331	80	2.794
31	2.314	81	2.608	31	2.253	81	2.639	31	2.351	81	2.814
32	2.324	82	2.608	32	2.263	82	2.639	32	2.351	82	2.824
33	2.324	83	2.608	33	2.273	83	2.639	33	2.351	83	2.834
34	2.324	84	2.608	34	2.273	84	2.649	34	2.351	84	2.854
35	2.334	85	2.618	35	2.283	85	2.659	35	2.382	85	2.854
36	2.344	86	2.649	36	2.283	86	2.669	36	2.392	86	2.854
37	2.344	87	2.659	37	2.294	87	2.669	37	2.392	87	2.904
38	2.354	88	2.720	38	2.294	88	2.669	38	2.392	88	2.924
39	2.354	89	2.720	39	2.304	89	2.750	39	2.402	89	2.995
40	2.365	90	2.750	40	2.324	90	2.760	40	2.402	90	3.015
41	2.365	91	2.760	41	2.324	91	2.781	41	2.402	91	3.035
42	2.365	92	2.771	42	2.334	92	2.791	42	2.432	92	3.055
43	2.365	93	2.781	43	2.334	93	2.831	43	2.442	93	3.085
44	2.365	94	2.811	44	2.344	94	2.842	44	2.452	94	3.085
45	2.375	95	2.842	45	2.344	95	2.862	45	2.462	95	3.095
46	2.375	96	2.933	46	2.344	96	3.004	46	2.462	96	3.095
47	2.375	97	2.943	47	2.344	97	3.105	47	2.465	97	3.115
48	2.375	98	3.055	48	2.344	98	3.237	48	2.472	98	3.125
49	2.375	99	3.126	49	2.344	99	3.308	49	2.472	99	3.346
50	2.395	100	3.582	50	2.354	100	3.461	50	2.472	100	3.387

Haynesville Vitrinite Reflectance Readings:

Haynesville Kerogen							
OCM #2							
Count	Ro	Count	Ro	Count	Ro	Count	Ro
1	0.800	26	1.712	51	1.978	76	2.327
2	1.076	27	1.712	52	1.978	77	2.358
3	1.107	28	1.753	53	1.989	78	2.378
4	1.148	29	1.753	54	1.989	79	2.388
5	1.179	30	1.773	55	2.009	80	2.399
6	1.210	31	1.794	56	2.009	81	2.429
7	1.343	32	1.804	57	2.019	82	2.511
8	1.353	33	1.814	58	2.050	83	2.563
9	1.360	34	1.835	59	2.050	84	2.583
10	1.404	35	1.835	60	2.071	85	2.604
11	1.460	36	1.835	61	2.091	86	2.604
12	1.476	37	1.876	62	2.101	87	2.716
13	1.517	38	1.896	63	2.112	88	2.737
14	1.527	39	1.907	64	2.112	89	2.747
15	1.538	40	1.907	65	2.132	90	2.850
16	1.548	41	1.907	66	2.163	91	2.880
17	1.558	42	1.917	67	2.163	92	2.901
18	1.599	43	1.927	68	2.173	93	2.921
19	1.609	44	1.927	69	2.214	94	2.983
20	1.609	45	1.927	70	2.214	95	3.167
21	1.640	46	1.937	71	2.235	96	3.249
22	1.661	47	1.948	72	2.255	97	3.249
23	1.702	48	1.958	73	2.265	98	3.260
24	1.702	49	1.968	74	2.276	99	3.649
25	1.712	50	1.968	75	2.286	100	3.895

Pyrolysis-GC Results:

			n-alkene/n-alkane ratio				
Sample	Isolation Method	Aromaticity (%)	C1-C36	C1-C5	C6-C10	C11-C14	C15+
Barnett (immature)	OCM #1	4.78	0.53	0.40	1.14	0.89	0.72
	OCM#2	4.68	0.49	0.40	1.20	0.91	0.78
	CCM	6.04	0.38	0.21	1.09	0.98	0.80
Monterey	OCM #1	5.74	0.48	0.36	0.92	0.73	0.60
	OCM#2	4.93	0.63	0.46	1.14	1.26	0.85
	CCM	5.36	0.41	0.31	0.78	0.78	0.69
Marcellus	OCM #1	6.87	0.55	0.43	1.01	0.70	0.56
	OCM#2	8.53	1.23	2.96	1.20	0.73	0.82
	CCM	6.91	1.02	1.57	1.14	0.69	0.61
Polish Shale	OCM #1	2.88	0.63	0.25	1.07	0.87	0.64
	OCM#2	8.48	0.50	0.39	1.06	0.38	0.53
	CCM	7.45	0.47	0.39	0.95	0.54	0.44
Haynesville	OCM#2	5.75	0.69	0.57	1.45	0.66	0.89
	CCM	5.51	0.35	0.30	1.13	0.54	0.56

Table showing the aromaticity and n-alkene/n-alkane ratios of the kerogen from the Py-GC results. Note the variability in the ratios and the aromaticity across methods. Greatest variability in the ratio was seen in the C1 to C5 range. Aromaticity was determined from the percent of aromatics out of all the measured compounds.

Barnett Shale (immature): Open-Conventional Method #1

Peak Label	Compound Name	Retention Time	Area	Height	Area%	Height%
NC1	Normal Alkane C1	6.485	2299817	55903	13.37	0.73
NO2	Normal Olefin C2	7.200	415516	514462	2.42	6.76
NC2	Normal Alkane C2	7.226	813119	1088768	4.73	14.30
NO3	Normal Olefin C3	7.339	568814	685454	3.31	9.01
NC3	Normal Alkane C3	7.383	387468	548768	2.25	7.21
NO4	Normal Olefin C4	7.878	407482	318773	2.37	4.19
NC4	Normal Alkane C4	7.972	231606	233919	1.35	3.07
NO5	Normal Olefin C5	9.541	178671	120212	1.04	1.58
NC5	Normal Alkane C5	9.851	168036	111049	0.98	1.46
NO6	Normal Olefin C6	13.319	172312	82789	1.00	1.09
NC6	Normal Alkane C6	13.823	129657	59454	0.75	0.78
BZ	Benzene	16.052	101873	42368	0.59	0.56
NO7	Normal Olefin C7	18.151	140587	60655	0.82	0.80
NC7	Normal Alkane C7	18.701	122591	51397	0.71	0.68
TOL	Toluene	21.138	179953	71272	1.05	0.94
NO8	Normal Olefin C8	22.817	122099	49470	0.71	0.65
NC8	Normal Alkane C8	23.332	106217	44176	0.62	0.58
EB	Ethylbenzene	25.342	49688	17604	0.29	0.23
MXYL	m-Xylene	25.714	122316	44987	0.71	0.59
PXYL	p-Xylene	25.764	59090	27086	0.34	0.36
OXYL	o-Xylene	26.648	74515	24335	0.43	0.32
23DMT	2-3 Dimethylthiophene	26.024	11144	4435	0.06	0.06
STY	Styrene	26.090	15597	6067	0.09	0.08
NO9	Normal Olefin C9	27.084	91291	38796	0.53	0.51
NC9	Normal Alkane C9	27.548	90666	36800	0.53	0.48
PH	Phenol	29.377	41423	13925	0.24	0.18
NO10	Normal Olefin C10	30.985	97597	35648	0.57	0.47
NC10	Normal Alkane C10	31.415	100263	38039	0.58	0.50
OCR	o-Cresol	32.396	33653	10681	0.20	0.14
MPCR	mp-Cresol	33.565	15184	5428	0.09	0.07
NO11	Normal Olefin C11	34.595	80452	28182	0.47	0.37
NC11	Normal Alkane C11	34.988	101279	40252	0.59	0.53
OEPH	o-Ethylphenol	36.558	11072	4997	0.06	0.07
PEPH	p-Ethylphenol	37.307	13105	5134	0.08	0.07
NO12	Normal Olefin C12	37.948	62176	22016	0.36	0.29
NC12	Normal Alkane C12	38.306	68625	23616	0.40	0.31
2MN	2-Methylnaphthalen	40.802	17556	7125	0.10	0.09
NO13	Normal Olefin C13	41.081	63709	18720	0.37	0.25
1MN	1-Methylnaphthalen	41.241	37126	8817	0.22	0.12
NC13	Normal Alkane C13	41.408	55383	17310	0.32	0.23
NO14	Normal Olefin C14	44.019	51176	16350	0.30	0.21
DMN	Dimethylnaphthalene	44.119	21761	4937	0.13	0.06
NC14	Normal Alkane C14	44.320	63278	18650	0.37	0.25
NO15	Normal Olefin C15	46.783	33771	11458	0.20	0.15

Barnett Shale (immature): Open-Conventional Method #1						
NC15	Normal Alkane C15	47.059	57176	15319	0.33	0.20
NO16	Normal Olefin C16	49.389	30283	9824	0.18	0.13
NC16	Normal Alkane C16	49.645	47036	13997	0.27	0.18
NO17	Normal Olefin C17	51.860	27410	8099	0.16	0.11
NC17	Normal Alkane C17	52.094	50451	15212	0.29	0.20
PREN	Pris-1-ene	52.347	15356	3934	0.09	0.05
PHEN	Phenanthrene	53.147	16680	3117	0.10	0.04
NO18	Normal Olefin C18	54.201	22757	6754	0.13	0.09
NC18	Normal Alkane C18	54.418	35269	11232	0.21	0.15
NO19	Normal Olefin C19	56.430	22451	5937	0.13	0.08
NC19	Normal Alkane C19	56.626	31749	10113	0.18	0.13
NO20	Normal Olefin C20	58.557	18095	5407	0.11	0.07
NC20	Normal Alkane C20	58.741	22000	7259	0.13	0.10
NO21	Normal Olefin C21	60.588	12543	4056	0.07	0.05
NC21	Normal Alkane C21	60.759	18258	5817	0.11	0.08
NO22	Normal Olefin C22	62.538	12655	3930	0.07	0.05
NC22	Normal Alkane C22	62.696	13317	4277	0.08	0.06
NO23	Normal Olefin C23	64.399	7980	2452	0.05	0.03
NC23	Normal Alkane C23	64.553	8440	3039	0.05	0.04
NO24	Normal Olefin C24	66.208	8588	2293	0.05	0.03
NC24	Normal Alkane C24	66.345	8749	2790	0.05	0.04
NO25	Normal Olefin C25	67.941	5508	1538	0.03	0.02
NC25	Normal Alkane C25	68.070	6332	1919	0.04	0.03
NO26	Normal Olefin C26	69.620	3948	1178	0.02	0.02
NC26	Normal Alkane C26	69.739	6802	1940	0.04	0.03
NO27	Normal Olefin C27	71.245	3586	992	0.02	0.01
NC27	Normal Alkane C27	71.366	6990	1678	0.04	0.02
NO28	Normal Olefin C28	72.850	6260	1634	0.04	0.02
NC28	Normal Alkane C28	72.974	4655	1330	0.03	0.02
NO29	Normal Olefin C29	74.531	3137	754	0.02	0.01
NC29	Normal Alkane C29	74.623	5869	1227	0.03	0.02
NO30	Normal Olefin C30	76.252	3238	830	0.02	0.01
NC30	Normal Alkane C30	76.348	5081	1091	0.03	0.01
NO31	Normal Olefin C31	78.083	2083	589	0.01	0.01
NC31	Normal Alkane C31	78.199	3835	978	0.02	0.01
NO32	Normal Olefin C32					
NC32	Normal Alkane C32					
NO33	Normal Olefin C33					
NC33	Normal Alkane C33					
NO34	Normal Olefin C34					
NC34	Normal Alkane C34					
NO35	Normal Olefin C35					
NC35	Normal Alkane C35					
NC36	Normal Alkane C36					

Barnett Shale (immature): Conventional Method #2

Peak Label	Compound Name	Retention Time	Area	Height	Area%	Height%
NC1	Normal Alkane C1	6.463	5170830	249175	18.04	1.78
NO2	Normal Olefin C2	6.993	935450	1075565	3.26	7.70
NC2	Normal Alkane C2	7.018	1655209	2145646	5.78	15.37
NO3	Normal Olefin C3	7.152	1252895	1473249	4.37	10.55
NC3	Normal Alkane C3	7.175	816487	1140267	2.85	8.17
NO4	Normal Olefin C4	7.649	813718	692863	2.84	4.96
NC4	Normal Alkane C4	7.736	443904	475392	1.55	3.41
NO5	Normal Olefin C5	9.276	332735	241382	1.16	1.73
NC5	Normal Alkane C5	9.595	291527	196935	1.02	1.41
NO6	Normal Olefin C6	13.100	281470	140731	0.98	1.01
NC6	Normal Alkane C6	13.630	206143	96448	0.72	0.69
BZ	Benzene	15.880	95742	47748	0.33	0.34
NO7	Normal Olefin C7	18.020	215730	94985	0.75	0.68
NC7	Normal Alkane C7	18.577	178000	77247	0.62	0.55
TOL	Toluene	21.007	348928	123163	1.22	0.88
NO8	Normal Olefin C8	22.726	179560	73314	0.63	0.53
NC8	Normal Alkane C8	23.248	150821	62331	0.53	0.45
EB	Ethylbenzene	25.228	88514	31096	0.31	0.22
MXYL	m-Xylene	25.608	203730	73702	0.71	0.53
PXYL	p-Xylene	25.657	97297	45291	0.34	0.32
OXYL	o-Xylene	26.534	125456	45833	0.44	0.33
23DMT	2-3 Dimethylthiophene	25.922	22799	6441	0.08	0.05
STY	Styrene	25.982	24291	5305	0.08	0.04
NO9	Normal Olefin C9	27.007	128405	56143	0.45	0.40
NC9	Normal Alkane C9	27.476	114786	49508	0.40	0.35
PH	Phenol	29.278	80637	27361	0.28	0.20
NO10	Normal Olefin C10	30.922	114750	43448	0.40	0.31
NC10	Normal Alkane C10	31.358	117485	47458	0.41	0.34
OCR	o-Cresol	32.243	14658	8477	0.05	0.06
MPCR	mp-Cresol	33.477	52997	15379	0.18	0.11
NO11	Normal Olefin C11	34.535	105619	40178	0.37	0.29
NC11	Normal Alkane C11	34.933	125339	48440	0.44	0.35
OEPH	o-Ethylphenol	36.387	34725	9238	0.12	0.07
PEPH	p-Ethylphenol	37.283	36876	10542	0.13	0.08
NO12	Normal Olefin C12	37.881	106598	31296	0.37	0.22
NC12	Normal Alkane C12	38.245	89886	33866	0.31	0.24
2MN	2-Methylnaphthalen	40.833	29805	7999	0.10	0.06
NO13	Normal Olefin C13	41.006	53622	20426	0.19	0.15
1MN	1-Methylnaphthalen	41.196	56001	15324	0.20	0.11
NC13	Normal Alkane C13	41.336	74414	26625	0.26	0.19
NO14	Normal Olefin C14	43.934	78777	22598	0.27	0.16
DMN	Dimethylnaphthalene	44.021	21223	6546	0.07	0.05
NC14	Normal Alkane C14	44.236	87729	26399	0.31	0.19
NO15	Normal Olefin C15	46.683	52278	14418	0.18	0.10

Barnett Shale (immature): Conventional Method #2						
NC15	Normal Alkane C15	46.961	65654	20678	0.23	0.15
NO16	Normal Olefin C16	49.275	56174	13996	0.20	0.10
NC16	Normal Alkane C16	49.534	47065	15723	0.16	0.11
NO17	Normal Olefin C17	51.734	37811	10121	0.13	0.07
NC17	Normal Alkane C17	51.971	48922	17091	0.17	0.12
PREN	Pris-1-ene	52.221	14807	3694	0.05	0.03
PHEN	Phenanthrene	52.996	6776	2361	0.02	0.02
NO18	Normal Olefin C18	54.063	19595	6342	0.07	0.05
NC18	Normal Alkane C18	54.280	46390	15303	0.16	0.11
NO19	Normal Olefin C19	56.277	17897	5380	0.06	0.04
NC19	Normal Alkane C19	56.477	33950	11676	0.12	0.08
NO20	Normal Olefin C20	58.382	18657	5178	0.07	0.04
NC20	Normal Alkane C20	58.569	32363	10422	0.11	0.07
NO21	Normal Olefin C21	60.397	13634	3837	0.05	0.03
NC21	Normal Alkane C21	60.566	20728	6482	0.07	0.05
NO22	Normal Olefin C22	62.323	9100	3002	0.03	0.02
NC22	Normal Alkane C22	62.482	11461	4110	0.04	0.03
NO23	Normal Olefin C23	64.170	4771	1656	0.02	0.01
NC23	Normal Alkane C23	64.311	7495	2501	0.03	0.02
NO24	Normal Olefin C24	65.945	6735	1482	0.02	0.01
NC24	Normal Alkane C24	66.082	6882	2106	0.02	0.02
NO25	Normal Olefin C25	67.658	3982	968	0.01	0.01
NC25	Normal Alkane C25	67.788	4462	1462	0.02	0.01
NO26	Normal Olefin C26	69.265	2665	631	0.01	0.00
NC26	Normal Alkane C26	69.431	5464	1004	0.02	0.01
NO27	Normal Olefin C27	70.925	939	404	0.00	0.00
NC27	Normal Alkane C27	71.035	2033	620	0.01	0.00
NO28	Normal Olefin C28	72.488	2056	578	0.01	0.00
NC28	Normal Alkane C28	72.588	2609	722	0.01	0.01
NO29	Normal Olefin C29					
NC29	Normal Alkane C29					
NO30	Normal Olefin C30					
NC30	Normal Alkane C30					
NO31	Normal Olefin C31					
NC31	Normal Alkane C31					
NO32	Normal Olefin C32					
NC32	Normal Alkane C32					
NO33	Normal Olefin C33					
NC33	Normal Alkane C33					
NO34	Normal Olefin C34					
NC34	Normal Alkane C34					
NO35	Normal Olefin C35					
NC35	Normal Alkane C35					
NC36	Normal Alkane C36					

Barnett Shale (immature): Conservative-Closed Method

Peak Label	Compound Name	Retention Time	Area	Height	Area%	Height%
NC1	Normal Alkane C1	6.303	7983881	176860	20.84	1.37
NO2	Normal Olefin C2	7.190	233820	230491	0.61	1.78
NC2	Normal Alkane C2	7.216	566007	591217	1.48	4.57
NO3	Normal Olefin C3	7.352	762076	912167	1.99	7.05
NC3	Normal Alkane C3	7.376	679102	766616	1.77	5.93
NO4	Normal Olefin C4	7.879	741535	602182	1.94	4.66
NC4	Normal Alkane C4	7.975	530914	544847	1.39	4.21
NO5	Normal Olefin C5	9.545	389507	262923	1.02	2.03
NC5	Normal Alkane C5	9.857	416500	268446	1.09	2.08
NO6	Normal Olefin C6	13.316	375174	176365	0.98	1.36
NC6	Normal Alkane C6	13.835	319885	138784	0.84	1.07
BZ	Benzene	16.073	610553	244268	1.59	1.89
NO7	Normal Olefin C7	18.168	303348	124425	0.79	0.96
NC7	Normal Alkane C7	18.722	300114	120532	0.78	0.93
TOL	Toluene	21.166	447807	159561	1.17	1.23
NO8	Normal Olefin C8	22.843	322126	119996	0.84	0.93
NC8	Normal Alkane C8	23.359	285614	110367	0.75	0.85
EB	Ethylbenzene	25.361	127543	43938	0.33	0.34
MXYL	m-Xylene	25.742	252928	85257	0.66	0.66
PXYL	p-Xylene	25.793	140190	69113	0.37	0.53
OXYL	o-Xylene	26.677	154413	51098	0.40	0.40
23DMT	2-3 Dimethylthiophene	26.040	31526	11356	0.08	0.09
STY	Styrene	26.113	53427	13073	0.14	0.10
NO9	Normal Olefin C9	27.113	254285	100440	0.66	0.78
NC9	Normal Alkane C9	27.581	261691	97165	0.68	0.75
PH	Phenol	29.406	102778	34550	0.27	0.27
NO10	Normal Olefin C10	31.019	262465	91391	0.69	0.71
NC10	Normal Alkane C10	31.449	229013	80387	0.60	0.62
OCR	o-Cresol	32.427	67634	22174	0.18	0.17
MPCR	mp-Cresol	33.594	50907	16244	0.13	0.13
NO11	Normal Olefin C11	34.629	218144	71095	0.57	0.55
NC11	Normal Alkane C11	35.021	188862	72586	0.49	0.56
OEPH	o-Ethylphenol	36.580	19760	10502	0.05	0.08
PEPH	p-Ethylphenol	37.353	51679	18193	0.13	0.14
NO12	Normal Olefin C12	37.983	171116	57206	0.45	0.44
NC12	Normal Alkane C12	38.342	171954	57796	0.45	0.45
2MN	2-Methylnaphthalen	40.839	43899	15519	0.11	0.12
NO13	Normal Olefin C13	41.116	156888	47662	0.41	0.37
1MN	1-Methylnaphthalen	41.273	81559	20682	0.21	0.16
NC13	Normal Alkane C13	41.445	163164	46839	0.43	0.36
NO14	Normal Olefin C14	44.058	132587	41538	0.35	0.32
DMN	Dimethylnaphthalene	44.164	47738	10745	0.12	0.08
NC14	Normal Alkane C14	44.359	165437	46567	0.43	0.36
NO15	Normal Olefin C15	46.821	88943	30017	0.23	0.23

Barnett Shale (immature) Closed-Conservative Method						
NC15	Normal Alkane C15	47.097	139221	38691	0.36	0.30
NO16	Normal Olefin C16	49.428	83761	24871	0.22	0.19
NC16	Normal Alkane C16	49.683	97772	30769	0.26	0.24
NO17	Normal Olefin C17	51.897	72462	19314	0.19	0.15
NC17	Normal Alkane C17	52.133	115476	30717	0.30	0.24
PREN	Pris-1-ene	52.380	29215	5956	0.08	0.05
PHEN	Phenanthrene	53.202	29060	4794	0.08	0.04
NO18	Normal Olefin C18	54.239	52324	16521	0.14	0.13
NC18	Normal Alkane C18	54.456	68395	21674	0.18	0.17
NO19	Normal Olefin C19	56.469	42868	13216	0.11	0.10
NC19	Normal Alkane C19	56.669	60218	19048	0.16	0.15
NO20	Normal Olefin C20	58.597	39793	11798	0.10	0.09
NC20	Normal Alkane C20	58.782	45514	14607	0.12	0.11
NO21	Normal Olefin C21	60.629	30857	9213	0.08	0.07
NC21	Normal Alkane C21	60.800	35833	11602	0.09	0.09
NO22	Normal Olefin C22	62.584	25411	7473	0.07	0.06
NC22	Normal Alkane C22	62.738	28055	8750	0.07	0.07
NO23	Normal Olefin C23	64.448	19319	5275	0.05	0.04
NC23	Normal Alkane C23	64.596	17632	6277	0.05	0.05
NO24	Normal Olefin C24	66.248	15420	4196	0.04	0.03
NC24	Normal Alkane C24	66.387	18761	5440	0.05	0.04
NO25	Normal Olefin C25	67.988	12764	3208	0.03	0.02
NC25	Normal Alkane C25	68.114	13199	4115	0.03	0.03
NO26	Normal Olefin C26	69.667	7630	2343	0.02	0.02
NC26	Normal Alkane C26	69.789	12427	3774	0.03	0.03
NO27	Normal Olefin C27	71.299	6216	1928	0.02	0.01
NC27	Normal Alkane C27	71.411	10868	2438	0.03	0.02
NO28	Normal Olefin C28	72.918	3799	1200	0.01	0.01
NC28	Normal Alkane C28	73.022	5434	1768	0.01	0.01
NO29	Normal Olefin C29	74.571	5860	1613	0.02	0.01
NC29	Normal Alkane C29	74.679	9841	2082	0.03	0.02
NO30	Normal Olefin C30	76.268	11068	1648	0.03	0.01
NC30	Normal Alkane C30	76.409	7417	1653	0.02	0.01
NO31	Normal Olefin C31					
NC31	Normal Alkane C31					
NO32	Normal Olefin C32					
NC32	Normal Alkane C32					
NO33	Normal Olefin C33					
NC33	Normal Alkane C33					
NO34	Normal Olefin C34					
NC34	Normal Alkane C34					
NO35	Normal Olefin C35					
NC35	Normal Alkane C35					
NC36	Normal Alkane C36					

Monterey Shale: Open-Conventional Method #1

Peak Label	Compound Name	Retention Time	Area	Height	Area%	Height%
NC1	Normal Alkane C1	6.656	1267694	34931	10.79	0.76
NO2	Normal Olefin C2	7.187	181625	191196	1.55	4.14
NC2	Normal Alkane C2	7.224	353789	438268	3.01	9.49
NO3	Normal Olefin C3	7.355	256739	302074	2.18	6.54
NC3	Normal Alkane C3	7.387	204155	314389	1.74	6.81
NO4	Normal Olefin C4	7.876	215027	163251	1.83	3.54
NC4	Normal Alkane C4	7.967	126583	132090	1.08	2.86
NO5	Normal Olefin C5	9.529	75637	52709	0.64	1.14
NC5	Normal Alkane C5	9.845	90482	60318	0.77	1.31
NO6	Normal Olefin C6	13.304	69380	33781	0.59	0.73
NC6	Normal Alkane C6	13.806	69828	30925	0.59	0.67
BZ	Benzene	16.037	61274	26162	0.52	0.57
NO7	Normal Olefin C7	18.131	60785	25057	0.52	0.54
NC7	Normal Alkane C7	18.687	69969	29199	0.60	0.63
TOL	Toluene	21.120	96197	39086	0.82	0.85
NO8	Normal Olefin C8	22.802	54892	21863	0.47	0.47
NC8	Normal Alkane C8	23.317	60865	24274	0.52	0.53
EB	Ethylbenzene	25.333	38494	14241	0.33	0.31
MXYL	m-Xylene	25.710	134664	49709	1.15	1.08
PXYL	p-Xylene	25.757	43282	21851	0.37	0.47
OXYL	o-Xylene	26.637	52961	19673	0.45	0.43
23DMT	2-3 Dimethylthiophene	26.026	4037	1887	0.03	0.04
STY	Styrene	26.081	10886	4106	0.09	0.09
NO9	Normal Olefin C9	27.068	43076	18435	0.37	0.40
NC9	Normal Alkane C9	27.537	51460	21668	0.44	0.47
PH	Phenol	29.376	74516	29254	0.63	0.63
NO10	Normal Olefin C10	30.974	64166	21776	0.55	0.47
NC10	Normal Alkane C10	31.408	66913	24794	0.57	0.54
OCR	o-Cresol	32.388	9669	3350	0.08	0.07
MPCR	mp-Cresol	33.561	25852	9338	0.22	0.20
NO11	Normal Olefin C11	34.589	46208	15854	0.39	0.34
NC11	Normal Alkane C11	34.982	72378	28537	0.62	0.62
OEPH	o-Ethylphenol	36.542	6134	3174	0.05	0.07
PEPH	p-Ethylphenol	37.310	22050	7374	0.19	0.16
NO12	Normal Olefin C12	37.943	36617	13084	0.31	0.28
NC12	Normal Alkane C12	38.302	52871	17806	0.45	0.39
2MN	2-Methylnaphthalen	40.805	19710	5780	0.17	0.13
NO13	Normal Olefin C13	41.078	40960	12461	0.35	0.27
1MN	1-Methylnaphthalen	41.245	46068	13234	0.39	0.29
NC13	Normal Alkane C13	41.407	48448	14682	0.41	0.32
NO14	Normal Olefin C14	44.015	49798	12885	0.42	0.28
DMN	Dimethylnaphthalene	44.109	21339	5026	0.18	0.11
NC14	Normal Alkane C14	44.320	64857	19332	0.55	0.42
NO15	Normal Olefin C15	46.785	29852	9593	0.25	0.21

Monterey Shale: Open-Conventional Method #1						
NC15	Normal Alkane C15	47.060	53469	15290	0.46	0.33
NO16	Normal Olefin C16	49.393	29720	8991	0.25	0.19
NC16	Normal Alkane C16	49.647	41513	13759	0.35	0.30
NO17	Normal Olefin C17	51.863	25929	7998	0.22	0.17
NC17	Normal Alkane C17	52.099	41013	12543	0.35	0.27
PREN	Pris-1-ene	52.352	11037	2476	0.09	0.05
PHEN	Phenanthrene	53.104	7086	1920	0.06	0.04
NO18	Normal Olefin C18	54.207	23221	7237	0.20	0.16
NC18	Normal Alkane C18	54.424	32087	10913	0.27	0.24
NO19	Normal Olefin C19	56.437	22014	6412	0.19	0.14
NC19	Normal Alkane C19	56.635	28430	9369	0.24	0.20
NO20	Normal Olefin C20	58.564	20648	6140	0.18	0.13
NC20	Normal Alkane C20	58.749	26513	8721	0.23	0.19
NO21	Normal Olefin C21	60.598	17582	4722	0.15	0.10
NC21	Normal Alkane C21	60.769	23421	7157	0.20	0.15
NO22	Normal Olefin C22	62.548	14138	4303	0.12	0.09
NC22	Normal Alkane C22	62.706	18324	5678	0.16	0.12
NO23	Normal Olefin C23	64.416	9309	2895	0.08	0.06
NC23	Normal Alkane C23	64.562	12096	4264	0.10	0.09
NO24	Normal Olefin C24	66.214	10512	2293	0.09	0.05
NC24	Normal Alkane C24	66.354	13601	4341	0.12	0.09
NO25	Normal Olefin C25	67.958	7182	2021	0.06	0.04
NC25	Normal Alkane C25	68.083	10642	3361	0.09	0.07
NO26	Normal Olefin C26	69.632	4167	1184	0.04	0.03
NC26	Normal Alkane C26	69.748	14518	3855	0.12	0.08
NO27	Normal Olefin C27	71.264	5845	1436	0.05	0.03
NC27	Normal Alkane C27	71.374	14463	3849	0.12	0.08
NO28	Normal Olefin C28	72.867	3570	967	0.03	0.02
NC28	Normal Alkane C28	72.988	10955	3254	0.09	0.07
NO29	Normal Olefin C29	74.519	3187	1038	0.03	0.02
NC29	Normal Alkane C29	74.631	17893	4178	0.15	0.09
NO30	Normal Olefin C30	76.250	5756	967	0.05	0.02
NC30	Normal Alkane C30	76.353	10672	2672	0.09	0.06
NO31	Normal Olefin C31	78.116	3230	813	0.03	0.02
NC31	Normal Alkane C31	78.206	13330	2596	0.11	0.06
NO32	Normal Olefin C32	80.133	2531	624	0.02	0.01
NC32	Normal Alkane C32	80.251	11663	1773	0.10	0.04
NO33	Normal Olefin C33	82.450	1621	427	0.01	0.01
NC33	Normal Alkane C33	82.583	6613	1062	0.06	0.02
NO34	Normal Olefin C34					
NC34	Normal Alkane C34	85.240	8661	986	0.07	0.02
NO35	Normal Olefin C35					
NC35	Normal Alkane C35	88.340	5415	752	0.05	0.02

Monterey Shale: Open-Conventional Method #2

Peak Label	Compound Name	Retention Time	Area	Height	Area%	Height%
NC1	Normal Alkane C1	6.397	1059212	25655	9.16	0.50
NO2	Normal Olefin C2	6.997	248831	285885	2.15	5.57
NC2	Normal Alkane C2	7.021	476655	636706	4.12	12.40
NO3	Normal Olefin C3	7.154	325082	424139	2.81	8.26
NC3	Normal Alkane C3	7.178	216993	362338	1.88	7.06
NO4	Normal Olefin C4	7.649	235745	190564	2.04	3.71
NC4	Normal Alkane C4	7.736	121174	129205	1.05	2.52
NO5	Normal Olefin C5	9.272	90296	64121	0.78	1.25
NC5	Normal Alkane C5	9.582	81412	57178	0.70	1.11
NO6	Normal Olefin C6	13.082	80416	41343	0.70	0.81
NC6	Normal Alkane C6	13.607	63300	30818	0.55	0.60
BZ	Benzene	15.860	26788	14847	0.23	0.29
NO7	Normal Olefin C7	17.990	65014	30889	0.56	0.60
NC7	Normal Alkane C7	18.554	60813	26772	0.53	0.52
TOL	Toluene	21.058	108201	47807	0.94	0.93
NO8	Normal Olefin C8	22.694	63682	25867	0.55	0.50
NC8	Normal Alkane C8	23.215	52381	22036	0.45	0.43
EB	Ethylbenzene	25.202	28241	10239	0.24	0.20
MXYL	m-Xylene	25.574	73526	32637	0.64	0.64
PXYL	p-Xylene	25.599	49710	28548	0.43	0.56
OXYL	o-Xylene	26.500	42165	14552	0.36	0.28
23DMT	2-3 Dimethylthiophene	25.876	5530	2005	0.05	0.04
STY	Styrene	25.964	11256	2661	0.10	0.05
NO9	Normal Olefin C9	26.976	51078	21355	0.44	0.42
NC9	Normal Alkane C9	27.445	42861	17915	0.37	0.35
PH	Phenol	29.253	76037	29992	0.66	0.58
NO10	Normal Olefin C10	30.895	50883	19696	0.44	0.38
NC10	Normal Alkane C10	31.328	53536	20278	0.46	0.39
OCR	o-Cresol	32.240	11367	6251	0.10	0.12
MPCR	mp-Cresol	33.451	28998	10426	0.25	0.20
NO11	Normal Olefin C11	34.515	74127	23492	0.64	0.46
NC11	Normal Alkane C11	34.903	59612	23901	0.52	0.47
OEPH	o-Ethylphenol	36.456	7449	4710	0.06	0.09
PEPH	p-Ethylphenol	37.290	6120	3811	0.05	0.07
NO12	Normal Olefin C12	37.858	57367	17613	0.50	0.34
NC12	Normal Alkane C12	38.218	44376	17195	0.38	0.33
2MN	2-Methylnaphthalen	40.643	23976	7930	0.21	0.15
NO13	Normal Olefin C13	40.979	46288	16292	0.40	0.32
1MN	1-Methylnaphthalen	41.157	44638	14435	0.39	0.28
NC13	Normal Alkane C13	41.312	34202	12661	0.30	0.25
NO14	Normal Olefin C14	43.913	55265	15888	0.48	0.31
DMN	Dimethylnaphthalene	44.001	11711	3327	0.10	0.06
NC14	Normal Alkane C14	44.211	47481	13526	0.41	0.26
NO15	Normal Olefin C15	46.666	42411	12586	0.37	0.25

Monterey Shale: Open-Conventional Method #2						
NC15	Normal Alkane C15	46.942	43868	14352	0.38	0.28
NO16	Normal Olefin C16	49.259	37377	11598	0.32	0.23
NC16	Normal Alkane C16	49.515	36178	12917	0.31	0.25
NO17	Normal Olefin C17	51.716	35530	10777	0.31	0.21
NC17	Normal Alkane C17	51.952	35781	12594	0.31	0.25
PREN	Pris-1-ene	52.203	11628	2936	0.10	0.06
PHEN	Phenanthrene	52.863	14394	2935	0.12	0.06
NO18	Normal Olefin C18	54.045	25210	8313	0.22	0.16
NC18	Normal Alkane C18	54.262	34040	12027	0.29	0.23
NO19	Normal Olefin C19	56.261	21571	6756	0.19	0.13
NC19	Normal Alkane C19	56.462	30054	9427	0.26	0.18
NO20	Normal Olefin C20	58.372	22991	6798	0.20	0.13
NC20	Normal Alkane C20	58.559	26151	8596	0.23	0.17
NO21	Normal Olefin C21	60.390	17568	5257	0.15	0.10
NC21	Normal Alkane C21	60.563	24052	6682	0.21	0.13
NO22	Normal Olefin C22	62.322	14255	4270	0.12	0.08
NC22	Normal Alkane C22	62.483	16162	5458	0.14	0.11
NO23	Normal Olefin C23	64.175	9335	3210	0.08	0.06
NC23	Normal Alkane C23	64.322	10414	3740	0.09	0.07
NO24	Normal Olefin C24	65.956	7327	2425	0.06	0.05
NC24	Normal Alkane C24	66.094	9877	3114	0.09	0.06
NO25	Normal Olefin C25	67.677	7990	2400	0.07	0.05
NC25	Normal Alkane C25	67.801	6672	2208	0.06	0.04
NO26	Normal Olefin C26	69.333	5551	1554	0.05	0.03
NC26	Normal Alkane C26	69.449	8619	1960	0.07	0.04
NO27	Normal Olefin C27	70.944	4271	1253	0.04	0.02
NC27	Normal Alkane C27	71.054	6031	1637	0.05	0.03
NO28	Normal Olefin C28	72.509	5000	1062	0.04	0.02
NC28	Normal Alkane C28	72.615	4798	1277	0.04	0.02
NO29	Normal Olefin C29	74.220	3703	1116	0.03	0.02
NC29	Normal Alkane C29	74.283	5276	1308	0.05	0.03
NO30	Normal Olefin C30					
NC30	Normal Alkane C30	75.426	8208	1284	0.07	0.03
NO31	Normal Olefin C31					
NC31	Normal Alkane C31	77.661	7598	1173	0.07	0.02
NO32	Normal Olefin C32					
NC32	Normal Alkane C32	79.705	5589	818	0.05	0.02
NO33	Normal Olefin C33					
NC33	Normal Alkane C33					
NO34	Normal Olefin C34					
NC34	Normal Alkane C34					
NO35	Normal Olefin C35					
NC35	Normal Alkane C35					
NC36	Normal Alkane C36					

Monterey Shale: Closed-Conservative Method

Peak Label	Compound Name	Retention Time	Area	Height	Area%	Height%
NC1	Normal Alkane C1	6.580	3642221	82841	12.22	0.61
NO2	Normal Olefin C2	7.095	509624	553543	1.71	4.09
NC2	Normal Alkane C2	7.123	1683451	2585061	5.65	19.09
NO3	Normal Olefin C3	7.250	880295	976322	2.95	7.21
NC3	Normal Alkane C3	7.282	927373	1271375	3.11	9.39
NO4	Normal Olefin C4	7.763	590667	454432	1.98	3.36
NC4	Normal Alkane C4	7.858	467970	491959	1.57	3.63
NO5	Normal Olefin C5	9.418	194465	130215	0.65	0.96
NC5	Normal Alkane C5	9.730	297806	195037	1.00	1.44
NO6	Normal Olefin C6	13.226	153997	75146	0.52	0.55
NC6	Normal Alkane C6	13.740	202695	89644	0.68	0.66
BZ	Benzene	15.990	169832	70776	0.57	0.52
NO7	Normal Olefin C7	18.102	125839	52234	0.42	0.39
NC7	Normal Alkane C7	18.660	192303	78530	0.65	0.58
TOL	Toluene	21.115	218925	78340	0.73	0.58
NO8	Normal Olefin C8	22.799	124315	46002	0.42	0.34
NC8	Normal Alkane C8	23.320	164880	64639	0.55	0.48
EB	Ethylbenzene	25.339	73082	25292	0.25	0.19
MXYL	m-Xylene	25.735	271032	85969	0.91	0.63
PXYL	p-Xylene	25.767	71192	46899	0.24	0.35
OXYL	o-Xylene	26.653	96110	31094	0.32	0.23
23DMT	2-3 Dimethylthiophene	26.030	13924	6346	0.05	0.05
STY	Styrene	26.091	18591	7196	0.06	0.05
NO9	Normal Olefin C9	27.082	91887	37820	0.31	0.28
NC9	Normal Alkane C9	27.550	125517	51441	0.42	0.38
PH	Phenol	29.411	264965	93657	0.89	0.69
NO10	Normal Olefin C10	30.997	134158	41352	0.45	0.31
NC10	Normal Alkane C10	31.430	124457	45431	0.42	0.34
OCR	o-Cresol	32.315	32089	11833	0.11	0.09
MPCR	mp-Cresol	33.593	86455	29782	0.29	0.22
NO11	Normal Olefin C11	34.618	100043	32846	0.34	0.24
NC11	Normal Alkane C11	35.008	108684	43754	0.36	0.32
OEPH	o-Ethylphenol	36.504	12010	4582	0.04	0.03
PEPH	p-Ethylphenol	37.391	8003	5792	0.03	0.04
NO12	Normal Olefin C12	37.977	81772	26726	0.27	0.20
NC12	Normal Alkane C12	38.331	104458	36654	0.35	0.27
2MN	2-Methylnaphthalen	40.865	55698	16374	0.19	0.12
NO13	Normal Olefin C13	41.106	81427	25477	0.27	0.19
1MN	1-Methylnaphthalen	41.284	119464	32275	0.40	0.24
NC13	Normal Alkane C13	41.449	111115	31868	0.37	0.24
NO14	Normal Olefin C14	44.066	116336	27841	0.39	0.21
DMN	Dimethylnaphthalene	44.176	63237	13661	0.21	0.10
NC14	Normal Alkane C14	44.376	159844	38993	0.54	0.29

Monterey Shale: Closed-Conservative Method						
NO15	Normal Olefin C15	46.843	68665	18718	0.23	0.14
NC15	Normal Alkane C15	47.120	121038	33474	0.41	0.25
NO16	Normal Olefin C16	49.456	69867	17510	0.23	0.13
NC16	Normal Alkane C16	49.714	82827	26948	0.28	0.20
NO17	Normal Olefin C17	51.933	55685	14439	0.19	0.11
NC17	Normal Alkane C17	52.169	87255	25714	0.29	0.19
PREN	Pris-1-ene	52.417	18553	4869	0.06	0.04
PHEN	Phenanthrene	53.166	22318	5479	0.07	0.04
NO18	Normal Olefin C18	54.281	43790	12977	0.15	0.10
NC18	Normal Alkane C18	54.500	64294	20731	0.22	0.15
NO19	Normal Olefin C19	56.517	37221	10836	0.12	0.08
NC19	Normal Alkane C19	56.717	52129	17817	0.17	0.13
NO20	Normal Olefin C20	58.651	35833	10972	0.12	0.08
NC20	Normal Alkane C20	58.836	49368	14748	0.17	0.11
NO21	Normal Olefin C21	60.689	27085	8193	0.09	0.06
NC21	Normal Alkane C21	60.862	47013	13743	0.16	0.10
NO22	Normal Olefin C22	62.639	25249	7169	0.08	0.05
NC22	Normal Alkane C22	62.801	32504	10070	0.11	0.07
NO23	Normal Olefin C23	64.515	18971	5009	0.06	0.04
NC23	Normal Alkane C23	64.658	22409	7418	0.08	0.05
NO24	Normal Olefin C24	66.332	9909	3933	0.03	0.03
NC24	Normal Alkane C24	66.453	20688	6378	0.07	0.05
NO25	Normal Olefin C25	68.061	11544	3533	0.04	0.03
NC25	Normal Alkane C25	68.181	12421	3541	0.04	0.03
NO26	Normal Olefin C26	69.732	8642	1938	0.03	0.01
NC26	Normal Alkane C26	69.850	15379	4058	0.05	0.03
NO27	Normal Olefin C27	71.354	7720	2034	0.03	0.02
NC27	Normal Alkane C27	71.475	12017	2852	0.04	0.02
NO28	Normal Olefin C28	72.972	2938	997	0.01	0.01
NC28	Normal Alkane C28	73.083	6117	1837	0.02	0.01
NO29	Normal Olefin C29	74.650	4825	1373	0.02	0.01
NC29	Normal Alkane C29	74.735	11220	2160	0.04	0.02
NO30	Normal Olefin C30	76.353	2997	971	0.01	0.01
NC30	Normal Alkane C30	76.482	6957	1504	0.02	0.01
NO31	Normal Olefin C31	78.255	2773	827	0.01	0.01
NC31	Normal Alkane C31	78.364	8813	1482	0.03	0.01
NO32	Normal Olefin C32					
NC32	Normal Alkane C32					
NO33	Normal Olefin C33					
NC33	Normal Alkane C33					
NO34	Normal Olefin C34					
NC34	Normal Alkane C34					
NO35	Normal Olefin C35					
NC35	Normal Alkane C35					
NC36	Normal Alkane C36					

Marcellus Shale: Open-Conventional Method #1

Peak Label	Compound Name	Retention Time	Area	Height	Area%	Height%
NC1	Normal Alkane C1	6.816	227077	7675	12.54	1.18
NO2	Normal Olefin C2	6.988	51556	56619	2.85	8.74
NC2	Normal Alkane C2	7.007	30393	42458	1.68	6.55
NO3	Normal Olefin C3	7.140	38949	45304	2.15	6.99
NC3	Normal Alkane C3	7.151	12241	14989	0.68	2.31
NO4	Normal Olefin C4	7.638	22449	17647	1.24	2.72
NC4	Normal Alkane C4	7.727	12298	8746	0.68	1.35
NO5	Normal Olefin C5	9.265	10345	7403	0.57	1.14
NC5	Normal Alkane C5	9.580	5874	3971	0.32	0.61
NO6	Normal Olefin C6	13.086	13714	6945	0.76	1.07
NC6	Normal Alkane C6	13.620	6021	2792	0.33	0.43
BZ	Benzene	15.850	17327	7346	0.96	1.13
NO7	Normal Olefin C7	18.013	11127	4922	0.61	0.76
NC7	Normal Alkane C7	18.577	6497	2956	0.36	0.46
TOL	Toluene	20.994	35868	15988	1.98	2.47
NO8	Normal Olefin C8	22.721	9878	4329	0.55	0.67
NC8	Normal Alkane C8	23.250	7018	2913	0.39	0.45
EB	Ethylbenzene	25.238	8333	3373	0.46	0.52
MXYL	m-Xylene	25.611	20158	8187	1.11	1.26
PXYL	p-Xylene	25.653	9841	4439	0.54	0.69
OXYL	o-Xylene	26.542	13589	5441	0.75	0.84
23DMT	2-3 Dimethylthiophene	25.909	560	179	0.03	0.03
STY	Styrene	26.034	901	387	0.05	0.06
NO9	Normal Olefin C9	27.016	9935	3388	0.55	0.52
NC9	Normal Alkane C9	27.485	10545	4252	0.58	0.66
PH	Phenol	29.296	2167	562	0.12	0.09
NO10	Normal Olefin C10	30.942	9901	3744	0.55	0.58
NC10	Normal Alkane C10	31.369	24077	9654	1.33	1.49
OCR	o-Cresol	32.257	4578	1554	0.25	0.24
MPCR	mp-Cresol	33.492	2397	980	0.13	0.15
NO11	Normal Olefin C11	34.561	10424	4083	0.58	0.63
NC11	Normal Alkane C11	34.953	30482	12792	1.68	1.97
OEPH	o-Ethylphenol	36.446	930	362	0.05	0.06
PEPH	p-Ethylphenol	37.381	225	176	0.01	0.03
NO12	Normal Olefin C12	37.910	13166	4261	0.73	0.66
NC12	Normal Alkane C12	38.273	12367	4956	0.68	0.76
2MN	2-Methylnaphthalen	40.757	3165	1084	0.17	0.17
NO13	Normal Olefin C13	41.042	8662	3435	0.48	0.53
1MN	1-Methylnaphthalen	41.239	2286	763	0.13	0.12
NC13	Normal Alkane C13	41.373	9343	3567	0.52	0.55
NO14	Normal Olefin C14	43.976	11528	4585	0.64	0.71
DMN	Dimethylnaphthalene	44.055	534	211	0.03	0.03
NC14	Normal Alkane C14	44.279	10653	3975	0.59	0.61
NO15	Normal Olefin C15	46.735	10435	3783	0.58	0.58

Marcellus Shale Open-conventional Method #1						
NC15	Normal Alkane C15	47.013	16313	6134	0.90	0.95
NO16	Normal Olefin C16	49.334	10813	3876	0.60	0.60
NC16	Normal Alkane C16	49.590	13826	4959	0.76	0.77
NO17	Normal Olefin C17	51.795	9007	2982	0.50	0.46
NC17	Normal Alkane C17	52.031	17734	6760	0.98	1.04
PREN	Pris-1-ene	52.285	3327	874	0.18	0.13
PHEN	Phenanthrene	53.049	1512	618	0.08	0.10
NO18	Normal Olefin C18	54.125	3710	1301	0.20	0.20
NC18	Normal Alkane C18	54.344	9212	3210	0.51	0.50
NO19	Normal Olefin C19	56.388	644	234	0.04	0.04
NC19	Normal Alkane C19	56.545	5221	1921	0.29	0.30
NO20	Normal Olefin C20	58.441	1196	333	0.07	0.05
NC20	Normal Alkane C20	58.646	4157	1561	0.23	0.24
NO21	Normal Olefin C21	60.479	238	175	0.01	0.03
NC21	Normal Alkane C21	60.654	2300	897	0.13	0.14
NO22	Normal Olefin C22	62.425	488	141	0.03	0.02
NC22	Normal Alkane C22	62.578	1024	392	0.06	0.06
NO23	Normal Olefin C23					
NC23	Normal Alkane C23	64.164	853	240	0.05	0.04
NO24	Normal Olefin C24					
NC24	Normal Alkane C24	66.206	585	179	0.03	0.03
NO25	Normal Olefin C25					
NC25	Normal Alkane C25					
NO26	Normal Olefin C26					
NC26	Normal Alkane C26					
NO27	Normal Olefin C27					
NC27	Normal Alkane C27					
NO28	Normal Olefin C28					
NC28	Normal Alkane C28					
NO29	Normal Olefin C29					
NC29	Normal Alkane C29					
NO30	Normal Olefin C30					
NC30	Normal Alkane C30					
NO31	Normal Olefin C31					
NC31	Normal Alkane C31					
NO32	Normal Olefin C32					
NC32	Normal Alkane C32					
NO33	Normal Olefin C33					
NC33	Normal Alkane C33					
NO34	Normal Olefin C34					
NC34	Normal Alkane C34					
NO35	Normal Olefin C35					
NC35	Normal Alkane C35					
NC36	Normal Alkane C36					

Marcellus Shale: Open-Conventional Method #2

Peak Label	Compound Name	Retention Time	Area	Height	Area%	Height%
NO2	Normal Olefin C2	7.191	87007	95122	2.25	6.62
NC2	Normal Alkane C2	7.215	40964	57113	1.06	3.97
NO3	Normal Olefin C3	7.348	79563	95127	2.06	6.62
NC3	Normal Alkane C3	7.373	17501	23927	0.45	1.66
NO4	Normal Olefin C4	7.866	70957	49741	1.84	3.46
NC4	Normal Alkane C4	7.958	18182	15015	0.47	1.04
NO5	Normal Olefin C5	9.524	26219	17678	0.68	1.23
NC5	Normal Alkane C5	9.833	12562	7816	0.33	0.54
NO6	Normal Olefin C6	13.292	33088	15581	0.86	1.08
NC6	Normal Alkane C6	13.811	13362	6070	0.35	0.42
BZ	Benzene	16.044	63213	27005	1.64	1.88
NO7	Normal Olefin C7	18.144	29908	12470	0.77	0.87
NC7	Normal Alkane C7	18.694	14684	5795	0.38	0.40
TOL	Toluene	21.135	109472	44741	2.83	3.11
NO8	Normal Olefin C8	22.817	27184	11316	0.70	0.79
NC8	Normal Alkane C8	23.330	17072	7003	0.44	0.49
EB	Ethylbenzene	25.349	17647	6369	0.46	0.44
MXYL	m-Xylene	25.708	38394	14628	0.99	1.02
PXYL	p-Xylene	25.763	18543	7793	0.48	0.54
OXYL	o-Xylene	26.653	32446	12523	0.84	0.87
23DMT	2-3 Dimethylthiophene	25.994	1826	920	0.05	0.06
STY	Styrene	26.098	1687	709	0.04	0.05
NO9	Normal Olefin C9	27.083	25384	10627	0.66	0.74
NC9	Normal Alkane C9	27.547	23344	9949	0.60	0.69
PH	Phenol	29.471	8020	2731	0.21	0.19
NO10	Normal Olefin C10	30.986	26112	10422	0.68	0.73
NC10	Normal Alkane C10	31.417	50015	20975	1.29	1.46
OCR	o-Cresol	32.375	1392	1146	0.04	0.08
MPCR	mp-Cresol	33.530	8005	2611	0.21	0.18
NO11	Normal Olefin C11	34.598	27184	10221	0.70	0.71
NC11	Normal Alkane C11	34.992	66694	27283	1.73	1.90
OEPH	o-Ethylphenol	36.575	6454	2114	0.17	0.15
PEPH	p-Ethylphenol	37.277	12312	3735	0.32	0.26
NO12	Normal Olefin C12	37.953	29752	10627	0.77	0.74
NC12	Normal Alkane C12	38.311	38060	13752	0.98	0.96
2MN	2-Methylnaphthalen	40.735	4544	1092	0.12	0.08
NO13	Normal Olefin C13	41.089	31859	10742	0.82	0.75
1MN	1-Methylnaphthalen	41.256	2345	643	0.06	0.04
NC13	Normal Alkane C13	41.416	33388	11271	0.86	0.78
NO14	Normal Olefin C14	44.031	38656	14296	1.00	0.99
DMN	Dimethylnaphthalene	44.103	2785	847	0.07	0.06
NC14	Normal Alkane C14	44.330	35321	12214	0.91	0.85
NO15	Normal Olefin C15	46.796	36227	12918	0.94	0.90
NC15	Normal Alkane C15	47.073	53012	18952	1.37	1.32

Marcellus Shale: Open-Conventional Method #2						
NO16	Normal Olefin C16	49.403	32387	11301	0.84	0.79
NC16	Normal Alkane C16	49.657	24185	8100	0.63	0.56
NO17	Normal Olefin C17	51.873	29597	9573	0.77	0.67
NC17	Normal Alkane C17	52.109	53357	18545	1.38	1.29
PREN	Pris-1-ene	52.349	1059	342	0.03	0.02
PHEN	Phenanthrene	53.032	708	295	0.02	0.02
NO18	Normal Olefin C18	54.214	9085	3025	0.24	0.21
NC18	Normal Alkane C18	54.431	6823	2111	0.18	0.15
NO19	Normal Olefin C19	56.441	2109	596	0.05	0.04
NC19	Normal Alkane C19	56.637	4677	1439	0.12	0.10
NO20	Normal Olefin C20	58.564	3765	1118	0.10	0.08
NC20	Normal Alkane C20	58.751	2782	849	0.07	0.06
NO21	Normal Olefin C21	60.570	5897	1061	0.15	0.07
NC21	Normal Alkane C21	60.771	2895	806	0.07	0.06
NO22	Normal Olefin C22	62.552	1636	500	0.04	0.03
NC22	Normal Alkane C22	62.709	1994	617	0.05	0.04
NO23	Normal Olefin C23	64.367	2806	767	0.07	0.05
NC23	Normal Alkane C23	64.568	1615	489	0.04	0.03
NO24	Normal Olefin C24	66.223	1868	494	0.05	0.03
NC24	Normal Alkane C24	66.362	1973	442	0.05	0.03
NO25	Normal Olefin C25	68.019	503	198	0.01	0.01
NC25	Normal Alkane C25	68.088	1016	317	0.03	0.02
NO26	Normal Olefin C26					
NC26	Normal Alkane C26	69.765	1297	316	0.03	0.02
NO27	Normal Olefin C27					
NC27	Normal Alkane C27					
NO28	Normal Olefin C28					
NC28	Normal Alkane C28					
NO29	Normal Olefin C29					
NC29	Normal Alkane C29					
NO30	Normal Olefin C30					
NC30	Normal Alkane C30					
NO31	Normal Olefin C31					
NC31	Normal Alkane C31					
NO32	Normal Olefin C32					
NC32	Normal Alkane C32					
NO33	Normal Olefin C33					
NC33	Normal Alkane C33					
NO34	Normal Olefin C34					
NC34	Normal Alkane C34					
NO35	Normal Olefin C35					
NC35	Normal Alkane C35					
NC36	Normal Alkane C36					

Marcellus Shale: Closed-Conservative Method

Peak Label	Compound Name	Retention Time	Area	Height	Area%	Height%
NO2	Normal Olefin C2	7.163	218835	231968	3.59	10.37
NC2	Normal Alkane C2	7.183	204675	241982	3.36	10.82
NO3	Normal Olefin C3	7.326	152372	176386	2.50	7.89
NC3	Normal Alkane C3	7.337	51650	73890	0.85	3.30
NO4	Normal Olefin C4	7.843	103094	76564	1.69	3.42
NC4	Normal Alkane C4	7.936	39416	38089	0.65	1.70
NO5	Normal Olefin C5	9.505	37028	25282	0.61	1.13
NC5	Normal Alkane C5	9.815	29047	18940	0.48	0.85
NO6	Normal Olefin C6	13.284	42488	19758	0.70	0.88
NC6	Normal Alkane C6	13.803	28923	13059	0.48	0.58
BZ	Benzene	16.044	72229	29206	1.19	1.31
NO7	Normal Olefin C7	18.146	36205	15680	0.59	0.70
NC7	Normal Alkane C7	18.698	33638	14269	0.55	0.64
TOL	Toluene	21.150	210966	87328	3.47	3.90
NO8	Normal Olefin C8	22.826	31221	13257	0.51	0.59
NC8	Normal Alkane C8	23.339	28988	12446	0.48	0.56
EB	Ethylbenzene	25.363	19854	7019	0.33	0.31
MXYL	m-Xylene	25.726	37132	14409	0.61	0.64
PXYL	p-Xylene	25.780	17151	7544	0.28	0.34
OXYL	o-Xylene	26.671	25137	9096	0.41	0.41
23DMT	2-3 Dimethylthiophene	26.009	3933	1057	0.06	0.05
STY	Styrene	26.114	1362	551	0.02	0.02
NO9	Normal Olefin C9	27.101	27742	11496	0.46	0.51
NC9	Normal Alkane C9	27.565	27226	11627	0.45	0.52
PH	Phenol	29.429	3600	775	0.06	0.03
NO10	Normal Olefin C10	31.009	35131	12816	0.58	0.57
NC10	Normal Alkane C10	31.437	32689	13232	0.54	0.59
OCR	o-Cresol	32.326	1928	790	0.03	0.04
MPCR	mp-Cresol	33.557	3028	860	0.05	0.04
NO11	Normal Olefin C11	34.623	29657	11409	0.49	0.51
NC11	Normal Alkane C11	35.011	38211	15450	0.63	0.69
OEPH	o-Ethylphenol	36.527	1648	577	0.03	0.03
PEPH	p-Ethylphenol	37.400	3177	1046	0.05	0.05
NO12	Normal Olefin C12	37.977	29966	11077	0.49	0.50
NC12	Normal Alkane C12	38.336	42448	16205	0.70	0.72
2MN	2-Methylnaphthalen	40.847	1856	1063	0.03	0.05
NO13	Normal Olefin C13	41.114	35934	12323	0.59	0.55
1MN	1-Methylnaphthalen	41.279	3148	817	0.05	0.04
NC13	Normal Alkane C13	41.443	53306	17603	0.88	0.79
NO14	Normal Olefin C14	44.056	37338	13806	0.61	0.62
DMN	Dimethylnaphthalene	44.130	1999	758	0.03	0.03
NC14	Normal Alkane C14	44.358	58947	20984	0.97	0.94
NO15	Normal Olefin C15	46.821	37811	13605	0.62	0.61
NC15	Normal Alkane C15	47.102	80609	28381	1.32	1.27

Marcellus Shale: Closed-Conservative Method						
NO16	Normal Olefin C16	49.432	48683	16459	0.80	0.74
NC16	Normal Alkane C16	49.686	54516	18175	0.90	0.81
NO17	Normal Olefin C17	51.900	36274	10291	0.60	0.46
NC17	Normal Alkane C17	52.141	105726	35099	1.74	1.57
PREN	Pris-1-ene	52.382	7816	2116	0.13	0.09
PHEN	Phenanthrene	53.182	12228	2201	0.20	0.10
NO18	Normal Olefin C18	54.245	45095	16012	0.74	0.72
NC18	Normal Alkane C18	54.458	38639	13201	0.63	0.59
NO19	Normal Olefin C19	56.521	3073	955	0.05	0.04
NC19	Normal Alkane C19	56.665	15011	4678	0.25	0.21
NO20	Normal Olefin C20	58.598	5002	1613	0.08	0.07
NC20	Normal Alkane C20	58.780	7423	2421	0.12	0.11
NO21	Normal Olefin C21	60.608	8249	1575	0.14	0.07
NC21	Normal Alkane C21	60.802	6045	1876	0.10	0.08
NO22	Normal Olefin C22	62.666	4132	1264	0.07	0.06
NC22	Normal Alkane C22	62.751	3415	1178	0.06	0.05
NO23	Normal Olefin C23	64.523	3795	851	0.06	0.04
NC23	Normal Alkane C23	64.604	3697	1030	0.06	0.05
NO24	Normal Olefin C24					
NC24	Normal Alkane C24	66.405	3796	805	0.06	0.04
NO25	Normal Olefin C25					
NC25	Normal Alkane C25	68.134	1190	379	0.02	0.02
NO26	Normal Olefin C26					
NC26	Normal Alkane C26					
NO27	Normal Olefin C27					
NC27	Normal Alkane C27					
NO28	Normal Olefin C28					
NC28	Normal Alkane C28					
NO29	Normal Olefin C29					
NC29	Normal Alkane C29					
NO30	Normal Olefin C30					
NC30	Normal Alkane C30					
NO31	Normal Olefin C31					
NC31	Normal Alkane C31					
NO32	Normal Olefin C32					
NC32	Normal Alkane C32					
NO33	Normal Olefin C33					
NC33	Normal Alkane C33					
NO34	Normal Olefin C34					
NC34	Normal Alkane C34					
NO35	Normal Olefin C35					
NC35	Normal Alkane C35					
NC36	Normal Alkane C36					

Polish Shale: Open-Conventional Method #1

Peak Label	Compound Name	Retention Time	Area	Height	Area%	Height%
NO2	Normal Olefin C2	7.176	38212	36940	1.04	3.18
NC2	Normal Alkane C2	7.191	23801	25840	0.65	2.22
NO3	Normal Olefin C3	7.338	24107	24401	0.66	2.10
NC3	Normal Alkane C3	7.360	8492	10163	0.23	0.87
NO4	Normal Olefin C4	7.856	16721	12794	0.46	1.10
NC4	Normal Alkane C4	7.945	5169	4367	0.14	0.38
NO5	Normal Olefin C5	9.518	7102	4500	0.19	0.39
NC5	Normal Alkane C5	9.822	3288	2072	0.09	0.18
NO6	Normal Olefin C6	13.282	7826	3287	0.21	0.28
NC6	Normal Alkane C6	13.673	3544	1120	0.10	0.10
BZ	Benzene	15.748	22088	7327	0.60	0.63
NO7	Normal Olefin C7	17.949	20942	7944	0.57	0.68
NC7	Normal Alkane C7	18.523	11482	4229	0.31	0.36
TOL	Toluene	21.025	18228	5588	0.50	0.48
NO8	Normal Olefin C8	22.747	10197	3446	0.28	0.30
NC8	Normal Alkane C8	23.269	6591	2078	0.18	0.18
EB	Ethylbenzene	25.289	3193	1098	0.09	0.09
MXYL	m-Xylene	25.727	12713	4078	0.35	0.35
PXYL	p-Xylene	25.794	4084	2020	0.11	0.17
OXYL	o-Xylene	26.658	13797	4172	0.38	0.36
23DMT	2-3 Dimethylthiophene					
STY	Styrene					
NO9	Normal Olefin C9	27.083	16907	6516	0.46	0.56
NC9	Normal Alkane C9	27.547	14660	5776	0.40	0.50
PH	Phenol	29.411	2979	704	0.08	0.06
NO10	Normal Olefin C10	30.989	24953	9622	0.68	0.83
NC10	Normal Alkane C10	31.418	39367	16023	1.07	1.38
OCR	o-Cresol	32.306	4906	1697	0.13	0.15
MPCR	mp-Cresol	33.638	5082	1584	0.14	0.14
NO11	Normal Olefin C11	34.605	50197	19908	1.37	1.71
NC11	Normal Alkane C11	34.996	77927	31720	2.12	2.73
OEPH	o-Ethylphenol	36.516	2226	764	0.06	0.07
PEPH	p-Ethylphenol	37.298	3141	2244	0.09	0.19
NO12	Normal Olefin C12	37.962	66494	24954	1.81	2.15
NC12	Normal Alkane C12	38.320	72807	28329	1.98	2.44
2MN	2-Methylnaphthalen	40.859	3259	1486	0.09	0.13
NO13	Normal Olefin C13	41.101	95907	34054	2.61	2.93
1MN	1-Methylnaphthalen	41.273	3719	952	0.10	0.08
NC13	Normal Alkane C13	41.430	121016	42627	3.30	3.67
NO14	Normal Olefin C14	44.045	131761	49037	3.59	4.22
DMN	Dimethylnaphthalene	44.110	3272	1662	0.09	0.14
NC14	Normal Alkane C14	44.344	124799	43382	3.40	3.73
NO15	Normal Olefin C15	46.802	76698	27569	2.09	2.37
NC15	Normal Alkane C15	47.084	125545	44102	3.42	3.80

Polish Shale: Open-Conventional Method #1						
NO16	Normal Olefin C16	49.404	35026	12410	0.95	1.07
NC16	Normal Alkane C16	49.658	36486	12922	0.99	1.11
NO17	Normal Olefin C17	51.872	25270	7917	0.69	0.68
NC17	Normal Alkane C17	52.109	55567	19134	1.51	1.65
PREN	Pris-1-ene	52.354	4252	1216	0.12	0.10
PHEN	Phenanthrene	53.118	3093	1318	0.08	0.11
NO18	Normal Olefin C18	54.212	4261	1228	0.12	0.11
NC18	Normal Alkane C18	54.426	10731	3494	0.29	0.30
NO19	Normal Olefin C19	56.439	1258	397	0.03	0.03
NC19	Normal Alkane C19	56.638	6885	2328	0.19	0.20
NO20	Normal Olefin C20	58.563	3206	962	0.09	0.08
NC20	Normal Alkane C20	58.748	3383	1229	0.09	0.11
NO21	Normal Olefin C21	60.574	3410	865	0.09	0.07
NC21	Normal Alkane C21	60.769	2034	683	0.06	0.06
NO22	Normal Olefin C22	62.552	709	231	0.02	0.02
NC22	Normal Alkane C22	62.708	1218	412	0.03	0.04
NO23	Normal Olefin C23	64.410	1703	265	0.05	0.02
NC23	Normal Alkane C23	64.561	1994	374	0.05	0.03
NO24	Normal Olefin C24					
NC24	Normal Alkane C24					
NO25	Normal Olefin C25					
NC25	Normal Alkane C25					
NO26	Normal Olefin C26					
NC26	Normal Alkane C26					
NO27	Normal Olefin C27					
NC27	Normal Alkane C27					
NO28	Normal Olefin C28					
NC28	Normal Alkane C28					
NO29	Normal Olefin C29					
NC29	Normal Alkane C29					
NO30	Normal Olefin C30					
NC30	Normal Alkane C30					
NO31	Normal Olefin C31					
NC31	Normal Alkane C31					
NO32	Normal Olefin C32					
NC32	Normal Alkane C32					
NO33	Normal Olefin C33					
NC33	Normal Alkane C33					
NO34	Normal Olefin C34					
NC34	Normal Alkane C34					
NO35	Normal Olefin C35					
NC35	Normal Alkane C35					
NC36	Normal Alkane C36					

Polish Shale: Open-Conventional Method #2

Peak Label	Compound Name	Retention Time	Area	Height	Area%	Height%
NO2	Normal Olefin C2	7.166	27310	29597	1.18	4.15
NC2	Normal Alkane C2	7.196	12134	16229	0.52	2.28
NO3	Normal Olefin C3	7.325	13154	13339	0.57	1.87
NC3	Normal Alkane C3	7.350	3912	4458	0.17	0.63
NO4	Normal Olefin C4	7.849	17160	10323	0.74	1.45
NC4	Normal Alkane C4	7.943	4553	2850	0.20	0.40
NO5	Normal Olefin C5	9.509	6308	3477	0.27	0.49
NC5	Normal Alkane C5	9.865	13725	8115	0.59	1.14
NO6	Normal Olefin C6	13.280	11310	5132	0.49	0.72
NC6	Normal Alkane C6	13.799	4427	1707	0.19	0.24
BZ	Benzene	16.035	24748	10111	1.07	1.42
NO7	Normal Olefin C7	18.135	11982	4778	0.52	0.67
NC7	Normal Alkane C7	18.692	5891	2251	0.25	0.32
TOL	Toluene	21.125	97627	40734	4.21	5.72
NO8	Normal Olefin C8	22.808	16365	5480	0.71	0.77
NC8	Normal Alkane C8	23.321	9359	3354	0.40	0.47
EB	Ethylbenzene	25.340	8475	2986	0.37	0.42
MXYL	m-Xylene	25.697	17550	7117	0.76	1.00
PXYL	p-Xylene	25.787	9495	3813	0.41	0.54
OXYL	o-Xylene	26.642	15899	5711	0.69	0.80
23DMT	2-3 Dimethylthiophene	25.997	889	453	0.04	0.06
STY	Styrene	26.091	1307	546	0.06	0.08
NO9	Normal Olefin C9	27.074	11777	4397	0.51	0.62
NC9	Normal Alkane C9	27.538	11818	4921	0.51	0.69
PH	Phenol	29.462	3707	1254	0.16	0.18
NO10	Normal Olefin C10	30.977	12423	4692	0.54	0.66
NC10	Normal Alkane C10	31.406	28964	12039	1.25	1.69
OCR	o-Cresol	32.400	1650	671	0.07	0.09
MPCR	mp-Cresol	33.521	5129	1760	0.22	0.25
NO11	Normal Olefin C11	34.588	12895	4666	0.56	0.65
NC11	Normal Alkane C11	34.979	41799	16810	1.80	2.36
OEPH	o-Ethylphenol	36.495	1455	452	0.06	0.06
PEPH	p-Ethylphenol	37.272	3447	1112	0.15	0.16
NO12	Normal Olefin C12	37.941	14920	5163	0.64	0.72
NC12	Normal Alkane C12	38.300	33034	12350	1.43	1.73
2MN	2-Methylnaphthalen	40.813	474	269	0.02	0.04
NO13	Normal Olefin C13	41.075	16106	5152	0.69	0.72
1MN	1-Methylnaphthalen	41.252	1818	442	0.08	0.06
NC13	Normal Alkane C13	41.406	45727	16960	1.97	2.38
NO14	Normal Olefin C14	44.015	18561	7034	0.80	0.99
DMN	Dimethylnaphthalene	44.074	982	379	0.04	0.05
NC14	Normal Alkane C14	44.318	42506	15650	1.83	2.20
NO15	Normal Olefin C15	46.778	16324	5528	0.70	0.78
NC15	Normal Alkane C15	47.054	24035	7968	1.04	1.12

Polish Shale: Open-Conventional Method #2						
NO16	Normal Olefin C16	49.387	14517	4728	0.63	0.66
NC16	Normal Alkane C16	49.640	12431	3996	0.54	0.56
NO17	Normal Olefin C17	51.856	11311	3356	0.49	0.47
NC17	Normal Alkane C17	52.089	19089	6406	0.82	0.90
PREN	Pris-1-ene	52.337	3420	911	0.15	0.13
PHEN	Phenanthrene	53.109	1853	684	0.08	0.10
NO18	Normal Olefin C18	54.198	4611	1469	0.20	0.21
NC18	Normal Alkane C18	54.413	8713	2887	0.38	0.41
NO19	Normal Olefin C19	56.428	2597	615	0.11	0.09
NC19	Normal Alkane C19	56.625	7696	2552	0.33	0.36
NO20	Normal Olefin C20	58.551	2486	738	0.11	0.10
NC20	Normal Alkane C20	58.737	5676	1854	0.24	0.26
NO21	Normal Olefin C21	60.560	3437	675	0.15	0.09
NC21	Normal Alkane C21	60.756	3431	1205	0.15	0.17
NO22	Normal Olefin C22	62.536	1899	569	0.08	0.08
NC22	Normal Alkane C22	62.692	2756	880	0.12	0.12
NO23	Normal Olefin C23	64.405	1164	343	0.05	0.05
NC23	Normal Alkane C23	64.551	2087	684	0.09	0.10
NO24	Normal Olefin C24	66.205	1280	368	0.06	0.05
NC24	Normal Alkane C24	66.344	2047	631	0.09	0.09
NO25	Normal Olefin C25	67.962	361	107	0.02	0.02
NC25	Normal Alkane C25	68.071	1693	597	0.07	0.08
NO26	Normal Olefin C26	69.626	432	204	0.02	0.03
NC26	Normal Alkane C26	69.743	3276	961	0.14	0.13
NO27	Normal Olefin C27	71.266	389	105	0.02	0.01
NC27	Normal Alkane C27	71.371	4535	1076	0.20	0.15
NO28	Normal Olefin C28	72.860	755	171	0.03	0.02
NC28	Normal Alkane C28	72.977	3703	963	0.16	0.14
NO29	Normal Olefin C29					
NC29	Normal Alkane C29	74.632	4884	1115	0.21	0.16
NO30	Normal Olefin C30	76.254	862	222	0.04	0.03
NC30	Normal Alkane C30	76.354	4593	928	0.20	0.13
NO31	Normal Olefin C31					
NC31	Normal Alkane C31	78.206	3103	691	0.13	0.10
NO32	Normal Olefin C32					
NC32	Normal Alkane C32	80.258	2474	483	0.11	0.07
NO33	Normal Olefin C33					
NC33	Normal Alkane C33	82.571	2203	354	0.10	0.05
NO34	Normal Olefin C34					
NC34	Normal Alkane C34	85.228	3921	364	0.17	0.05
NO35	Normal Olefin C35					
NC35	Normal Alkane C35	88.322	2398	298	0.10	0.04
NC36	Normal Alkane C36					

Polish Shale: Closed-Conservative Method

Peak Label	Compound Name	Retention Time	Area	Height	Area%	Height%
NO2	Normal Olefin C2	7.191	33778	34958	2.36	7.64
NC2	Normal Alkane C2	7.203	14445	17907	1.01	3.91
NO3	Normal Olefin C3	7.348	26083	29302	1.82	6.40
NC3	Normal Alkane C3	7.375	7072	8113	0.49	1.77
NO4	Normal Olefin C4	7.869	20653	12910	1.44	2.82
NC4	Normal Alkane C4	7.961	6831	4641	0.48	1.01
NO5	Normal Olefin C5	9.528	6028	4042	0.42	0.88
NC5	Normal Alkane C5	9.841	2891	1891	0.20	0.41
NO6	Normal Olefin C6	13.303	8113	3669	0.57	0.80
NC6	Normal Alkane C6	13.820	3773	1667	0.26	0.36
BZ	Benzene	16.060	17151	6911	1.20	1.51
NO7	Normal Olefin C7	18.158	7011	2839	0.49	0.62
NC7	Normal Alkane C7	18.707	4651	1761	0.32	0.38
TOL	Toluene	21.149	37247	14647	2.60	3.20
NO8	Normal Olefin C8	22.832	6688	2627	0.47	0.57
NC8	Normal Alkane C8	23.344	4815	2018	0.34	0.44
EB	Ethylbenzene	25.370	6281	2191	0.44	0.48
MXYL	m-Xylene	25.728	14551	5605	1.02	1.22
PXYL	p-Xylene	25.784	6974	2922	0.49	0.64
OXYL	o-Xylene	26.674	10755	3845	0.75	0.84
23DMT	2-3 Dimethylthiophene	26.024	819	216	0.06	0.05
STY	Styrene	26.116	767	313	0.05	0.07
NO9	Normal Olefin C9	27.104	6789	2576	0.47	0.56
NC9	Normal Alkane C9	27.567	7797	3101	0.54	0.68
PH	Phenol	29.419	354	105	0.02	0.02
NO10	Normal Olefin C10	31.008	6851	2626	0.48	0.57
NC10	Normal Alkane C10	31.435	16377	6687	1.14	1.46
OCR	o-Cresol	32.326	3116	1158	0.22	0.25
MPCR	mp-Cresol	33.549	1822	712	0.13	0.16
NO11	Normal Olefin C11	34.621	7158	2669	0.50	0.58
NC11	Normal Alkane C11	35.010	24160	9606	1.69	2.10
OEPH	o-Ethylphenol	36.533	949	272	0.07	0.06
PEPH	p-Ethylphenol	37.406	1838	605	0.13	0.13
NO12	Normal Olefin C12	37.977	7646	2678	0.53	0.59
NC12	Normal Alkane C12	38.333	10243	3975	0.71	0.87
2MN	2-Methylnaphthalen	40.862	529	263	0.04	0.06
NO13	Normal Olefin C13	41.111	7834	2492	0.55	0.54
1MN	1-Methylnaphthalen	41.276	769	176	0.05	0.04
NC13	Normal Alkane C13	41.437	13568	4490	0.95	0.98
NO14	Normal Olefin C14	44.050	9606	3522	0.67	0.77
DMN	Dimethylnaphthalene	44.130	458	195	0.03	0.04
NC14	Normal Alkane C14	44.349	12001	4039	0.84	0.88
NO15	Normal Olefin C15	46.813	9442	3047	0.66	0.67
NC15	Normal Alkane C15	47.088	18699	6447	1.31	1.41

Polish Shale: Closed-Conservative Method						
NO16	Normal Olefin C16	49.422	8646	2682	0.60	0.59
NC16	Normal Alkane C16	49.675	12281	3981	0.86	0.87
NO17	Normal Olefin C17	51.890	8207	2437	0.57	0.53
NC17	Normal Alkane C17	52.124	21215	6839	1.48	1.49
PREN	Pris-1-ene	52.372	4200	1050	0.29	0.23
PHEN	Phenanthrene	53.146	2290	799	0.16	0.17
NO18	Normal Olefin C18	54.234	2052	567	0.14	0.12
NC18	Normal Alkane C18	54.447	9007	2883	0.63	0.63
NO19	Normal Olefin C19	56.510	961	303	0.07	0.07
NC19	Normal Alkane C19	56.662	9801	3183	0.68	0.70
NO20	Normal Olefin C20	58.586	1394	387	0.10	0.08
NC20	Normal Alkane C20	58.774	6990	2406	0.49	0.53
NO21	Normal Olefin C21	60.597	2336	480	0.16	0.10
NC21	Normal Alkane C21	60.797	4082	1418	0.28	0.31
NO22	Normal Olefin C22	62.584	628	190	0.04	0.04
NC22	Normal Alkane C22	62.738	1875	646	0.13	0.14
NO23	Normal Olefin C23					
NC23	Normal Alkane C23	64.602	1003	303	0.07	0.07
NO24	Normal Olefin C24					
NC24	Normal Alkane C24	66.399	727	214	0.05	0.05
NO25	Normal Olefin C25					
NC25	Normal Alkane C25	68.133	377	129	0.03	0.03
NO26	Normal Olefin C26					
NC26	Normal Alkane C26	69.819	685	162	0.05	0.04
NO27	Normal Olefin C27					
NC27	Normal Alkane C27					
NO28	Normal Olefin C28					
NC28	Normal Alkane C28					
NO29	Normal Olefin C29					
NC29	Normal Alkane C29					
NO30	Normal Olefin C30					
NC30	Normal Alkane C30					
NO31	Normal Olefin C31					
NC31	Normal Alkane C31					
NO32	Normal Olefin C32					
NC32	Normal Alkane C32					
NO33	Normal Olefin C33					
NC33	Normal Alkane C33					
NO34	Normal Olefin C34					
NC34	Normal Alkane C34					
NO35	Normal Olefin C35					
NC35	Normal Alkane C35					
NC36	Normal Alkane C36					

Haynesville Shale: Open-Conventional Method #2

Peak Label	Compound Name	Retention Time	Area	Height	Area%	Height%
NO2	Normal Olefin C2	6.996	82810	94997	3.65	10.67
NC2	Normal Alkane C2	7.012	37309	50900	1.64	5.72
NO3	Normal Olefin C3	7.146	67068	85576	2.95	9.61
NC3	Normal Alkane C3	7.157	17680	25362	0.78	2.85
NO4	Normal Olefin C4	7.633	46511	34415	2.05	3.87
NC4	Normal Alkane C4	7.731	18416	12747	0.81	1.43
NO5	Normal Olefin C5	9.269	16985	11524	0.75	1.29
NC5	Normal Alkane C5	9.573	7162	4627	0.32	0.52
NO6	Normal Olefin C6	13.076	18448	9410	0.81	1.06
NC6	Normal Alkane C6	13.609	6323	2825	0.28	0.32
BZ	Benzene	15.838	29486	12716	1.30	1.43
NO7	Normal Olefin C7	18.001	14486	6713	0.64	0.75
NC7	Normal Alkane C7	18.567	5991	2614	0.26	0.29
TOL	Toluene	20.981	31657	13863	1.39	1.56
NO8	Normal Olefin C8	22.716	13245	5714	0.58	0.64
NC8	Normal Alkane C8	23.237	6402	2813	0.28	0.32
EB	Ethylbenzene	25.226	7352	2730	0.32	0.31
MXYL	m-Xylene	25.590	15666	6283	0.69	0.71
PXYL	p-Xylene	25.644	7554	3402	0.33	0.38
OXYL	o-Xylene	26.528	10841	4205	0.48	0.47
23DMT	2-3 Dimethylthiophene	25.900	896	359	0.04	0.04
STY	Styrene	25.968	322	136	0.01	0.02
NO9	Normal Olefin C9	27.004	12541	4755	0.55	0.53
NC9	Normal Alkane C9	27.475	8768	3653	0.39	0.41
PH	Phenol	29.275	2867	838	0.13	0.09
NO10	Normal Olefin C10	30.929	13004	5021	0.57	0.56
NC10	Normal Alkane C10	31.357	22024	9375	0.97	1.05
OCR	o-Cresol	32.260	3843	1745	0.17	0.20
MPCR	mp-Cresol	33.481	3764	1234	0.17	0.14
NO11	Normal Olefin C11	34.548	13461	5472	0.59	0.61
NC11	Normal Alkane C11	34.941	36944	16204	1.63	1.82
OEPH	o-Ethylphenol	36.431	5364	1605	0.24	0.18
PEPH	p-Ethylphenol	37.145	7131	2890	0.31	0.32
NO12	Normal Olefin C12	37.895	28016	6994	1.23	0.79
NC12	Normal Alkane C12	38.264	17991	7337	0.79	0.82
2MN	2-Methylnaphthalen	40.687	598	344	0.03	0.04
NO13	Normal Olefin C13	41.029	12889	5209	0.57	0.59
1MN	1-Methylnaphthalen	41.144	742	292	0.03	0.03
NC13	Normal Alkane C13	41.366	24683	9482	1.09	1.07
NO14	Normal Olefin C14	43.968	17972	6928	0.79	0.78
DMN	Dimethylnaphthalene	44.042	1960	721	0.09	0.08
NC14	Normal Alkane C14	44.272	30348	11472	1.34	1.29
NO15	Normal Olefin C15	46.725	15469	5190	0.68	0.58
NC15	Normal Alkane C15	47.003	19085	6757	0.84	0.76

Haynesville Shale: Open-Conventional Method #2						
NO16	Normal Olefin C16	49.324	13683	5071	0.60	0.57
NC16	Normal Alkane C16	49.580	10109	3699	0.45	0.42
NO17	Normal Olefin C17	51.784	9350	3100	0.41	0.35
NC17	Normal Alkane C17	52.020	11928	4610	0.53	0.52
PREN	Pris-1-ene	52.276	881	265	0.04	0.03
PHEN	Phenanthrene	53.036	506	130	0.02	0.01
NO18	Normal Olefin C18	54.116	1844	657	0.08	0.07
NC18	Normal Alkane C18	54.335	3468	1129	0.15	0.13
NO19	Normal Olefin C19	56.351	1332	327	0.06	0.04
NC19	Normal Alkane C19	56.535	1738	595	0.08	0.07
NO20	Normal Olefin C20	58.429	1335	329	0.06	0.04
NC20	Normal Alkane C20	58.638	1339	456	0.06	0.05
NO21	Normal Olefin C21	60.643	968	357	0.04	0.04
NC21	Normal Alkane C21	60.843	906	238	0.04	0.03
NO22	Normal Olefin C22	62.412	432	137	0.02	0.02
NC22	Normal Alkane C22	62.569	836	303	0.04	0.03
NO23	Normal Olefin C23					
NC23	Normal Alkane C23	64.414	686	209	0.03	0.02
NO24	Normal Olefin C24					
NC24	Normal Alkane C24	66.191	515	182	0.02	0.02
NO25	Normal Olefin C25					
NC25	Normal Alkane C25					
NO26	Normal Olefin C26					
NC26	Normal Alkane C26					
NO27	Normal Olefin C27					
NC27	Normal Alkane C27					
NO28	Normal Olefin C28					
NC28	Normal Alkane C28					
NO29	Normal Olefin C29					
NC29	Normal Alkane C29					
NO30	Normal Olefin C30					
NC30	Normal Alkane C30					
NO31	Normal Olefin C31					
NC31	Normal Alkane C31					
NO32	Normal Olefin C32					
NC32	Normal Alkane C32					
NO33	Normal Olefin C33					
NC33	Normal Alkane C33					
NO34	Normal Olefin C34					
NC34	Normal Alkane C34					
NO35	Normal Olefin C35					
NC35	Normal Alkane C35					
NC36	Normal Alkane C36					

Haynesville Shale: Closed-Conservative Method

Peak Label	Compound Name	Retention Time	Area	Height	Area%	Height%
NO2	Normal Olefin C2	7.176	151053	152554	4.86	12.85
NC2	Normal Alkane C2	7.190	132348	192013	4.26	16.17
NO3	Normal Olefin C3	7.337	120751	143925	3.88	12.12
NC3	Normal Alkane C3	7.357	43081	58694	1.39	4.94
NO4	Normal Olefin C4	7.855	72753	49633	2.34	4.18
NC4	Normal Alkane C4	7.947	26296	21101	0.85	1.78
NO5	Normal Olefin C5	9.520	16350	11107	0.53	0.94
NC5	Normal Alkane C5	9.828	10829	7038	0.35	0.59
NO6	Normal Olefin C6	13.295	15695	7091	0.50	0.60
NC6	Normal Alkane C6	13.813	10689	4799	0.34	0.40
BZ	Benzene	16.055	32605	12922	1.05	1.09
NO7	Normal Olefin C7	18.154	11881	4846	0.38	0.41
NC7	Normal Alkane C7	18.708	8395	3353	0.27	0.28
TOL	Toluene	21.149	64048	25409	2.06	2.14
NO8	Normal Olefin C8	22.830	9865	3979	0.32	0.34
NC8	Normal Alkane C8	23.346	7617	3217	0.24	0.27
EB	Ethylbenzene	25.368	10108	3639	0.33	0.31
MXYL	m-Xylene	25.724	25746	9465	0.83	0.80
PXYL	p-Xylene	25.783	11237	5101	0.36	0.43
OXYL	o-Xylene	26.674	12991	4790	0.42	0.40
23DMT	2-3 Dimethylthiophene	26.020	1641	445	0.05	0.04
STY	Styrene	26.115	1345	564	0.04	0.05
NO9	Normal Olefin C9	27.102	8309	3385	0.27	0.29
NC9	Normal Alkane C9	27.565	8506	3413	0.27	0.29
PH	Phenol	29.418	1014	252	0.03	0.02
NO10	Normal Olefin C10	31.007	7997	3108	0.26	0.26
NC10	Normal Alkane C10	31.435	12403	5005	0.40	0.42
OCR	o-Cresol	32.326	1671	635	0.05	0.05
MPCR	mp-Cresol	33.550	1484	531	0.05	0.04
NO11	Normal Olefin C11	34.621	7779	2899	0.25	0.24
NC11	Normal Alkane C11	35.009	14897	5814	0.48	0.49
OEPH	o-Ethylphenol	36.534	871	284	0.03	0.02
PEPH	p-Ethylphenol	37.400	2104	645	0.07	0.05
NO12	Normal Olefin C12	37.976	7587	2580	0.24	0.22
NC12	Normal Alkane C12	38.332	10723	4159	0.34	0.35
2MN	2-Methylnaphthalen	40.846	466	289	0.01	0.02
NO13	Normal Olefin C13	41.111	8084	2413	0.26	0.20
1MN	1-Methylnaphthalen	41.270	1333	289	0.04	0.02
NC13	Normal Alkane C13	41.435	17577	5758	0.57	0.48
NO14	Normal Olefin C14	44.048	8769	3185	0.28	0.27
DMN	Dimethylnaphthalene	44.126	778	287	0.03	0.02
NC14	Normal Alkane C14	44.348	16381	5577	0.53	0.47
NO15	Normal Olefin C15	46.812	6871	2401	0.22	0.20
NC15	Normal Alkane C15	47.086	13923	4864	0.45	0.41

Haynesville Shale: Closed-Conservative Method						
NO16	Normal Olefin C16	49.419	7113	2411	0.23	0.20
NC16	Normal Alkane C16	49.673	10465	3494	0.34	0.29
NO17	Normal Olefin C17	51.888	7347	1964	0.24	0.17
NC17	Normal Alkane C17	52.121	15745	5269	0.51	0.44
PREN	Pris-1-ene	52.368	3160	792	0.10	0.07
PHEN	Phenanthrene	53.148	1748	608	0.06	0.05
NO18	Normal Olefin C18	54.229	2347	685	0.08	0.06
NC18	Normal Alkane C18	54.444	5928	1969	0.19	0.17
NO19	Normal Olefin C19	56.520	1321	346	0.04	0.03
NC19	Normal Alkane C19	56.658	5548	1650	0.18	0.14
NO20	Normal Olefin C20	58.585	1895	564	0.06	0.05
NC20	Normal Alkane C20	58.772	2683	902	0.09	0.08
NO21	Normal Olefin C21	60.599	2546	687	0.08	0.06
NC21	Normal Alkane C21	60.795	1727	592	0.06	0.05
NO22	Normal Olefin C22	62.584	506	167	0.02	0.01
NC22	Normal Alkane C22	62.736	1078	368	0.03	0.03
NO23	Normal Olefin C23					
NC23	Normal Alkane C23	64.604	729	260	0.02	0.02
NO24	Normal Olefin C24					
NC24	Normal Alkane C24	66.399	1053	274	0.03	0.02
NO25	Normal Olefin C25					
NC25	Normal Alkane C25	68.128	500	185	0.02	0.02
NO26	Normal Olefin C26					
NC26	Normal Alkane C26					
NO27	Normal Olefin C27					
NC27	Normal Alkane C27					
NO28	Normal Olefin C28					
NC28	Normal Alkane C28					
NO29	Normal Olefin C29					
NC29	Normal Alkane C29					
NO30	Normal Olefin C30					
NC30	Normal Alkane C30					
NO31	Normal Olefin C31					
NC31	Normal Alkane C31					
NO32	Normal Olefin C32					
NC32	Normal Alkane C32					
NO33	Normal Olefin C33					
NC33	Normal Alkane C33					
NO34	Normal Olefin C34					
NC34	Normal Alkane C34					
NO35	Normal Olefin C35					
NC35	Normal Alkane C35					
NC36	Normal Alkane C36					